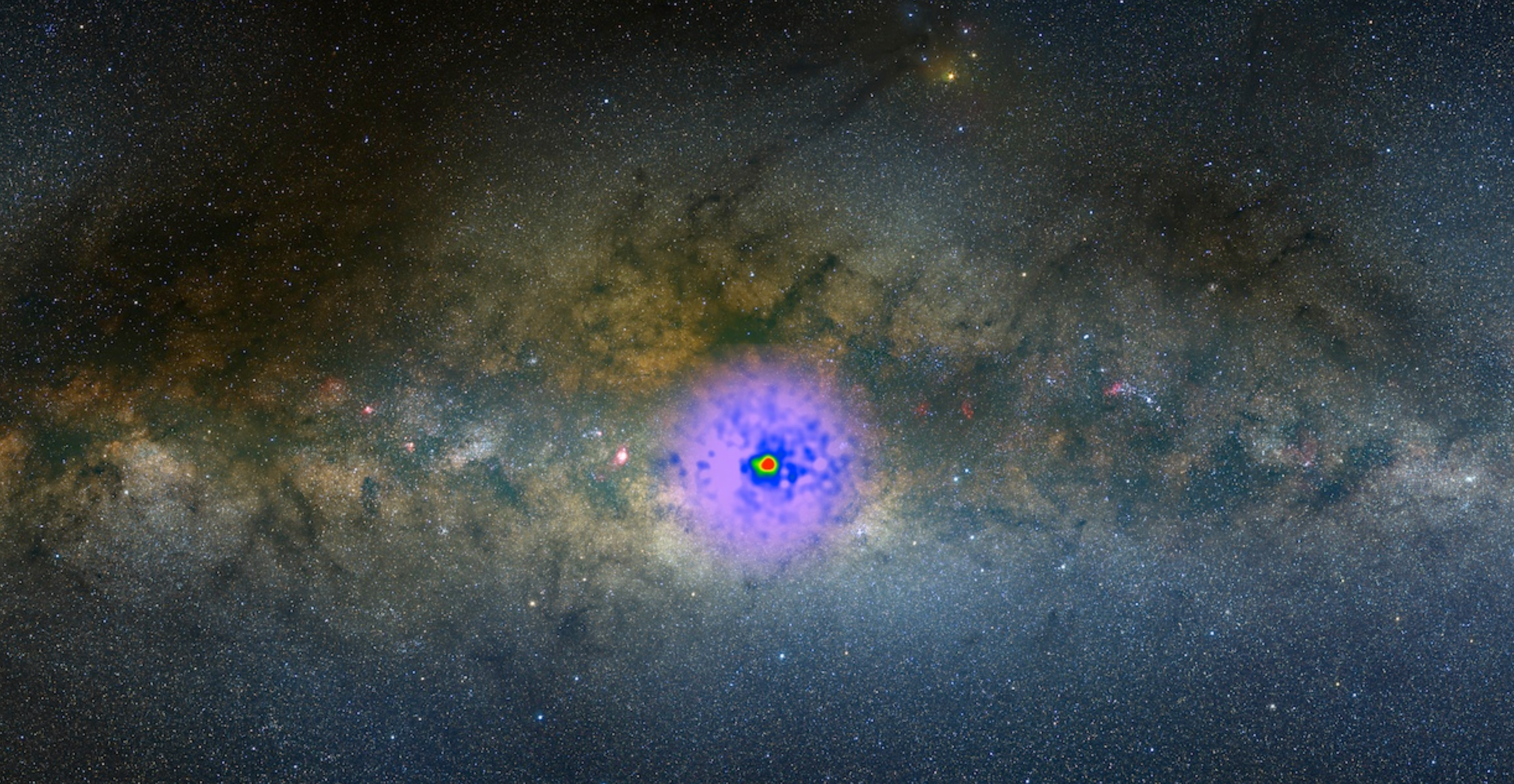

The Galactic Center Gamma-Ray Excess

Tim Linden

Boston University
High Energy Physics Seminar
October 31, 2018

The Ohio State University
Center for Cosmology and Astroparticle Physics

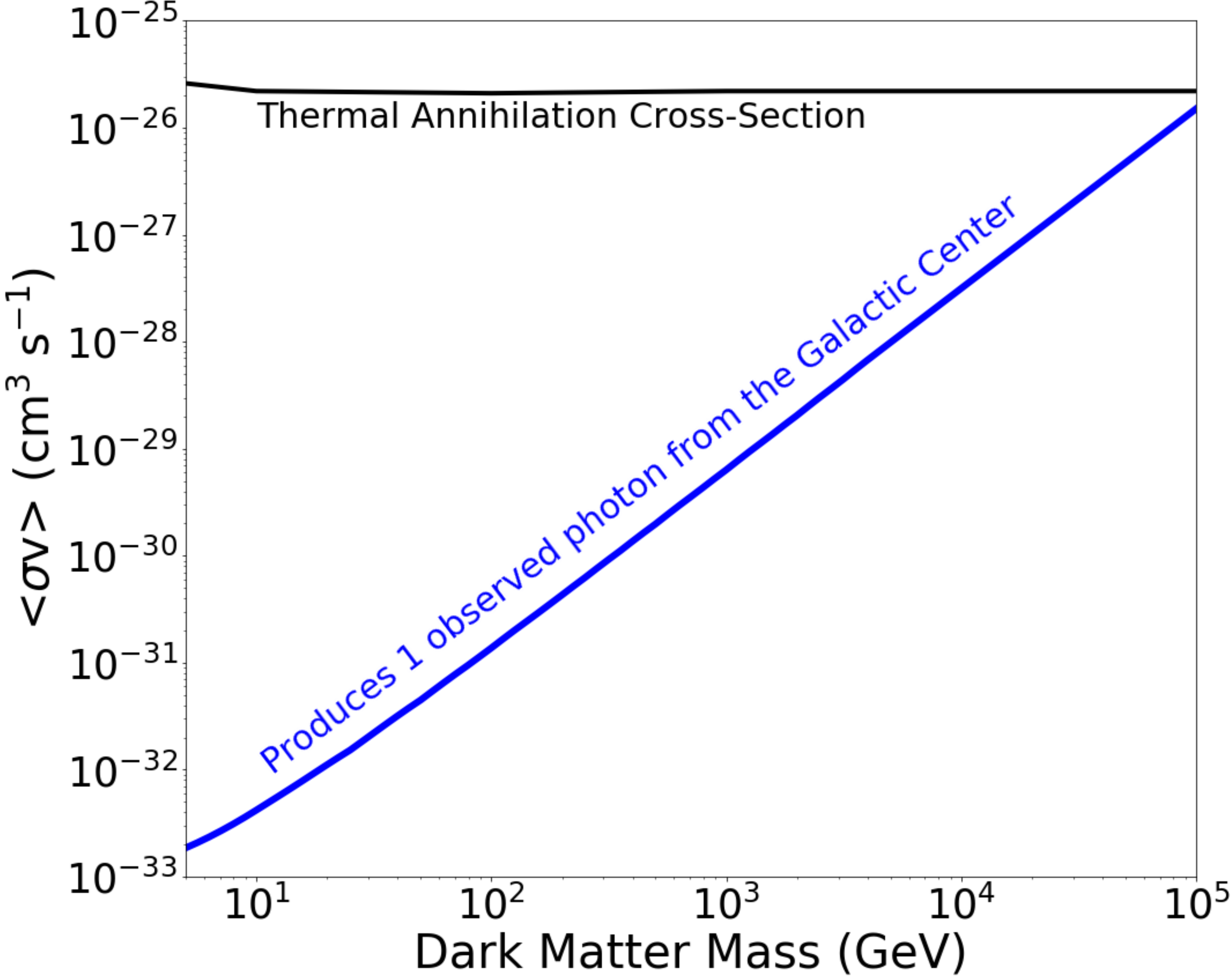

Thermal Annihilation Cross-Section
Produces 1 observed photon from the Galactic Center
$\langle\sigma v\rangle$ (cm^3 s^{-1})
Dark Matter Mass (GeV)
10^{-25}
10^{-26}
10^{-27}
10^{-28}
10^{-29}
10^{-30}
10^{-31}
10^{-32}
10^{-33}
10^{1}
10^{2}
10^{3}
10^{4}
10^{5}

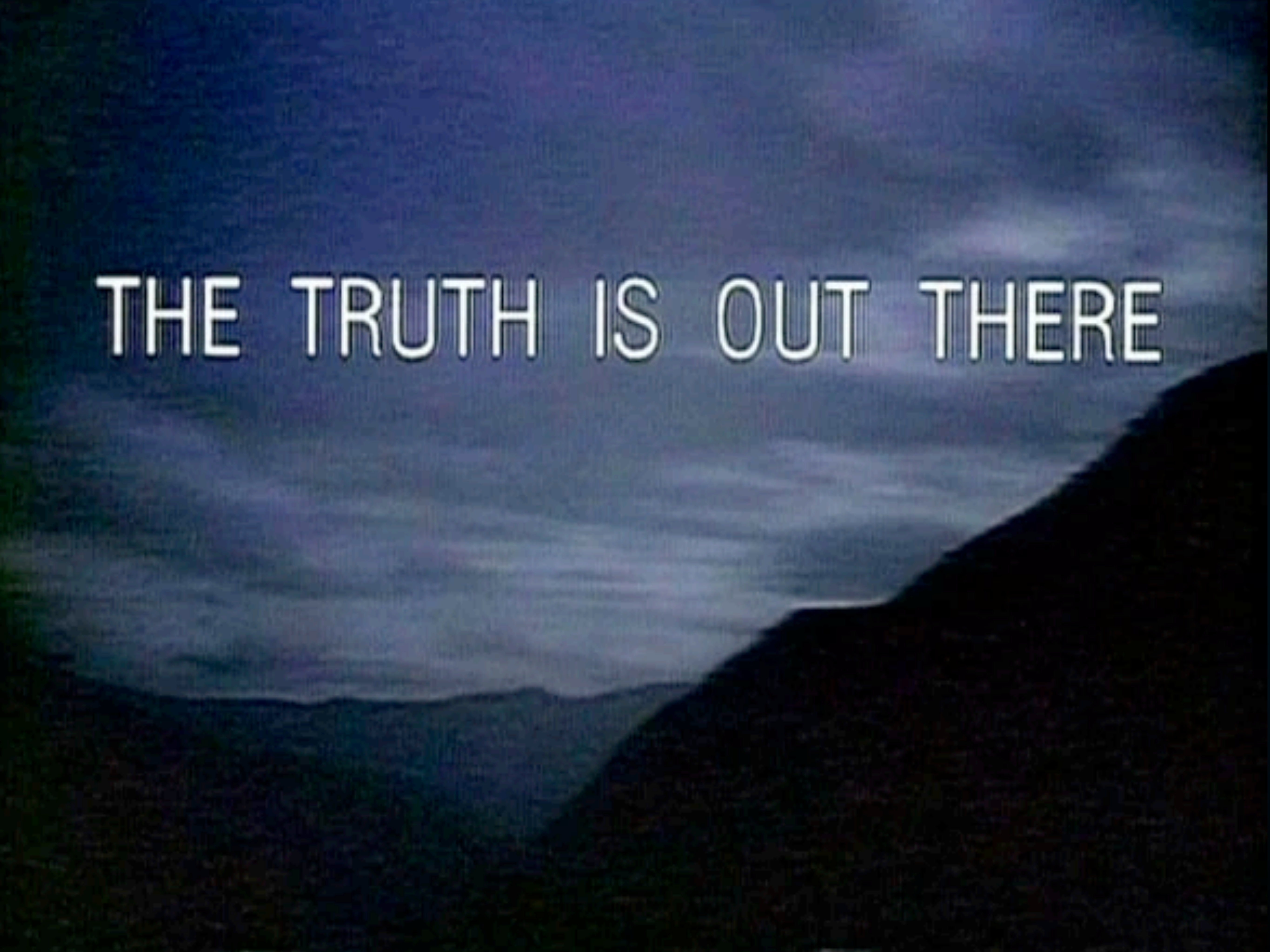
THE TRUTH IS OUT THERE

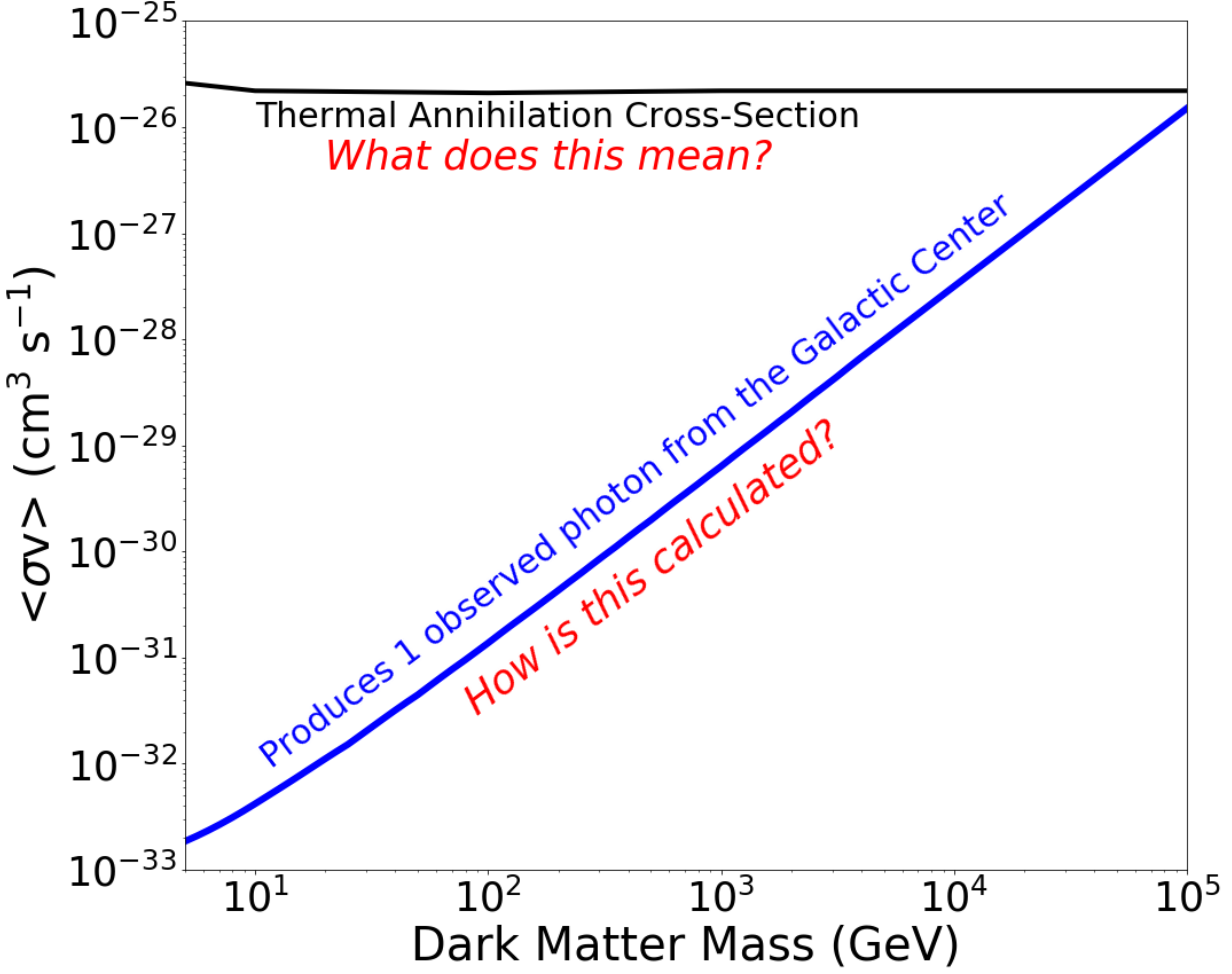

Thermal Annihilation Cross-Section
What does this mean?
Produces 1 observed photon from the Galactic Center
How is this calculated?
$\langle\sigma v\rangle$ (cm^3 s^{-1})
Dark Matter Mass (GeV)
10^{-25}
10^{-26}
10^{-27}
10^{-28}
10^{-29}
10^{-30}
10^{-31}
10^{-32}
10^{-33}
10^{1}
10^{2}
10^{3}
10^{4}
10^{5}

The WIMP Miracle

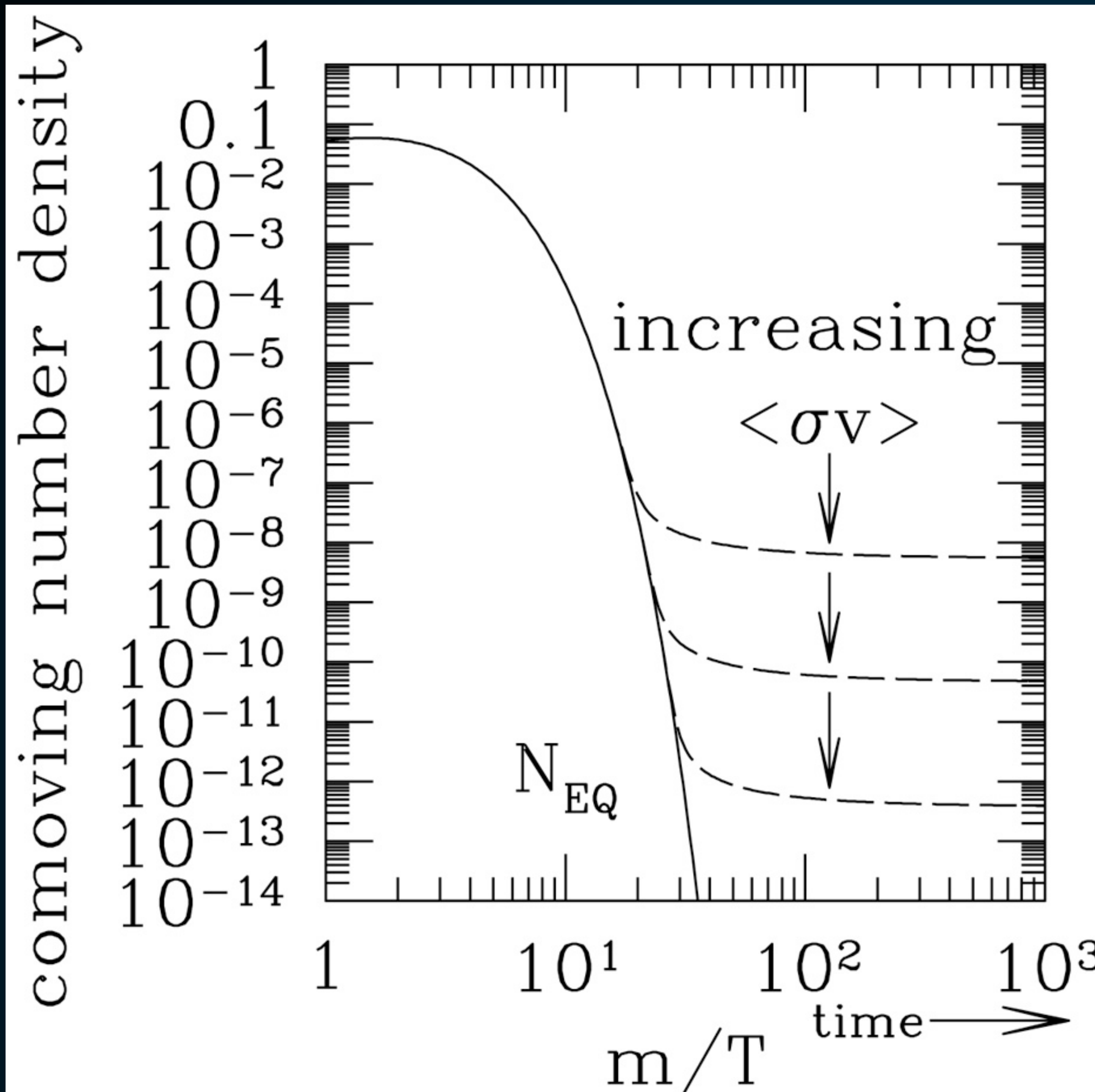

A particle with a weak interaction cross-section and a mass on the weak scale is expected to naturally obtain the correct relic abundance through thermal freeze-out in the Earth universe.

$$\frac{\Omega_\chi}{0.2} = \frac{x_{f.o}}{20}\left(\frac{10^{-8}\ \mathrm{GeV}^{-2}}{\sigma}\right)$$

$$< \sigma v > \ \sim \ 10^{-8}\,\mathrm{GeV}^{-2}\left(3 \times 10^{-28}\right)\mathrm{GeV}^2\mathrm{cm}^2\ 10^{10}\frac{\mathrm{cm}}{\mathrm{s}}$$

$$\boxed{< \sigma v > \ \sim \ 3 \times 10^{-26}\ \frac{\mathrm{cm}^3}{\mathrm{s}}}$$

The Thermal Miracle

WIMP Miracle

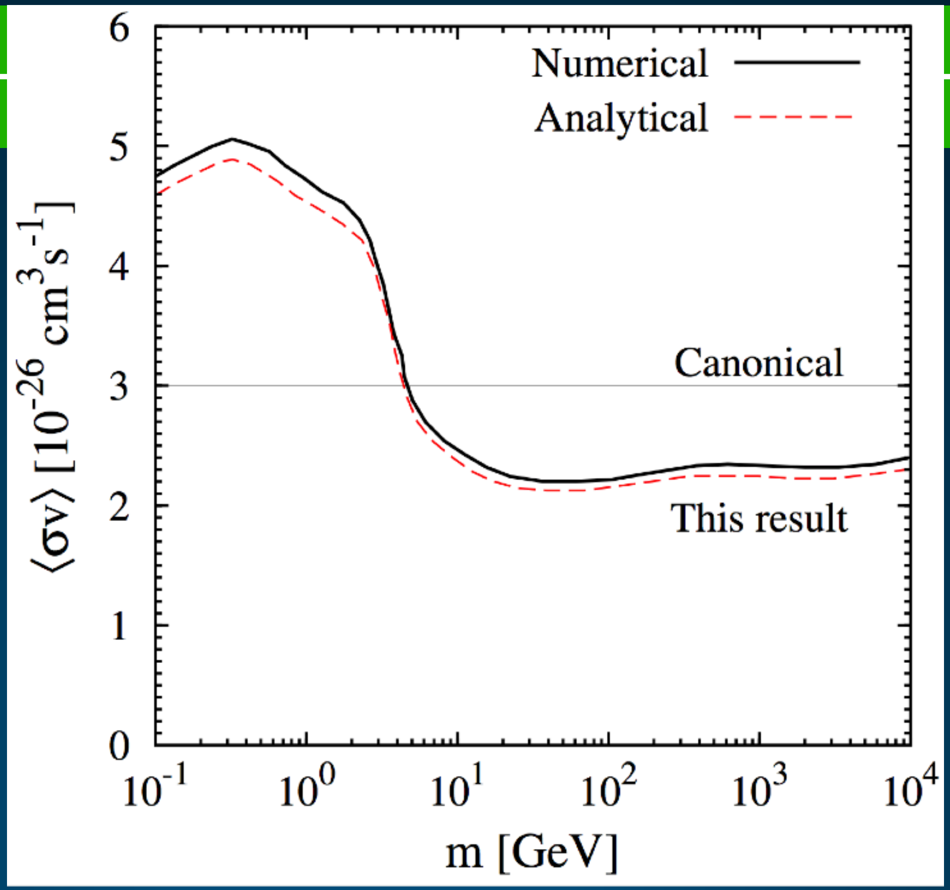

Steigman et al. (1204.3622)

N_{eff}

>3 MeV

$$N_{\rm eff} = N_\nu \left(\frac{4}{11}\right)^{-4/3}\left(\frac{T_\nu}{T_\gamma}\right)^4$$

$$N_{\rm eff}^{\rm equil} = N_\nu\left[1+\frac{1}{N_\nu}\sum_{i=1}^{n}\frac{g_i}{2}F\left(\frac{m_i}{T_d}\right)\right]^{4/3}$$

Unitarity

< 124 TeV

$$\sigma \sim \frac{g^2}{m_\chi^4}$$

$$g \lesssim 4\pi$$

$$\frac{\Omega_\chi}{0.2} \gtrsim 10^{-8}\ {\rm GeV}^{-2}\left(\frac{m_\chi^2}{4\pi}\right)$$

$$x_f = ln\left(\frac{m_\chi^3 < \sigma v >}{H_{x=1}}\right)$$

Thermal WIMPs - The Most Boring Model

1 new particle (can be motivated by more-complex physics)

1 new conserved quantity ("dark matter-ness", r-parity)

1 (maybe 0) new forces

Thermal WIMPs - The Most Boring Model

1 new particle (can be motivated by more-complex physics)

1 new conserved quantity ("dark matter-ness", r-parity)

1 (maybe 0) new forces

Ruling out this model leaves only *more* interesting possibilities.

Dark Matter Complementarity

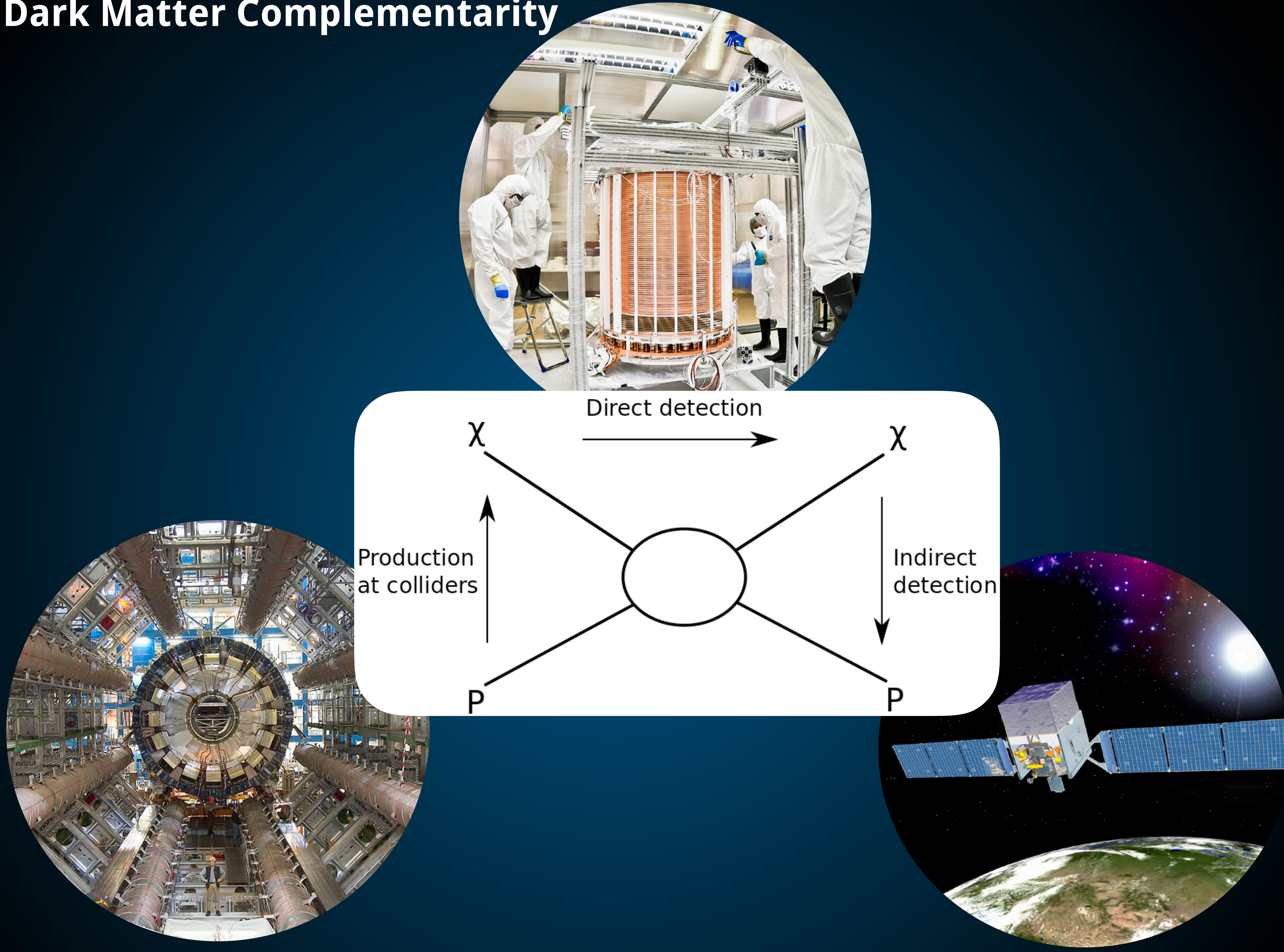

Dark Matter Complementarity

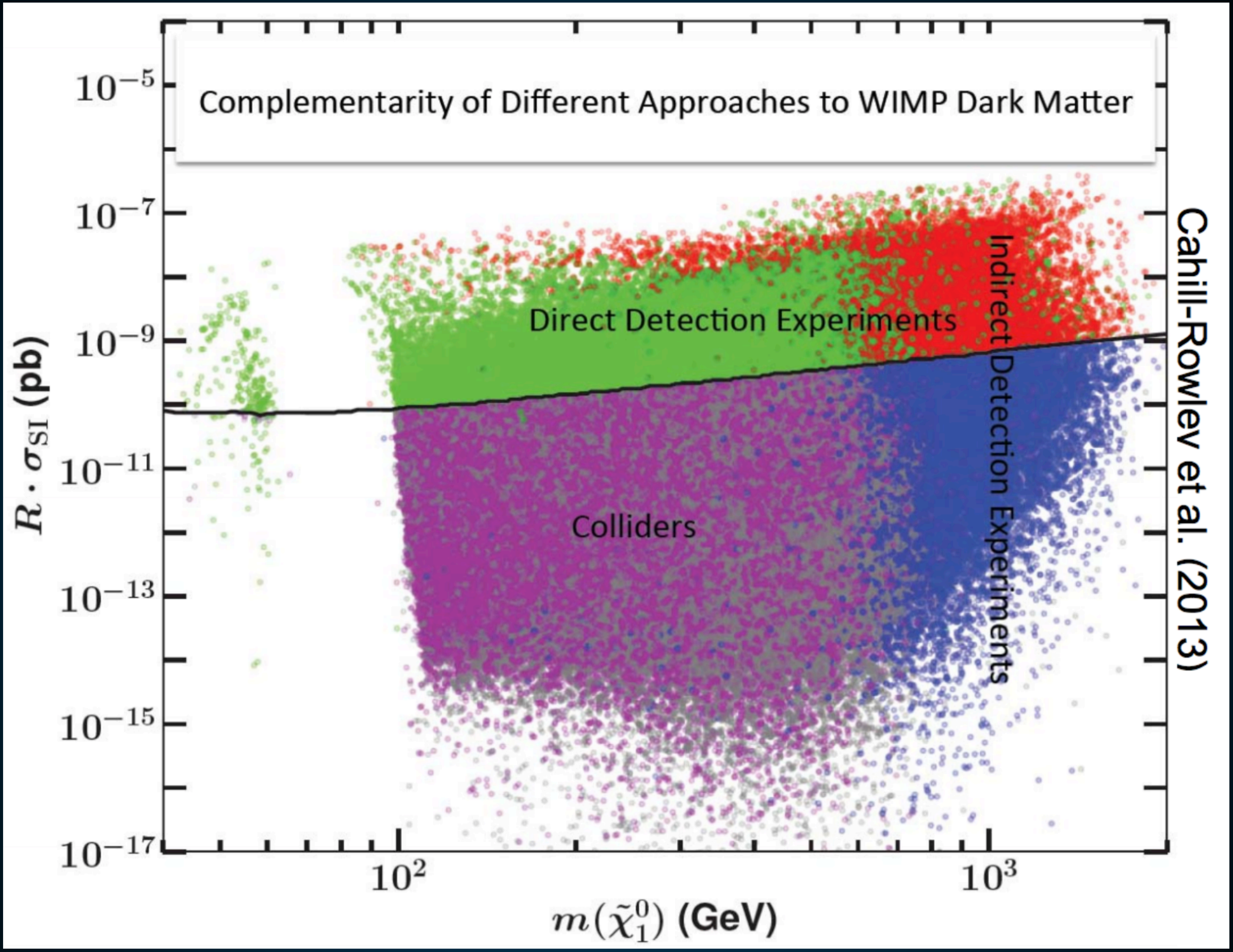

Dark Matter Complementarity

Gambit Collaboration (1705.07917)

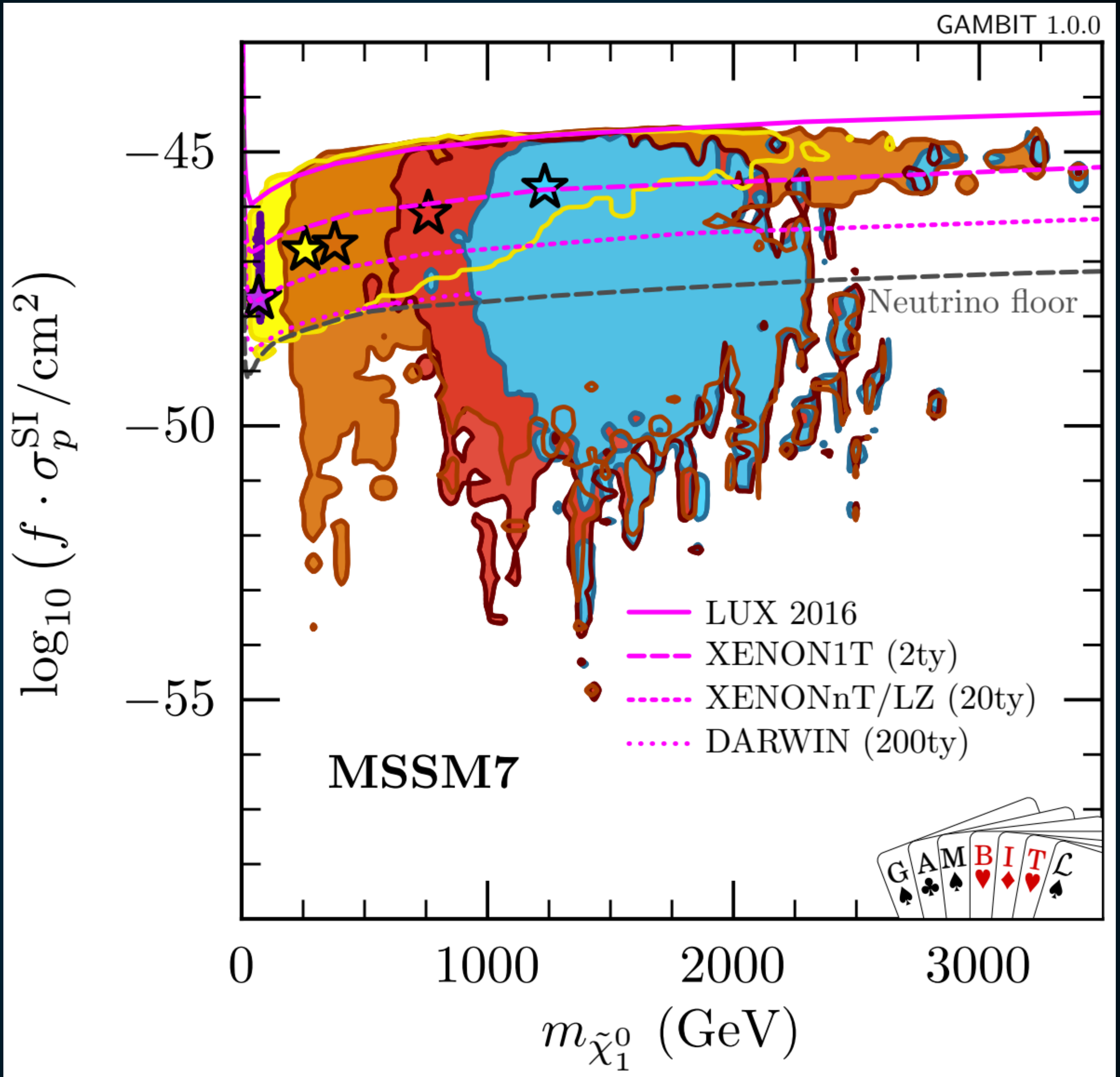

Why Indirect Detection?

$$\langle \sigma v \rangle \sim 10^{-8}\ \mathrm{GeV}^{-2}\left(3 \times 10^{-28}\ \mathrm{GeV}^2\ \mathrm{cm}^2\right)\ 10^{10}\ \frac{\mathrm{cm}}{\mathrm{s}} = 3 \times 10^{-26}\ \frac{\mathrm{cm}^3}{\mathrm{s}}$$

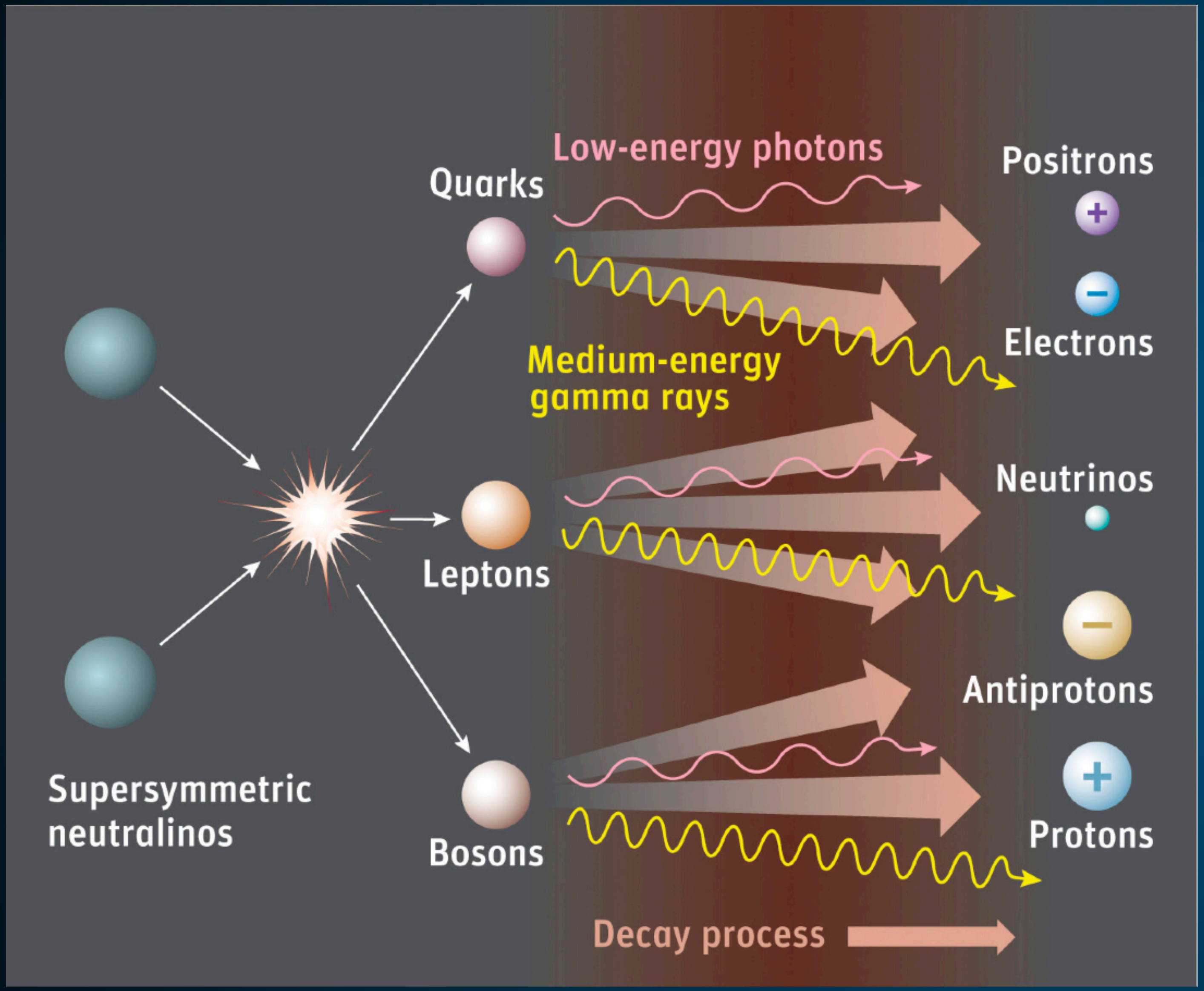

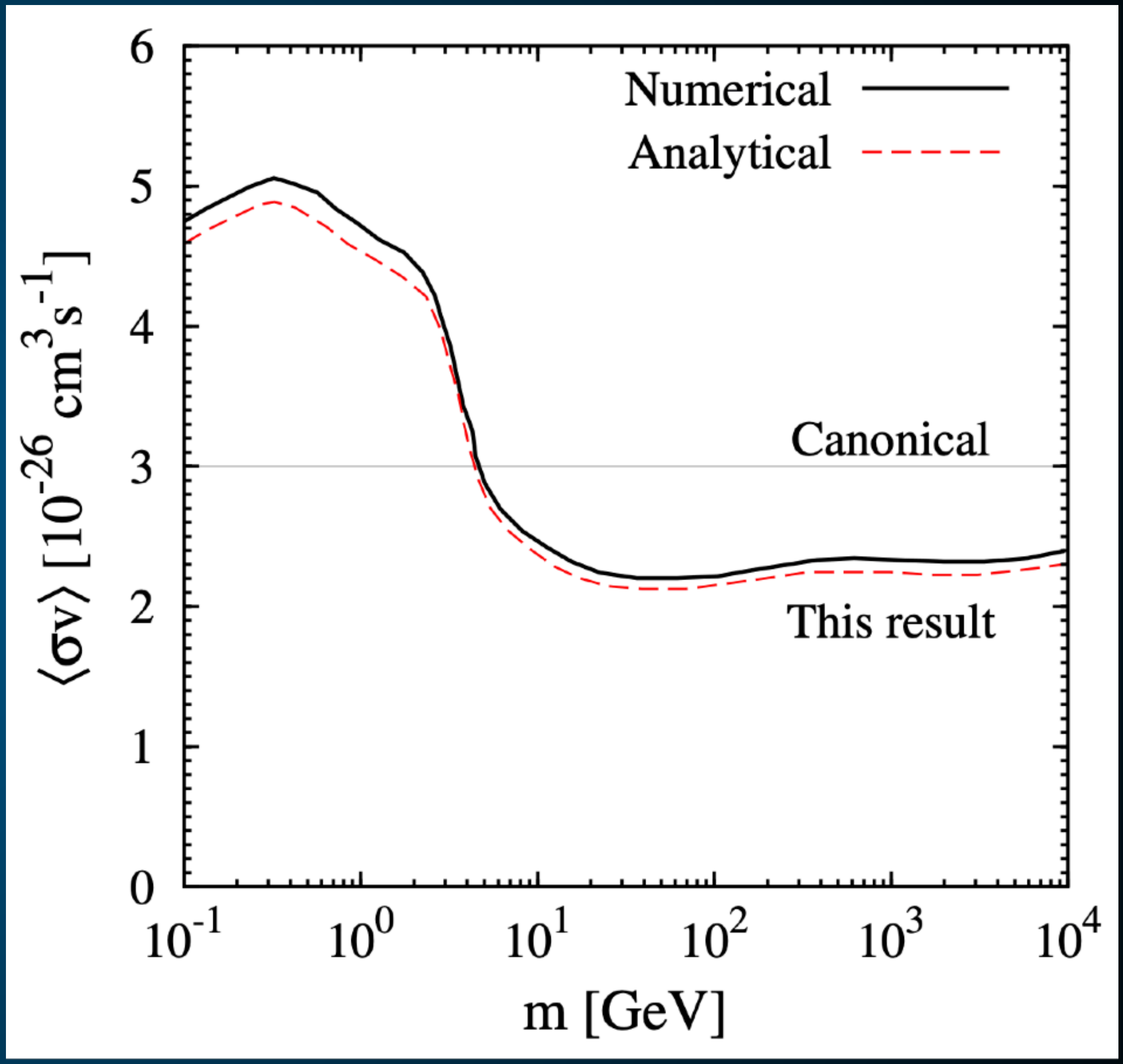

Steigman et al. (1204.3622)

Why Gamma-Rays?

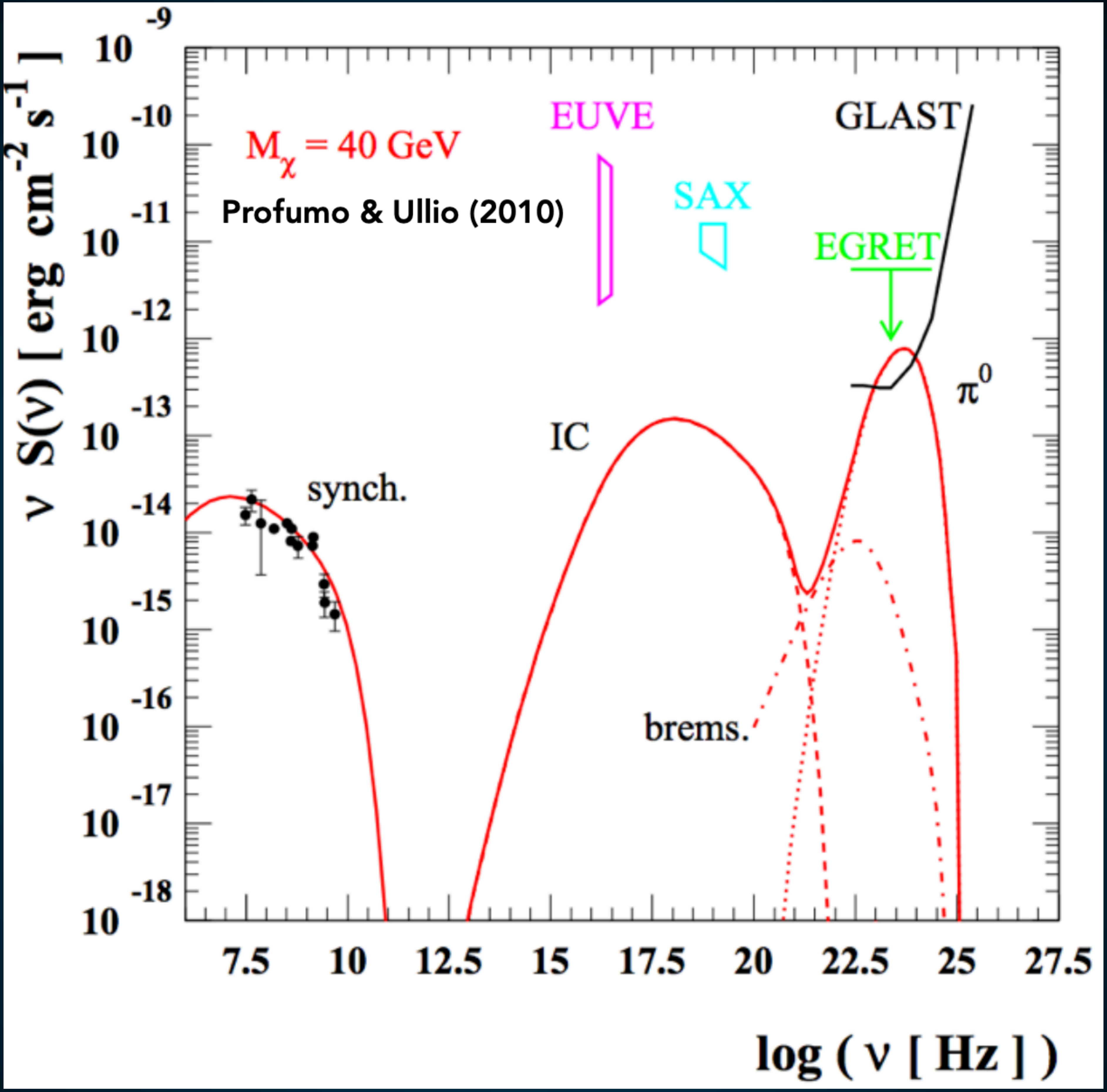

Why Gamma-Rays?

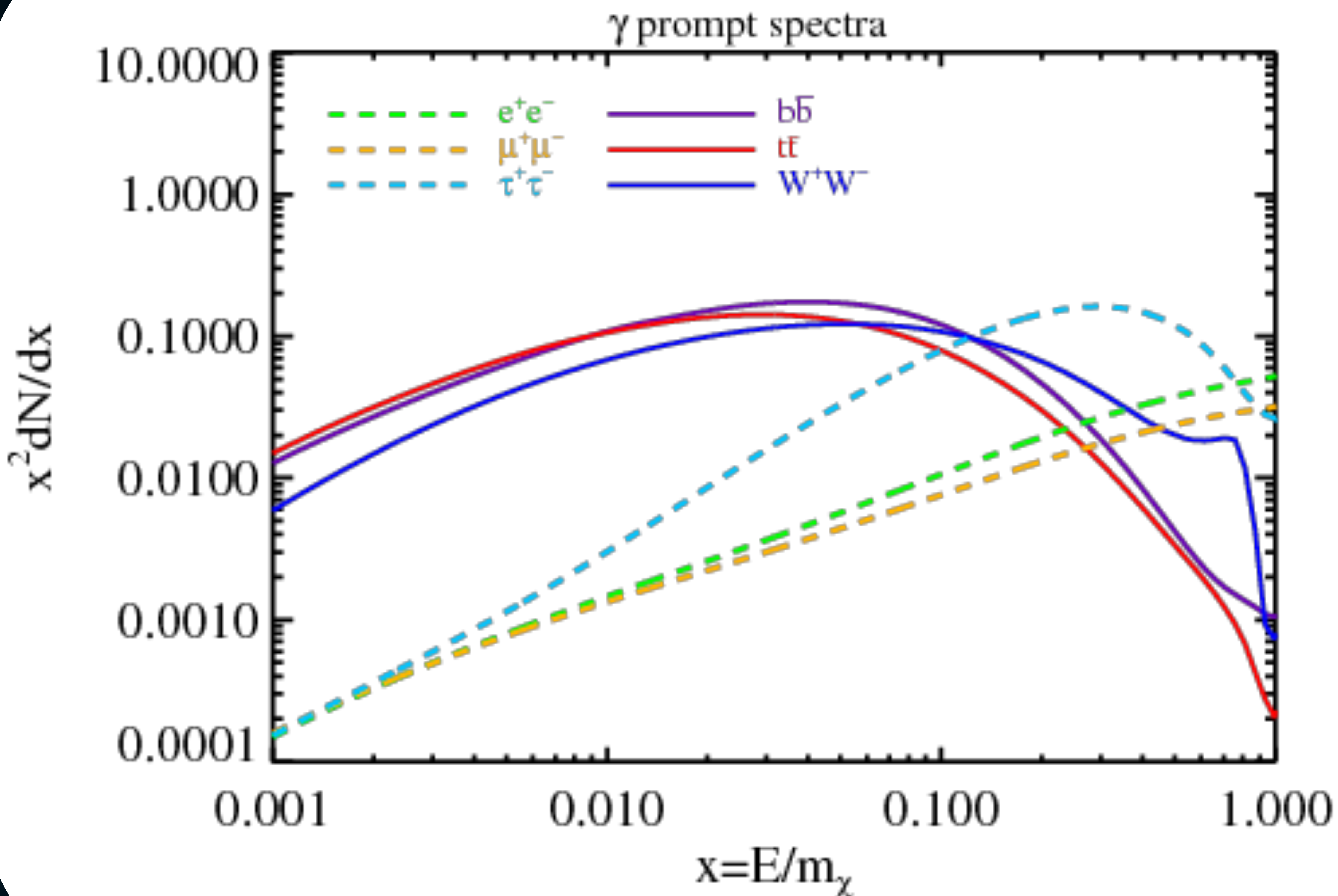

Why the Galactic Center?

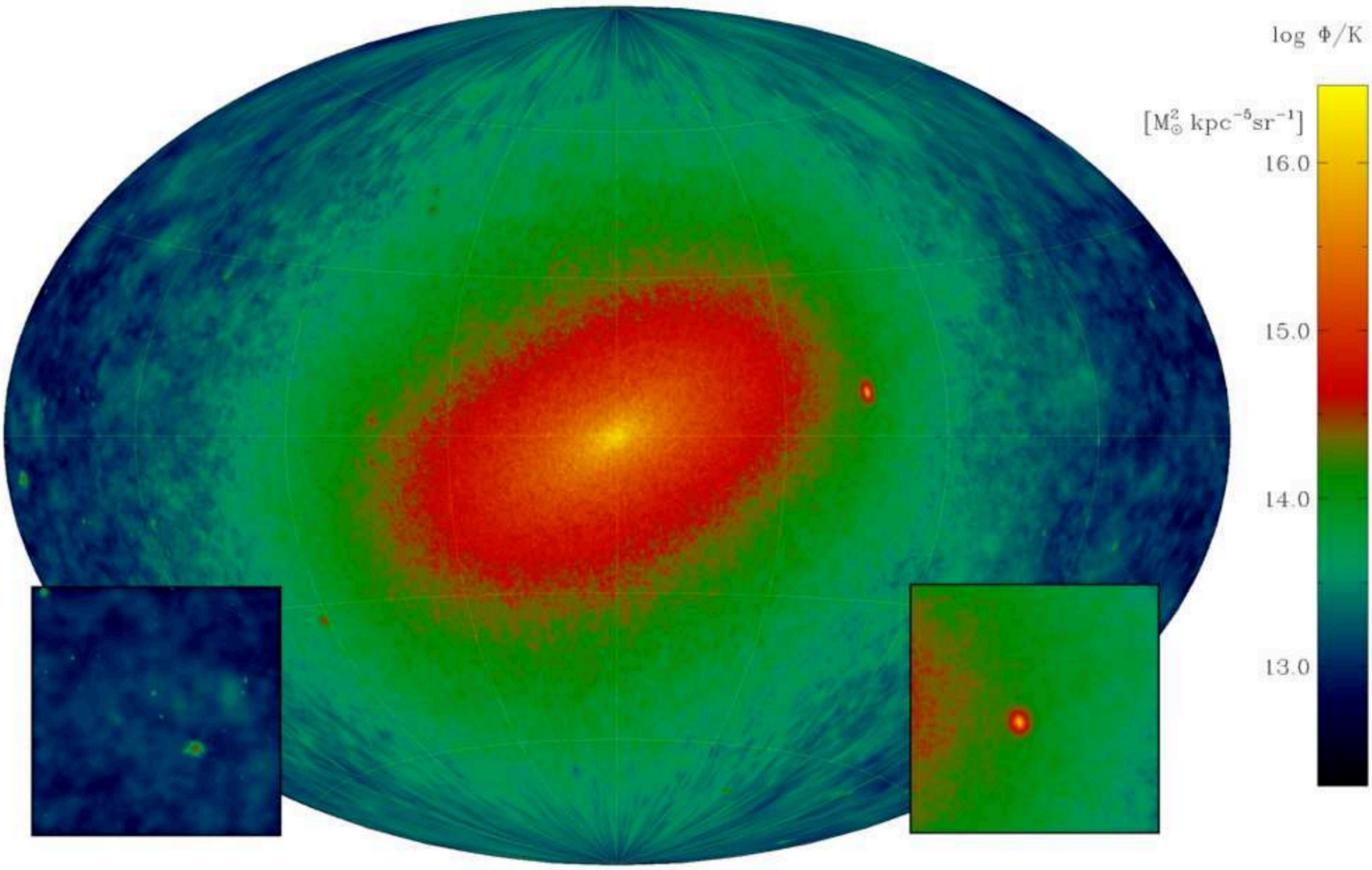

Why Indirect Detection?

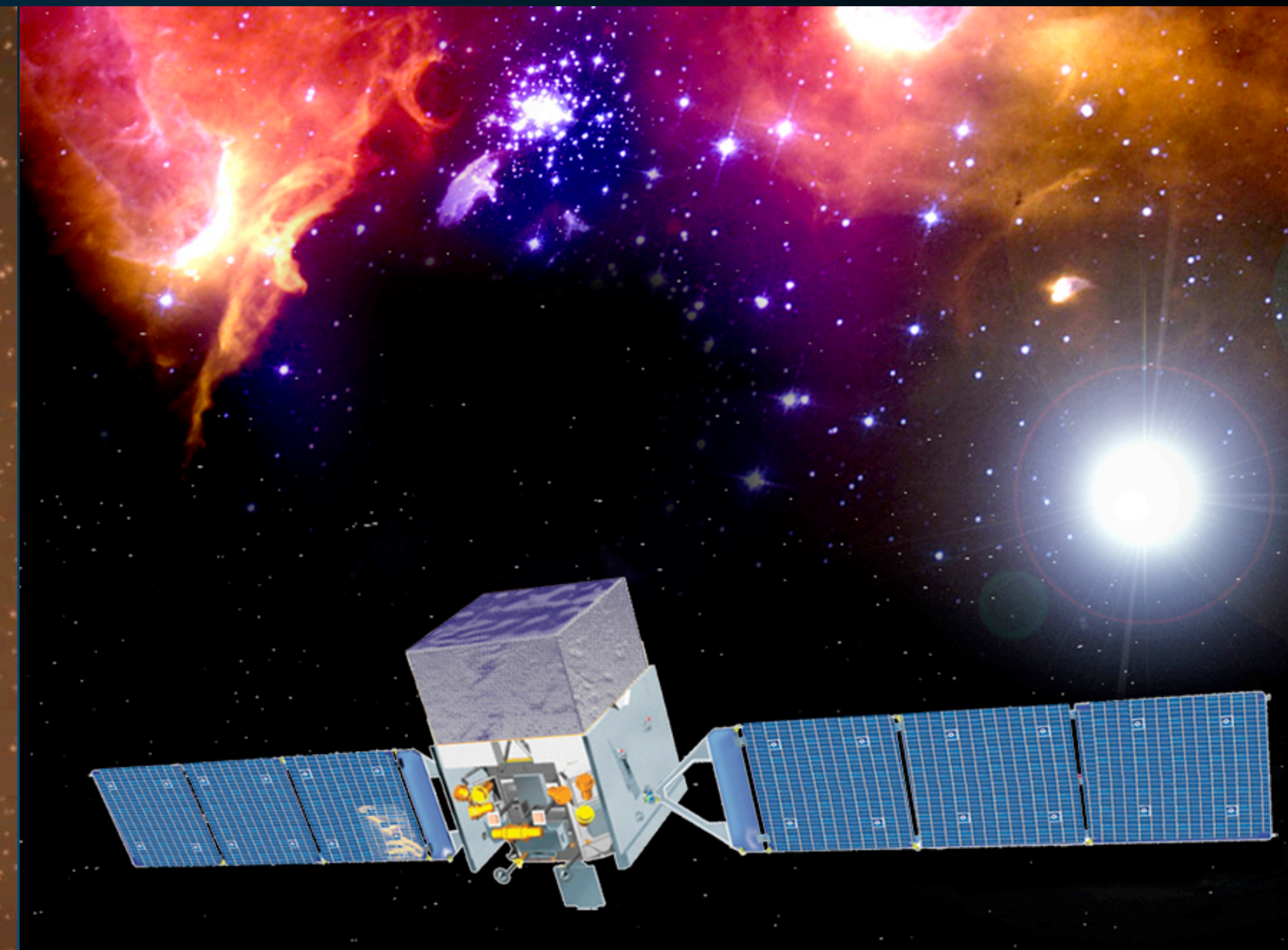

- **For a standard dark matter density profile, the annihilation rate within 5^{o} of the Galactic center is ~1×10^{38} ann s^{-1}.**

- **For a 1 m^{2} instrument, this produces a flux of 10^{-4} ann s^{-1}.**

A Startling Coincidence

- **Model:**
  - **100 GeV dark matter particle annihilates to bb**
  - **Annihilation Rate is Thermal Cross-Section**

- **Expected Galactic Center Flux (above 1 GeV):**
  - **2×10^{-11} erg cm^{-2} s^{-1}**

- **Observed Flux:**
  - **1×10^{-10} erg cm^{-2} s^{-1}**

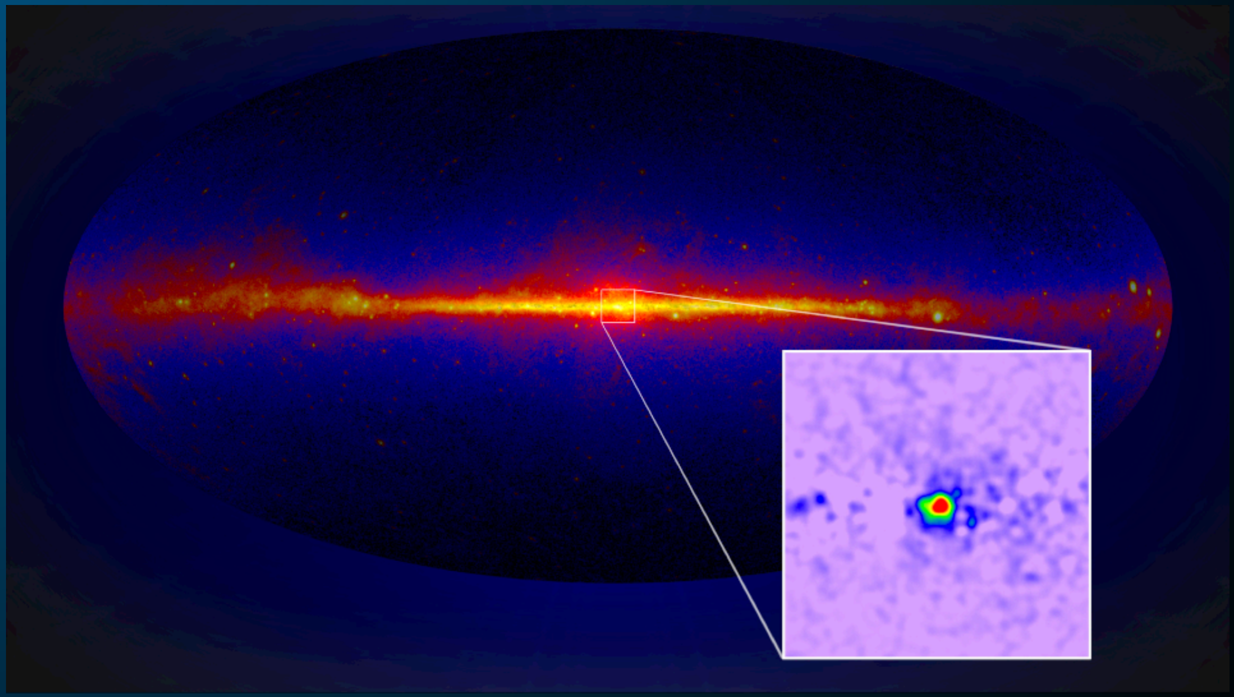

A Startling Coincidence

- **Model:**
  - **100 GeV dark matter particle annihilates to bb**
  - **Annihilation Rate is Thermal Cross-Section**
- **Expected Galactic Center Radio Flux:**
  - **2×10^{-13} erg cm^{-2} s^{-1}**
- **Observed Flux:**
  - **5×10^{-10} erg cm^{-2} s^{-1}**

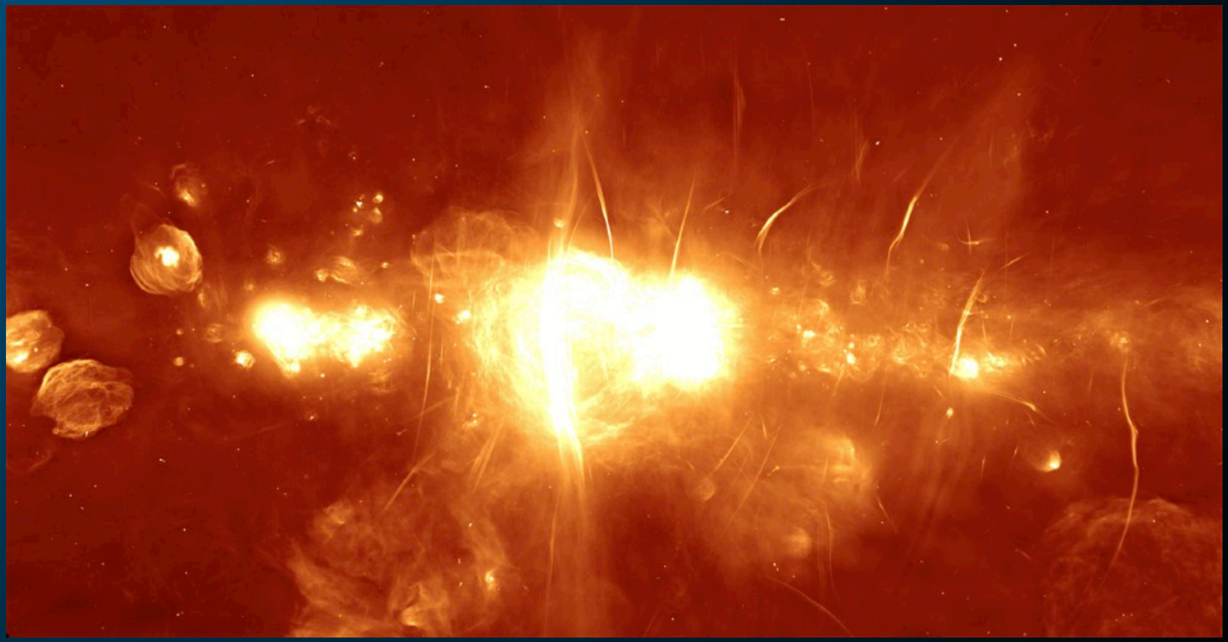

The Galactic Center is Complicated

- 400 pc x 80 pc
- 10^7 M_o of gas in Molecular Clouds
- Conditions similar to nearby starburst galaxies

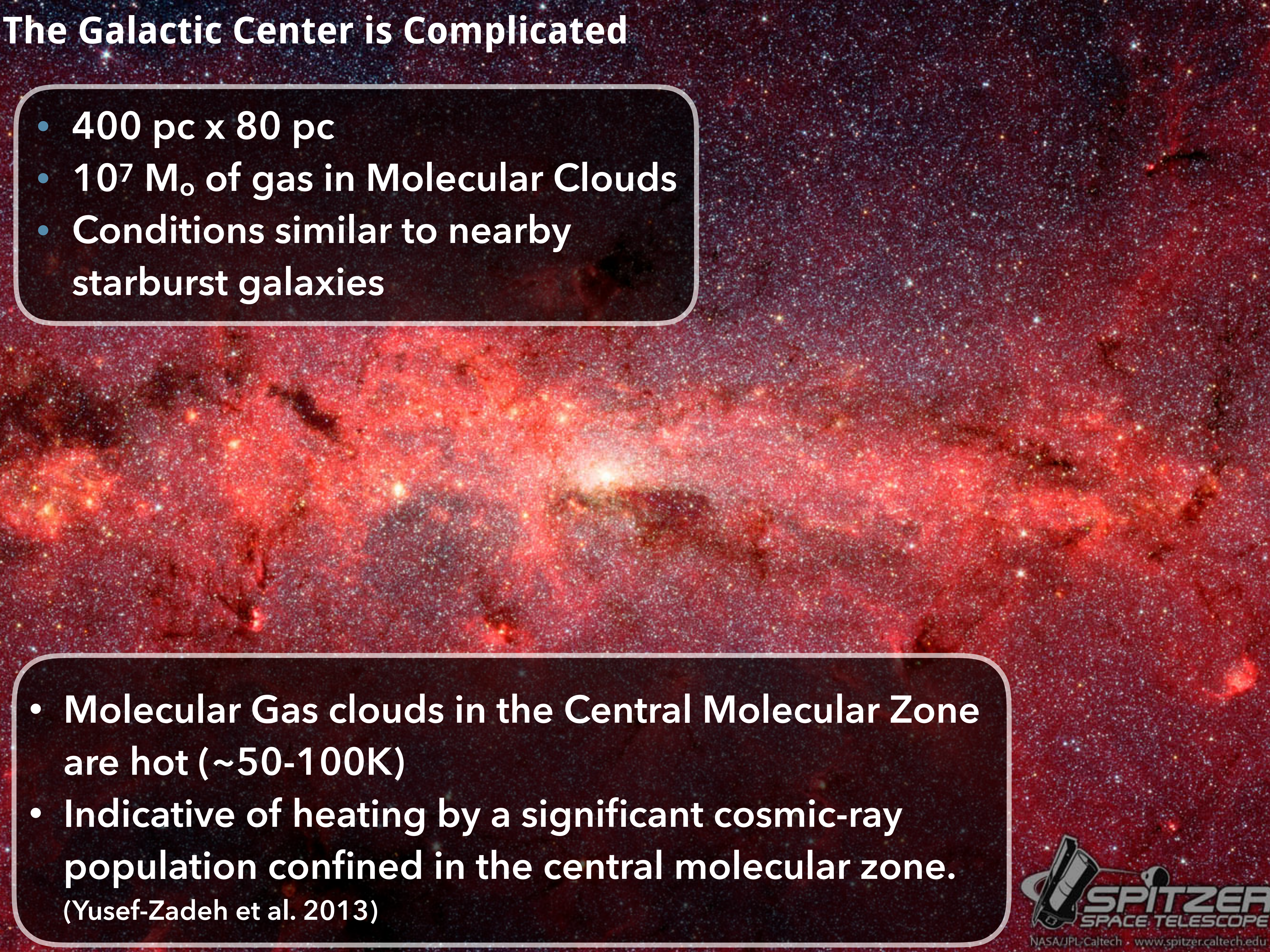

- Molecular Gas clouds in the Central Molecular Zone are hot (~50-100K)
- Indicative of heating by a significant cosmic-ray population confined in the central molecular zone.

(Yusef-Zadeh et al. 2013)

The Galactic Center is Complicated

Galactic Center is a dense star-forming environment.

3-20% of total Milky Way Star Formation

2-4% - ISOGAL Survey Immer et al. (2012)
2.5-5% - Young Stellar Objects Yusef-Zadeh et al. (2009)
5-10% - Infrared Flux Longmore et al. (2013)
10-20% - Wolf-Rayet Stars Rosslowe & Crowther (2014)
2% - Far-IR Flux Thompson et al. (2007)
2.5-6% - SN1a Schanne et al. (2007)

- **The Supernovae of these stars produce 10^{51} erg!**

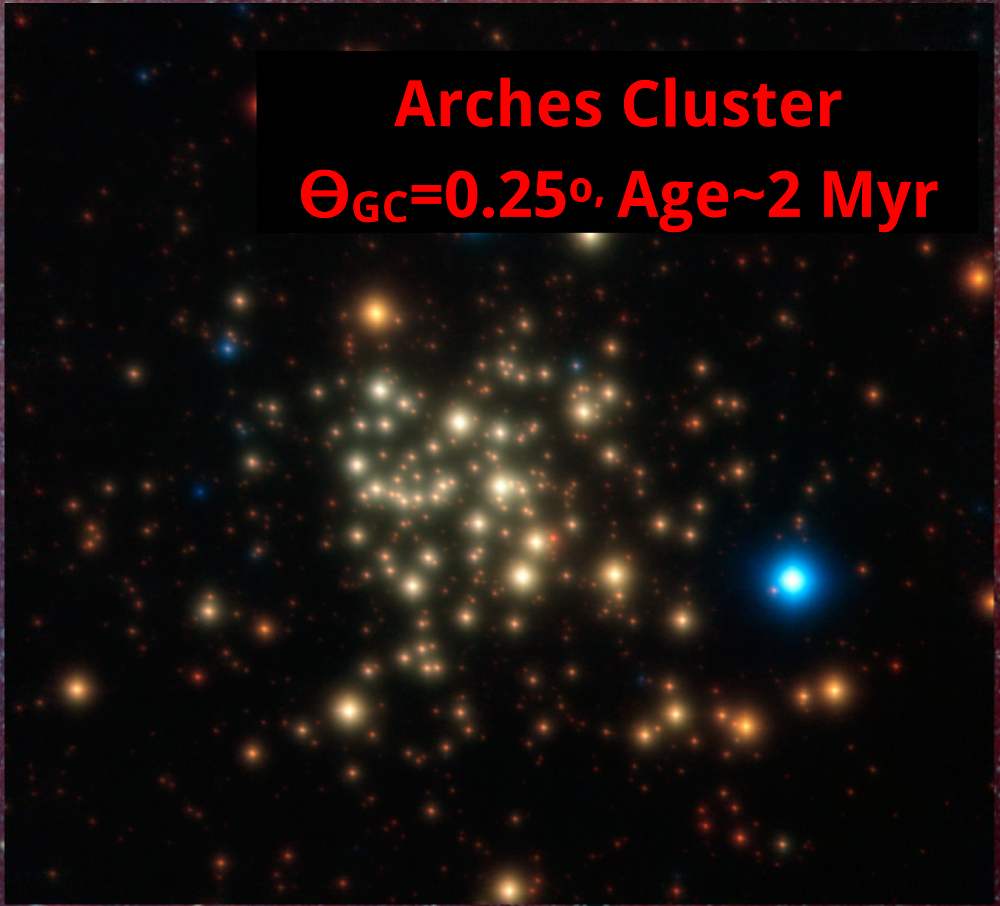

The Galactic Center is Complicated

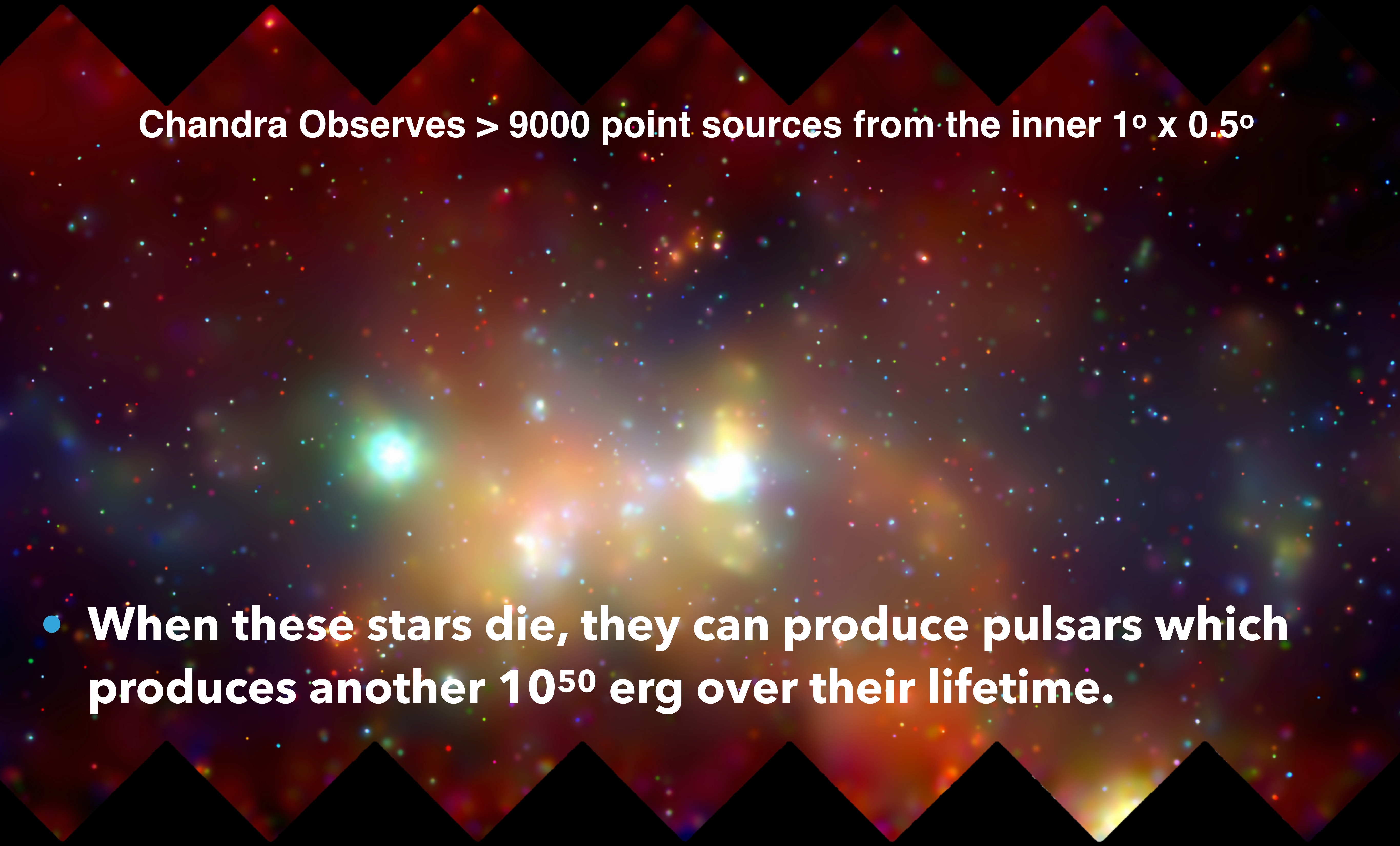

Chandra Observes > 9000 point sources from the inner 1° x 0.5°

- **When these stars die, they can produce pulsars which produces another 10^{50} erg over their lifetime.**

Galactic Center is a Bright Multi-Wavelength Source

Fermi Bubbles

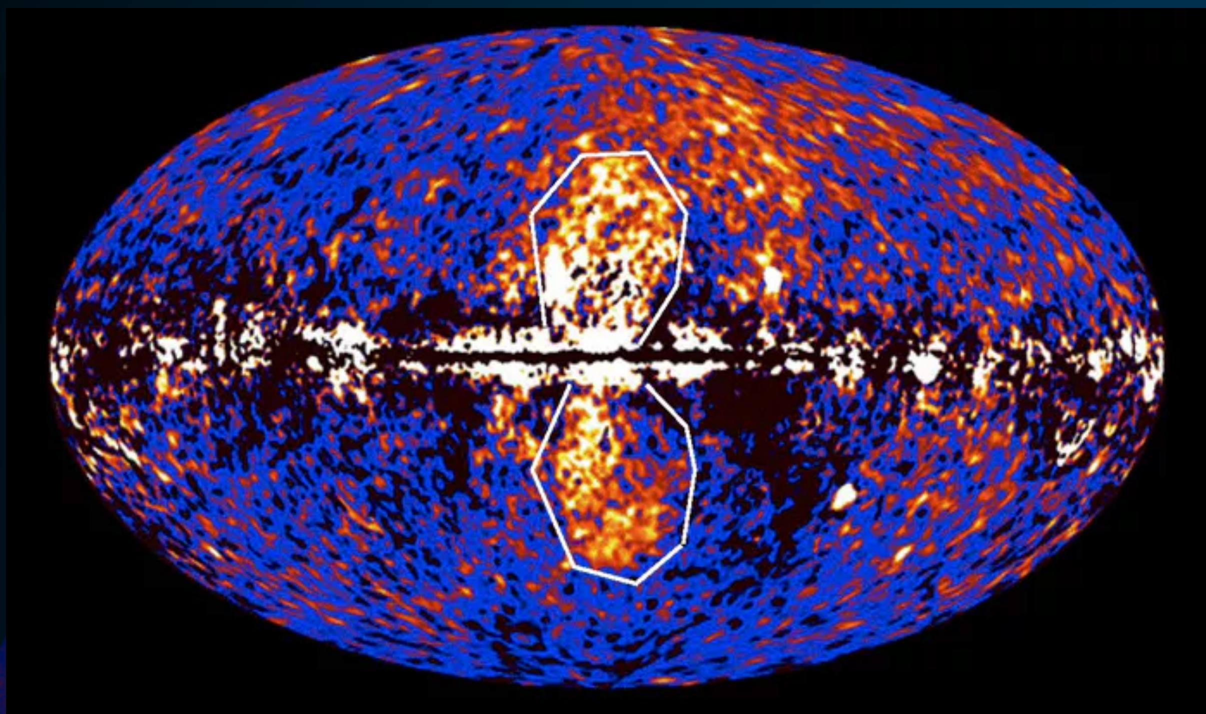

Integral 511 keV Excess

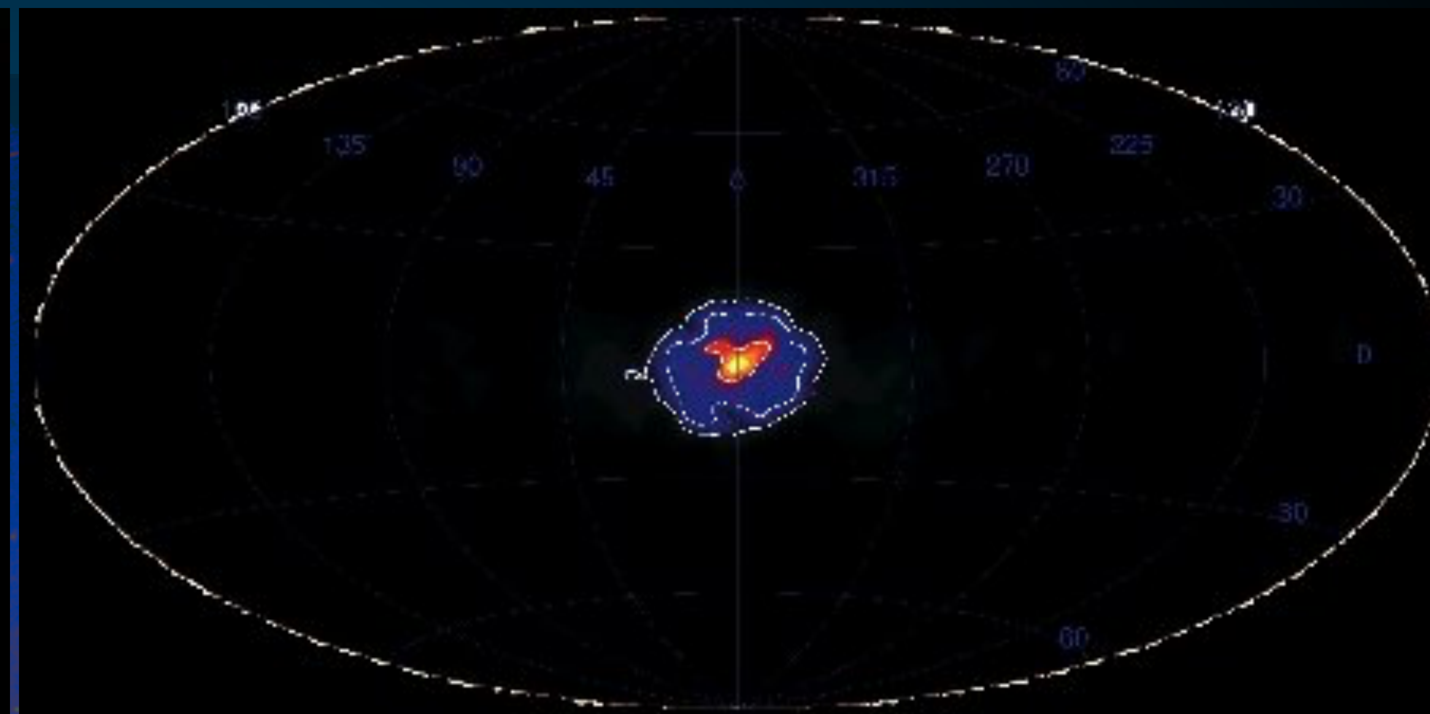

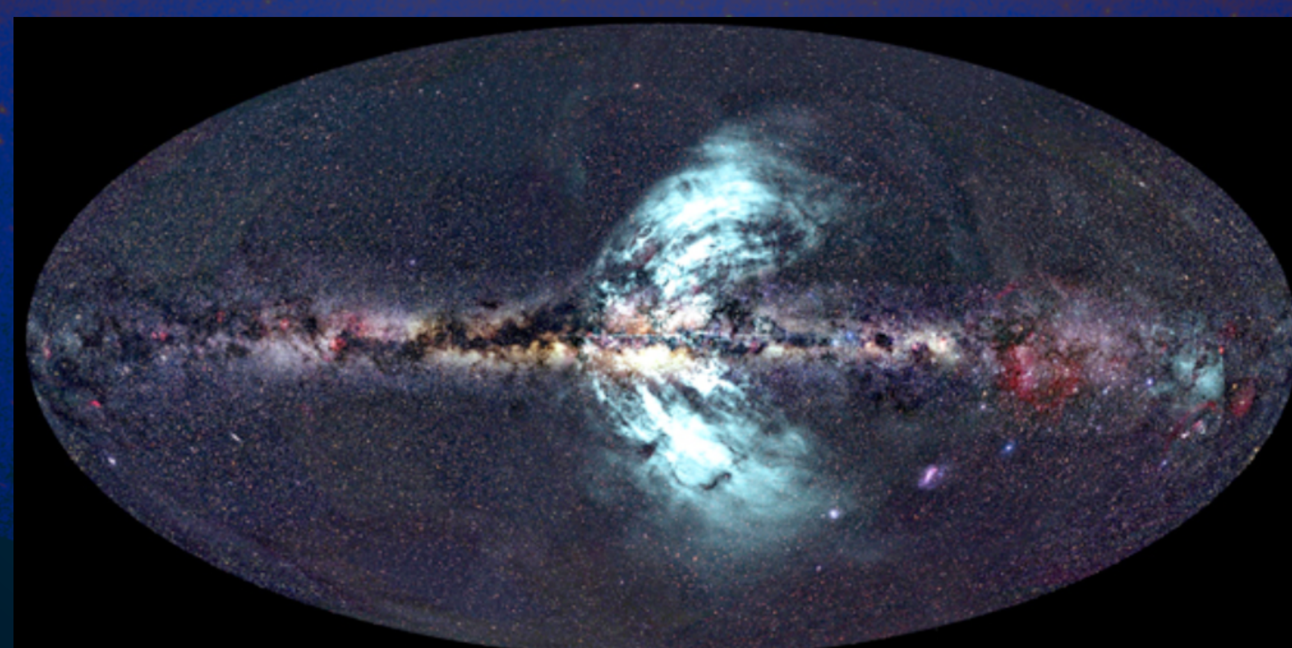

WMAP/PLANCK Haze

COSMIC-RAY ACCELERATION AND PROPAGATION

Start with a source of relativistic cosmic-rays

- Supernova Explosions
- Supernova Remnants
- Pulsars
- Shocks/Mergers

COSMIC-RAY ACCELERATION AND PROPAGATION

Start with a source of relativistic cosmic-rays

cosmic rays propagate

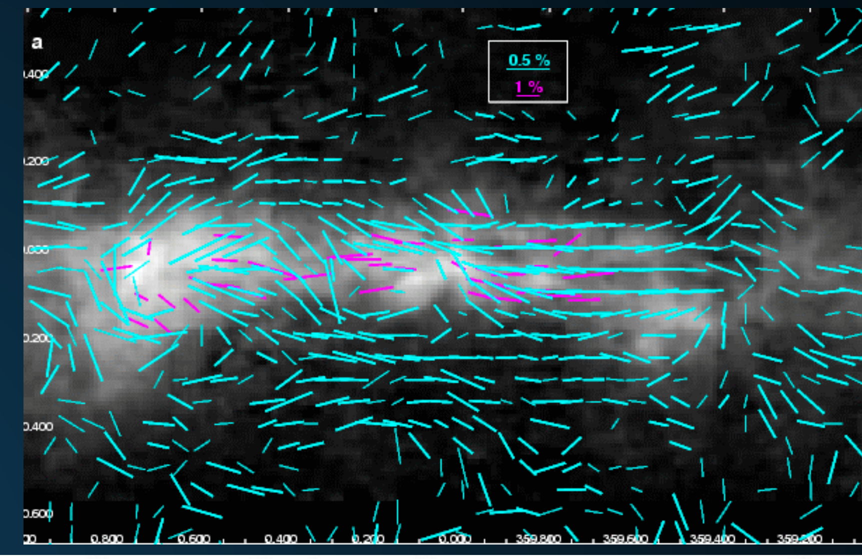

$$\frac{\partial \psi}{\partial t} = q(\vec{r},p) + \vec{\nabla}\cdot(D_{xx}\vec{\nabla}\psi - \vec{V}\psi) + \frac{\partial}{\partial p} p^2 D_{pp} \frac{\partial}{\partial p}\frac{1}{p^2}\psi - \frac{\partial}{\partial p}\left[\dot{p}\psi - \frac{p}{3}(\vec{\nabla}\cdot\vec{V})\psi\right] - \frac{1}{\tau_f}\psi - \frac{1}{\tau_r}\psi$$

Solved Numerically:
e.g. Galprop

- **If they propagate to Earth, can be detected:**
  - **AMS-02/PAMELA**
  - **CREAM/HEAT/CAPRICE**

COSMIC-RAY ACCELERATION AND PROPAGATION

Start with a source of relativistic cosmic-rays

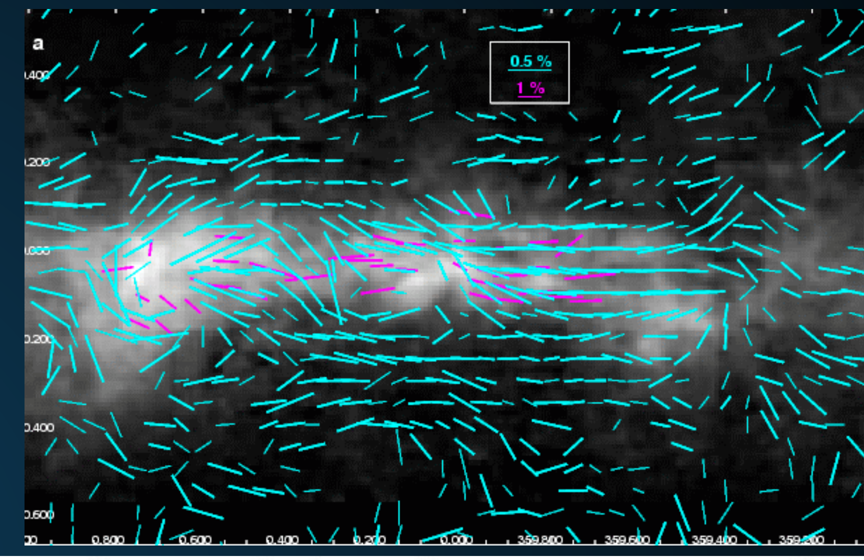

cosmic rays propagate

$$\frac{\partial \psi}{\partial t} = q(\vec{r},p) + \vec{\nabla}\cdot(D_{xx}\vec{\nabla}\psi - \vec{V}\psi) + \frac{\partial}{\partial p}p^2 D_{pp}\frac{\partial}{\partial p}\frac{1}{p^2}\psi - \frac{\partial}{\partial p}\left[\dot{p}\psi - \frac{p}{3}(\vec{\nabla}\cdot\vec{V})\psi\right] - \frac{1}{\tau_f}\psi - \frac{1}{\tau_r}\psi$$

Solved Numerically:
e.g. Galprop

Gas/ISRF

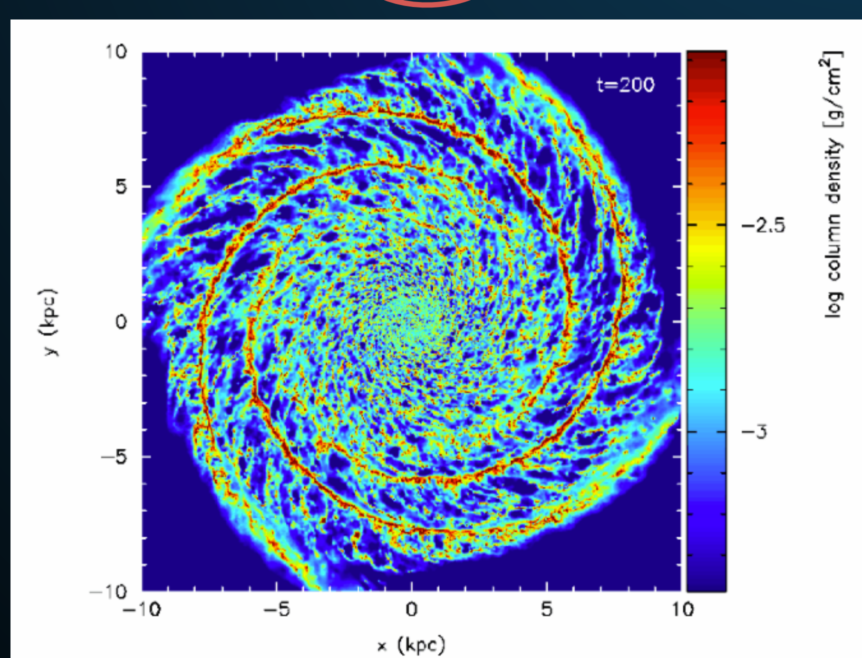

- **Alternatively can collide with Galactic gas or the interstellar radiation field.**

COSMIC-RAY ACCELERATION AND PROPAGATION

Start with a source of relativistic cosmic-rays

cosmic rays propagate

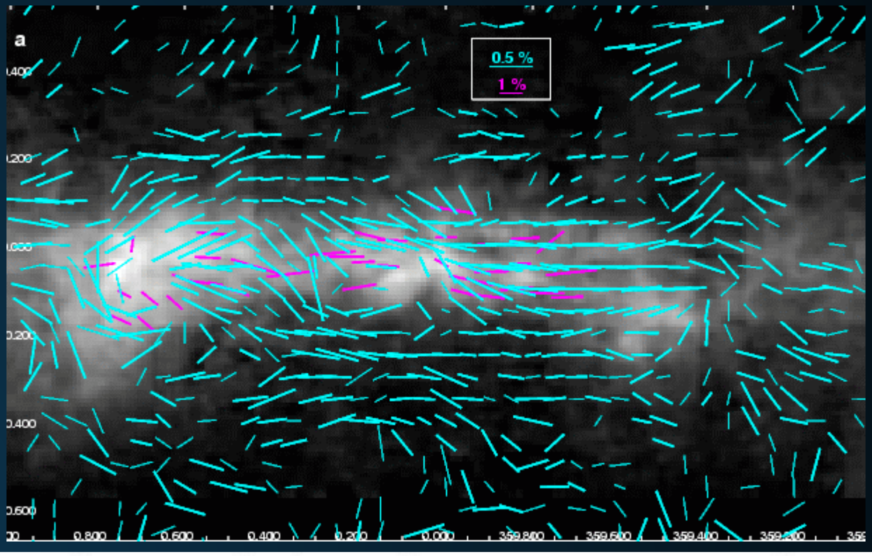

$$\frac{\partial \psi}{\partial t} = q(\vec{r},p) + \vec{\nabla}\cdot(D_{xx}\vec{\nabla}\psi - \vec{V}\psi) + \frac{\partial}{\partial p}p^2 D_{pp}\frac{\partial}{\partial p}\frac{1}{p^2}\psi - \frac{\partial}{\partial p}\left[\dot{p}\psi - \frac{p}{3}(\vec{\nabla}\cdot\vec{V})\psi\right] - \frac{1}{\tau_f}\psi - \frac{1}{\tau_r}\psi$$

Solved Numerically:
e.g. Galprop

Gas/ISRF

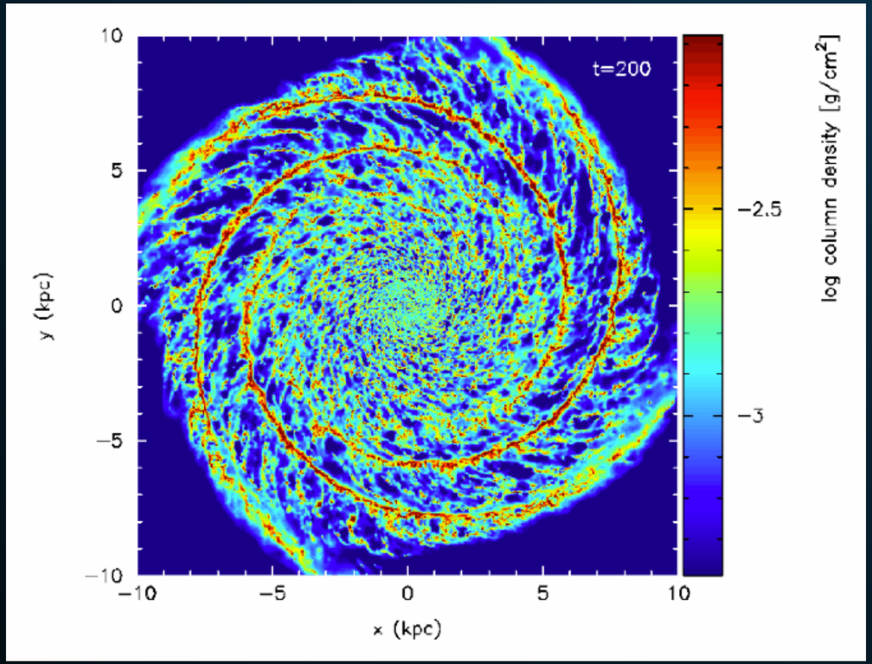

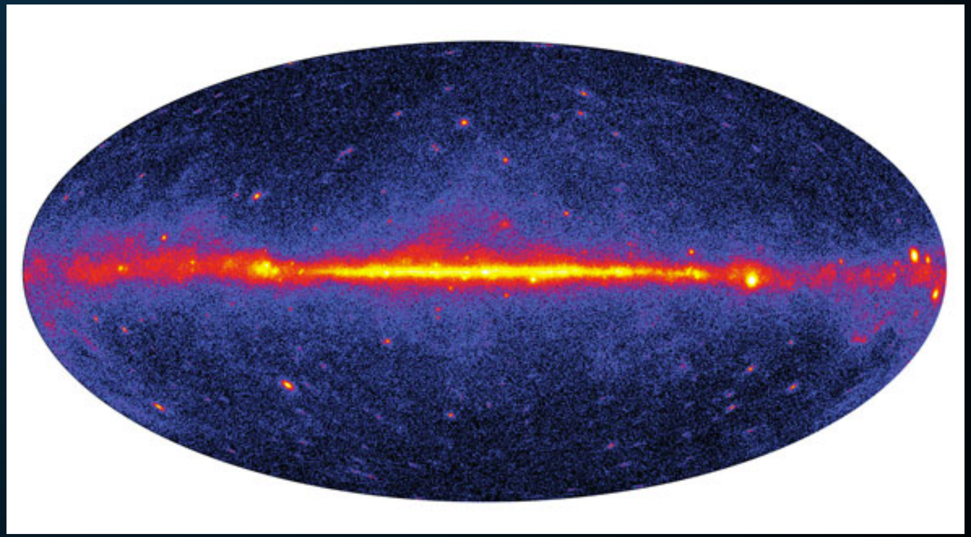

Energetic Arguments Fail

A Startling Coincidence

- **Model:**
  - **100 GeV dark matter particle annihilates to bb**
  - **Annihilation Rate is Thermal Cross-Section**
- **Expected Galactic Center Flux (above 1 GeV):**
  - **2×10^{-11} erg cm^{-2} s^{-1}**
- **Observed Flux:**
  - **1×10^{-10} erg cm^{-2} s^{-1}**

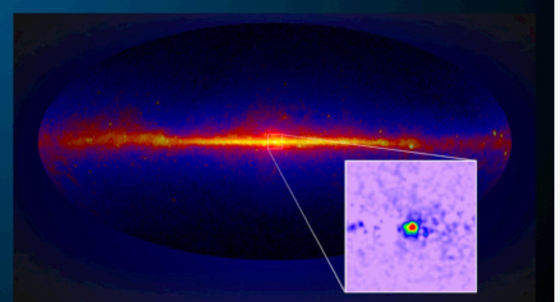

Supernovae:

A Supernovae produces ~10^{51} erg of energy.

~10% to CR protons.

Assuming 1 Galactic center SN every 250 years (10% the Galactic Rate), this provides an energy flux of 1.3×10^{40} erg s^{-1}.

If these cosmic-rays are trapped for 10 kyr in a 100 pc box ($D_0 = 5 \times 10^{28}$ cm^2 s-1), filled with Hydrogen gas at density 100 cm^{-2}, this will produce a total gamma-ray emission:

$$6.7 \times 10^{37} \text{ erg s}^{-1}$$ ✔

Energetic Arguments Fail

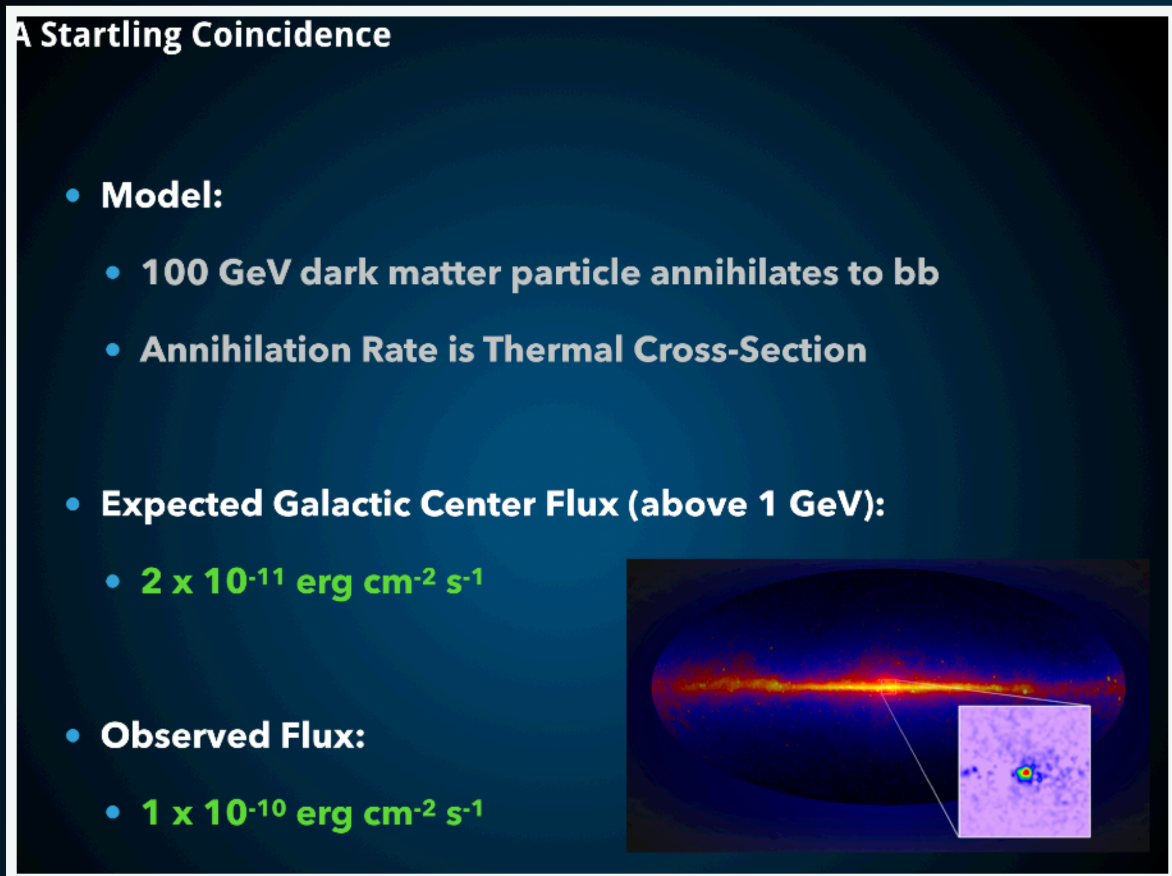

Sgr A*:

A tidal disruption event releases ~10^{45} erg s^{-1} for a period of ~0.2 yr.

Sgr A* is expected to produce a tidal disruption event every ~10^5 yr, producing a time-averaged energy output of 2 x 10^{39} erg s^{-1}.

If these CRs are primarily leptonic, and the electrons remain trapped in a region with a 40 eV cm^{-3} ISRF and a 200 μG magnetic field the gamma-ray flux from inverse Compton scattering is:

$$7.0 \times 10^{37} \text{ erg s}^{-1}$$ ✔

Energetic Arguments Fail

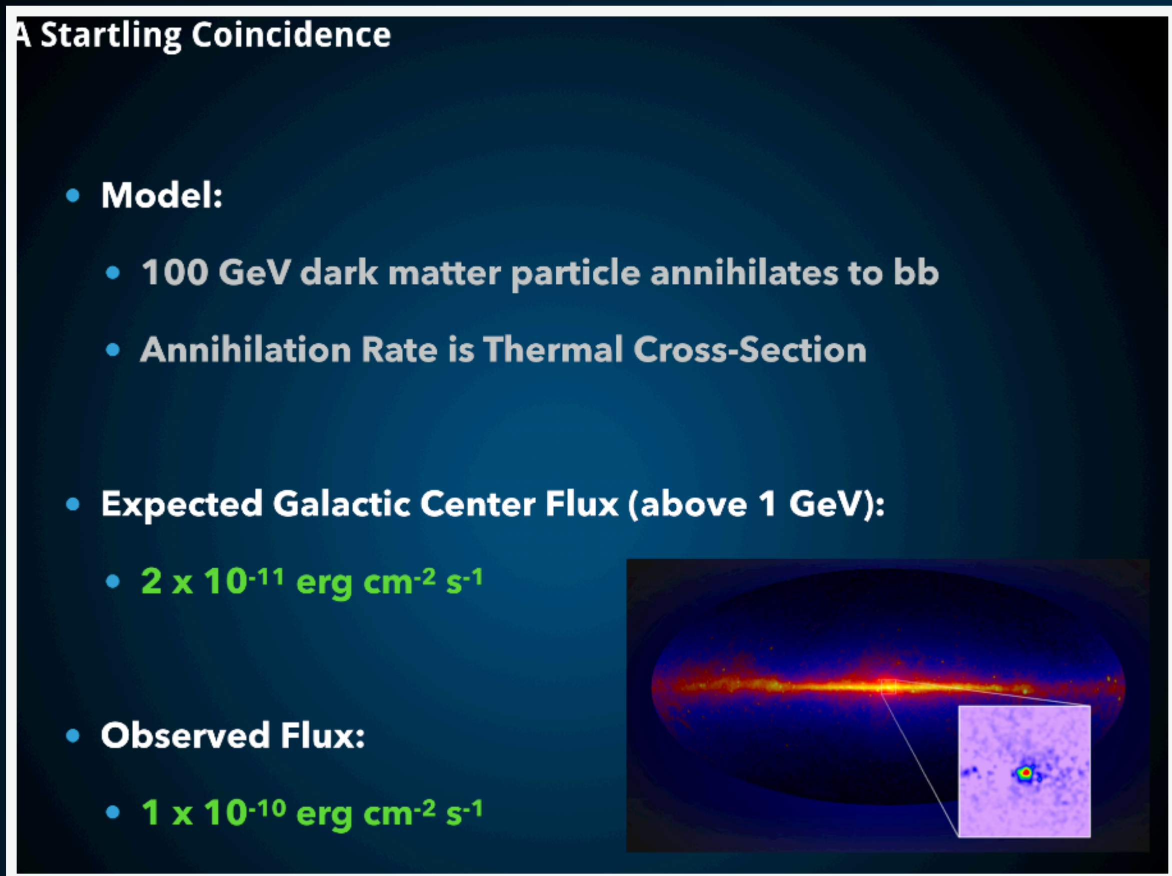

Pulsars

MSPs observed in the galactic field are fit by a population with a mean gamma-ray flux of 3 x 10^{34} erg s^{-1}. (Hooper & Mohlabeng 2015)

Given the population of 129 MSPs among 124 globular clusters (with a total stellar mass ~5 x 10^{7} M_o). For the 1 x 10^{9} M_o of stars formed in the inner degree of the Milky Way, we get:

7.7 x 10^{37} erg s^{-1} ✔

Energetic Arguments Fail

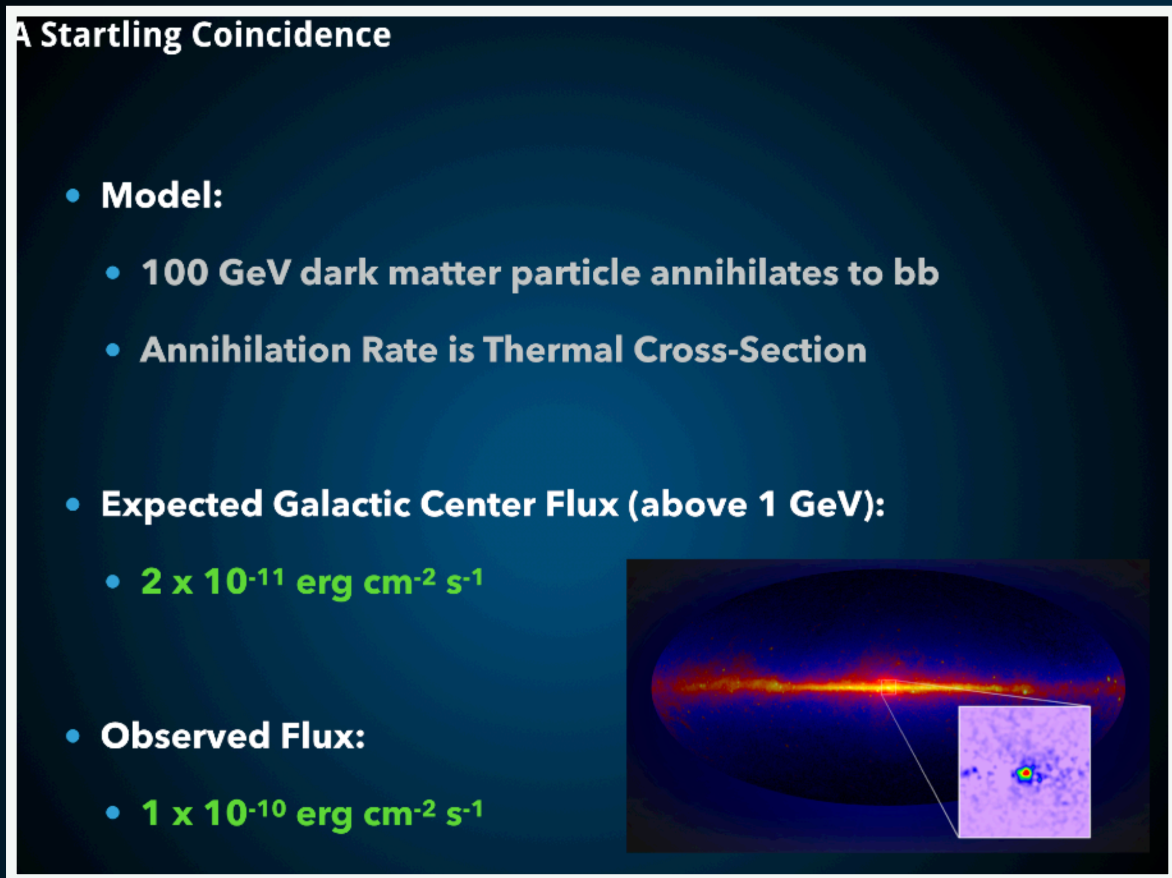

Dark Matter

For a 35 GeV dark matter particle annihilating at the thermal cross-section to bb, and a slightly adiabatically contracted $r^{-1.35}$ density profile.

The dark matter annihilation rate is 8.6 x 10^{38} ann s^{-1}, which produces a gamma-ray flux of:

$$6.9 \times 10^{36} \text{ erg s}^{-1}$$ ✔

Two Regions of Interest

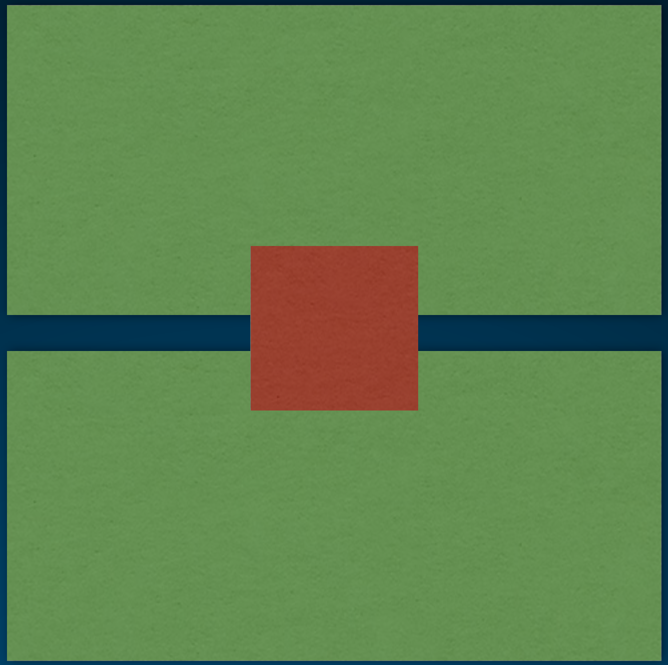

INNER GALAXY

- Mask galactic plane (e.g. $|b| > 1^{o}$), and consider 40^{o} x 40^{o} box
- Bright point sources masked at 2^{o}
- Use likelihood analysis, allowing the diffuse templates to float in each energy bin
- Background systematics controlled

GALACTIC CENTER

- Box around the GC (10^{o} x 10^{o})
- Include and model all point sources
- Use likelihood analysis to calculate the spectrum and intensity of each source
- Bright Signal

Conclusion:
Every Model is Correct

Is this (theorist) heaven?

or is this hell?

A Template Based Model

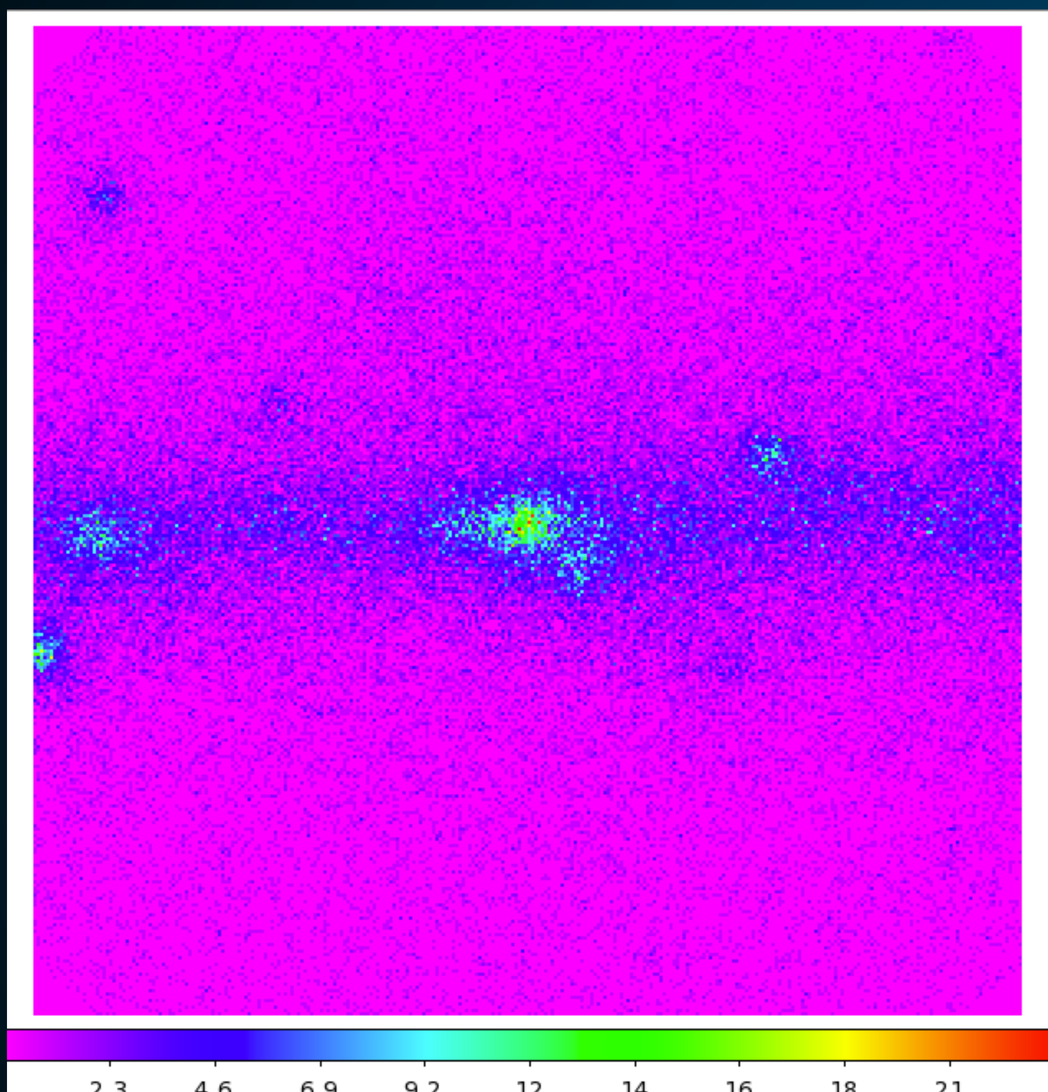

Data

750 — 950 MeV

Best Angular Resolution Cut

10º x 10º ROI

=

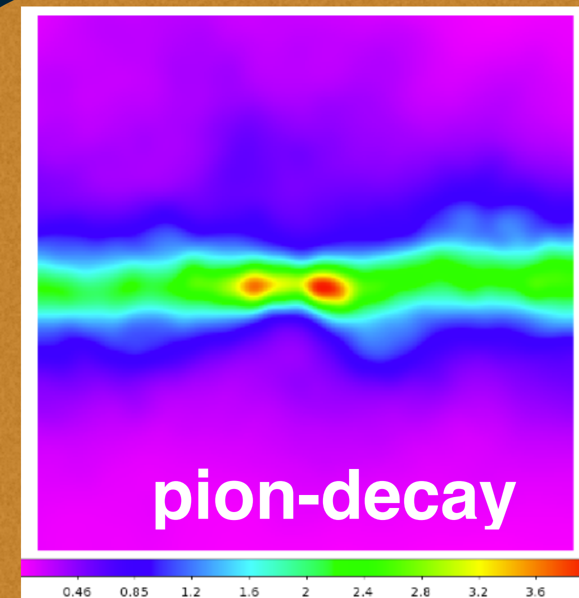

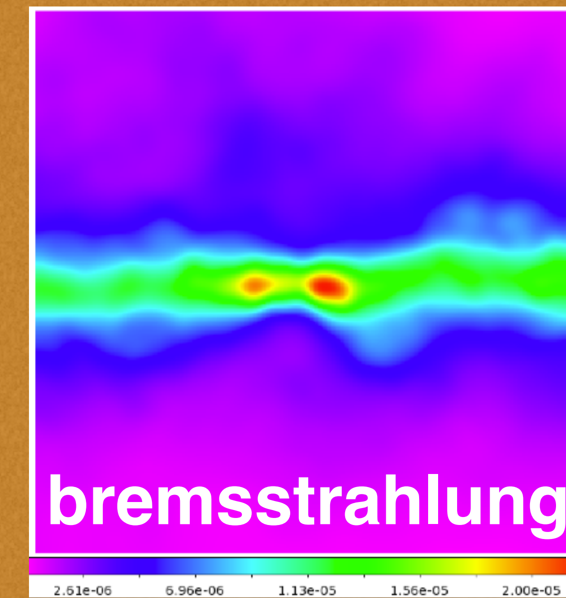

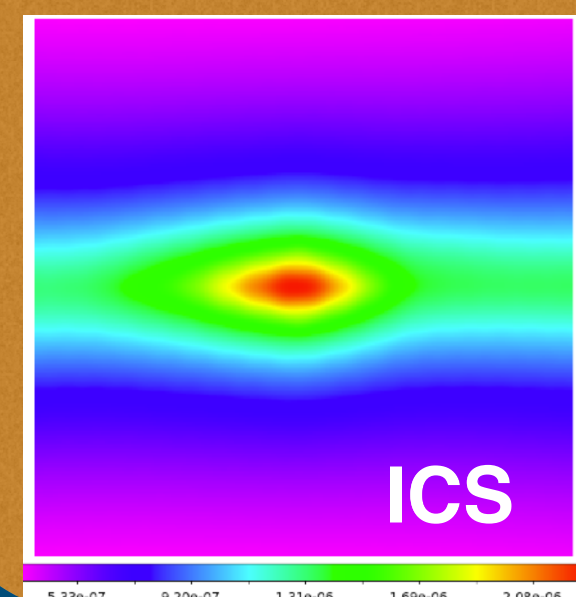

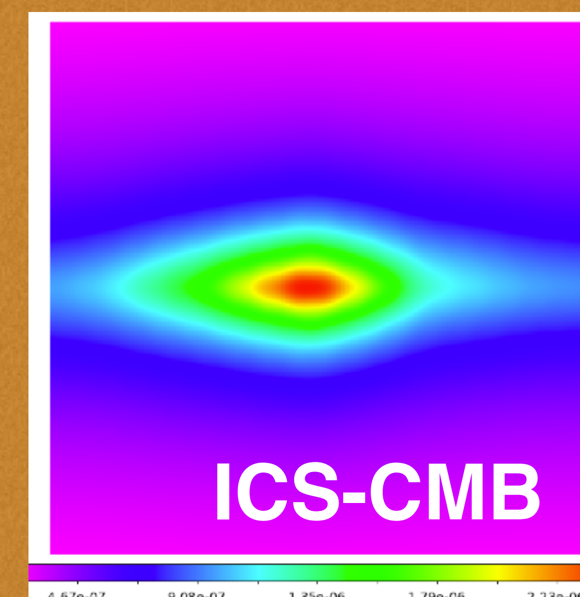

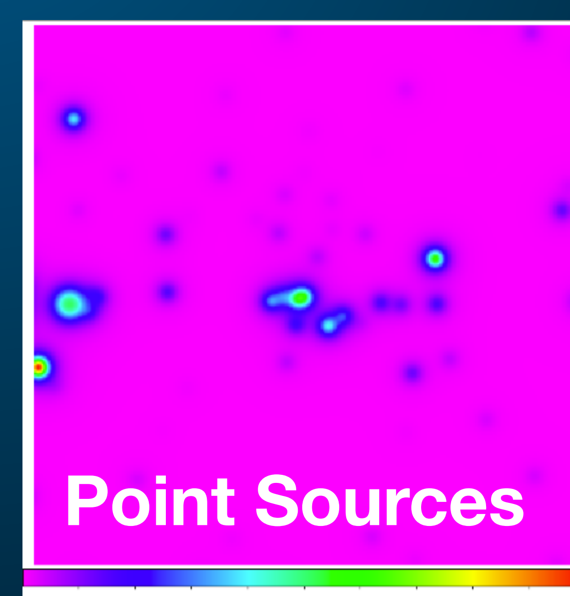

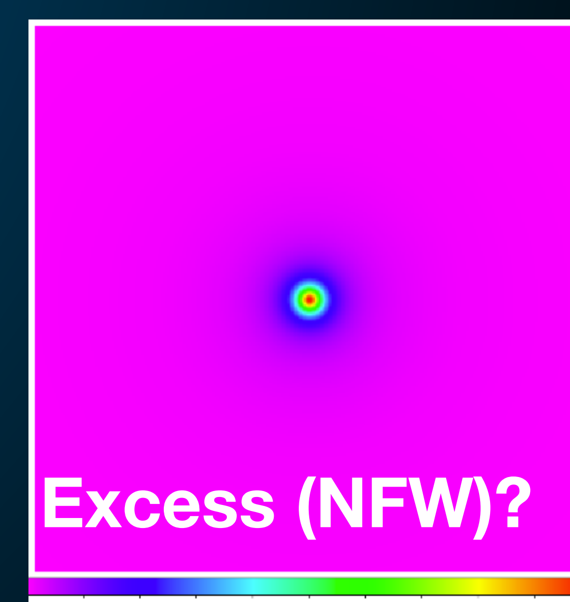

An Excess!

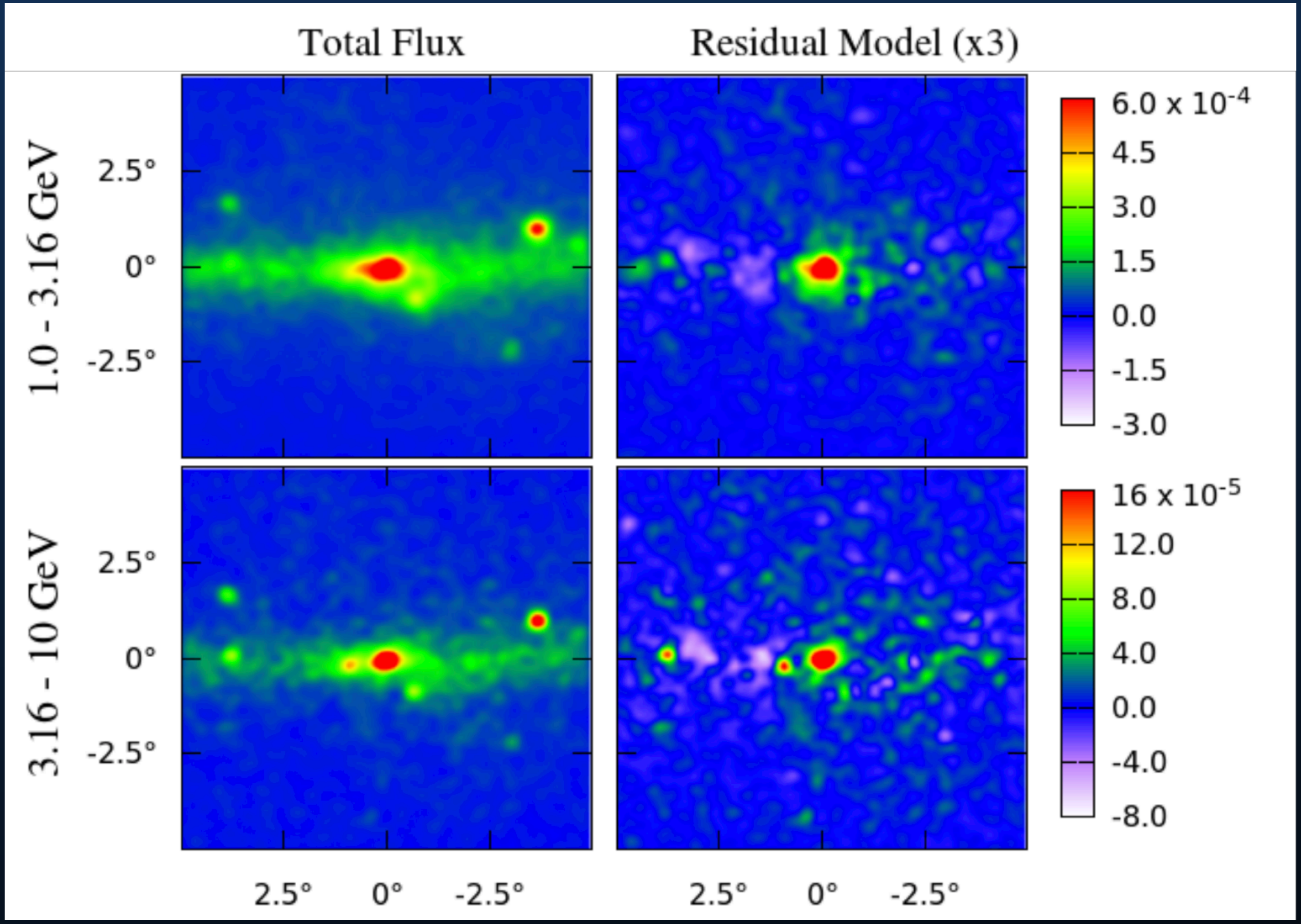

<u>There are four resilient features of the GeV Excess:</u>

1.) High Luminosity of ~2×10^{37} erg s^{-1}

An Excess!

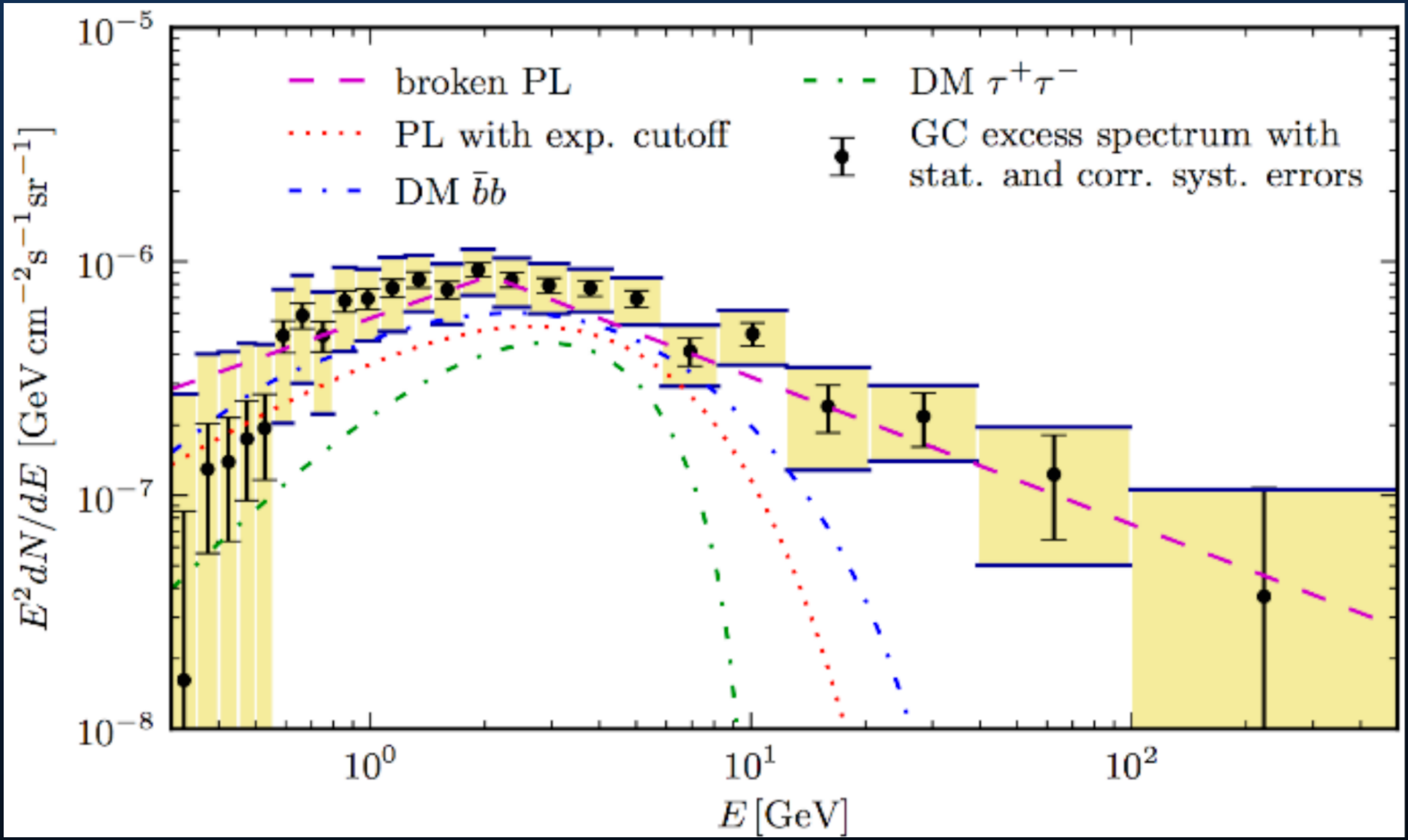

There are four resilient features of the GeV Excess:

2.) A hard gamma-ray spectrum peaking at ~2 GeV.

An Excess!

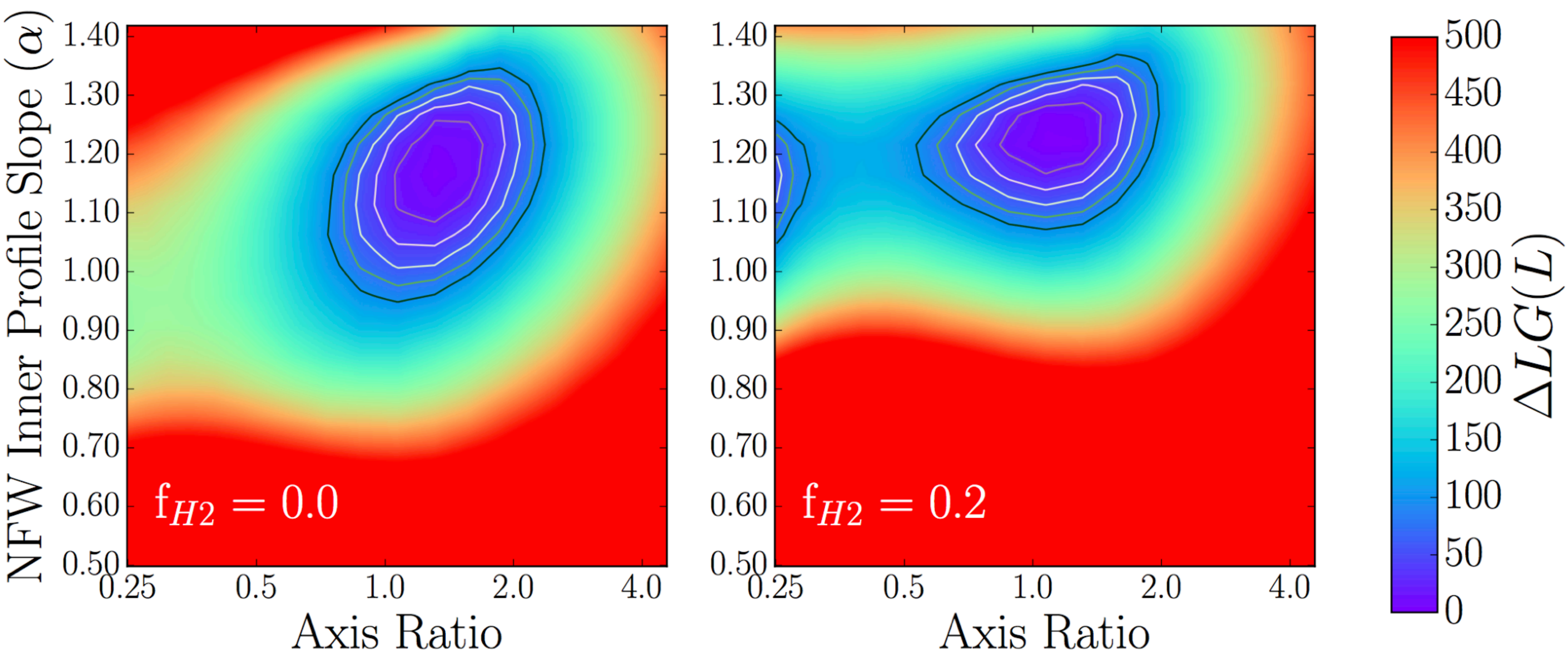

<u>There are four resilient features of the GeV Excess:</u>

3.) A roughly spherically symmetric emission morphology.

An Excess!

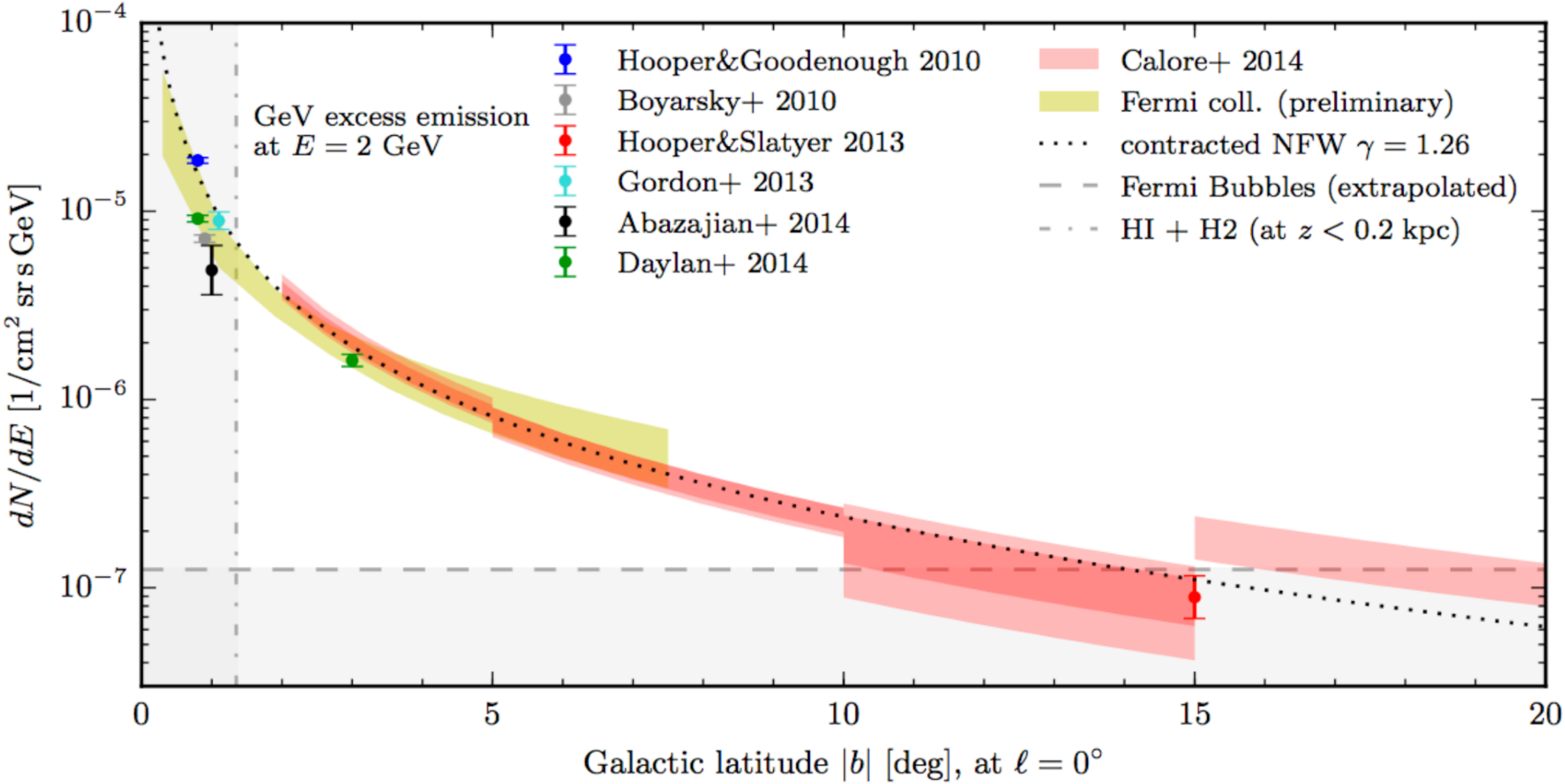

There are four resilient features of the GeV Excess:

4.) Extension from roughly 0.1° to >10° from the Galactic Center.

Other Features Can Depend on the Modeling

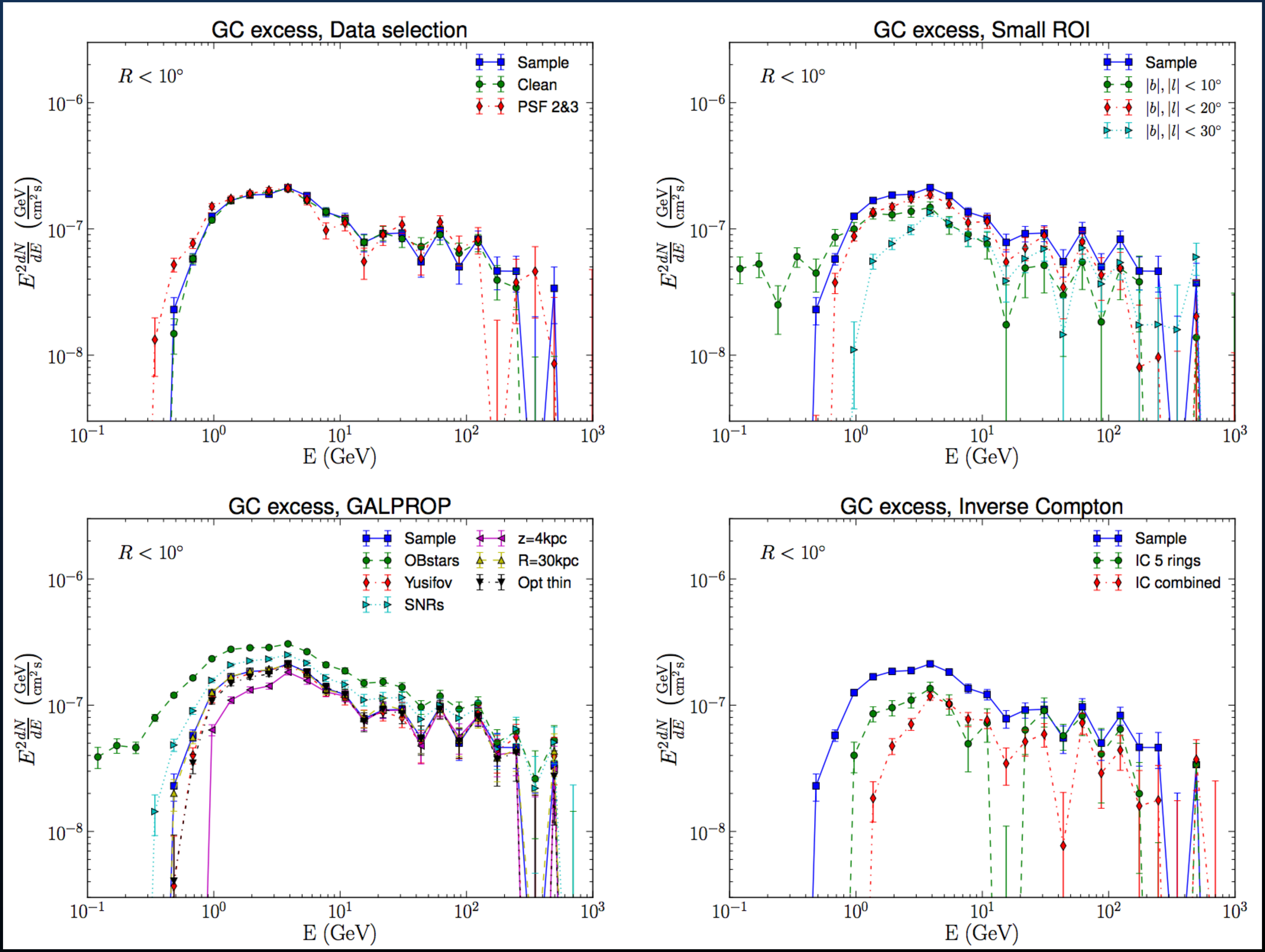

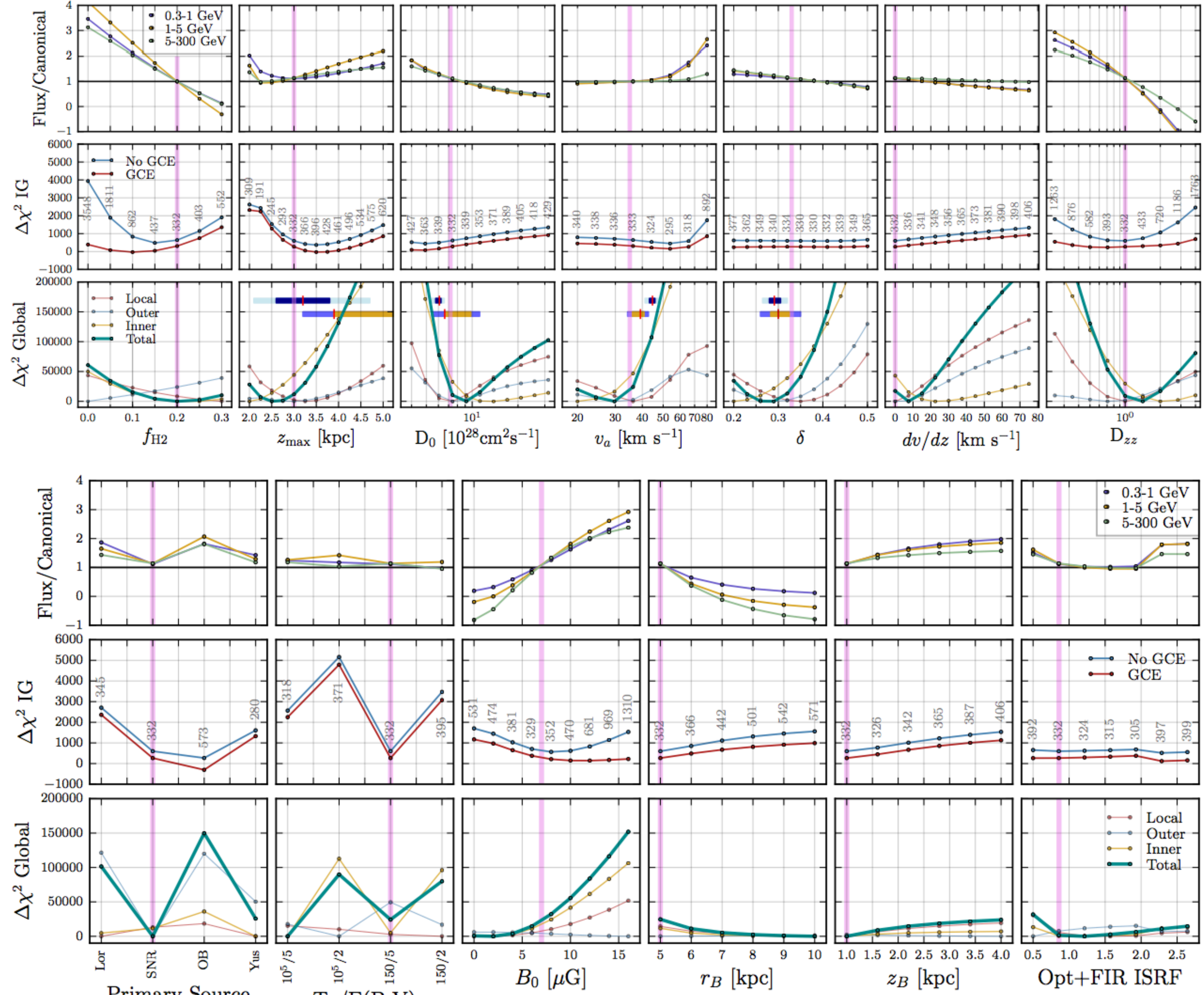

Flux/Canonical
0.3-1 GeV
1-5 GeV
5-300 GeV
Δχ² IG
No GCE
GCE
Δχ² Global
Local
Outer
Inner
Total
f_H2
z_max [kpc]
D_0 [10^28 cm^2 s^-1]
v_a [km s^-1]
δ
dv/dz [km s^-1]
D_zz
Lor
SNR
OB
Yus
10^5/5
10^5/2
150/5
150/2
B_0 [μG]
r_B [kpc]
z_B [kpc]
Opt+FIR ISRF

Significant Freedom

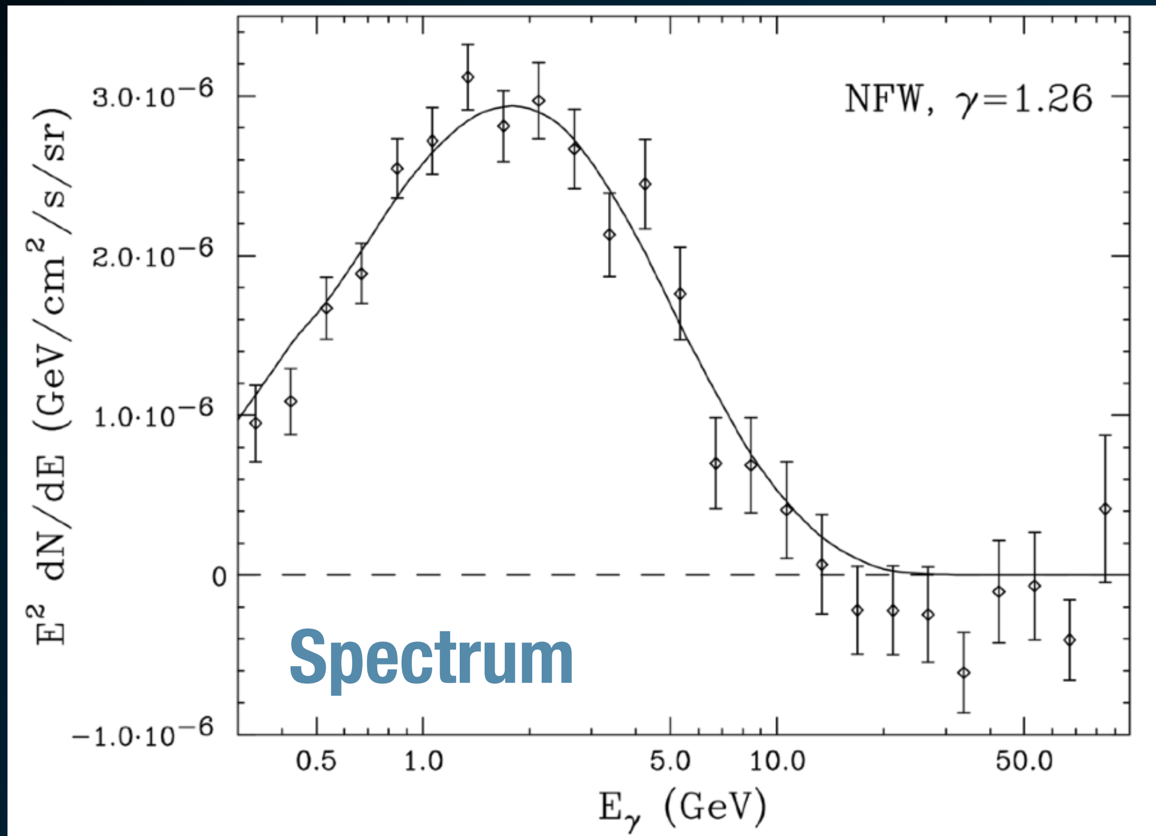

Constrained

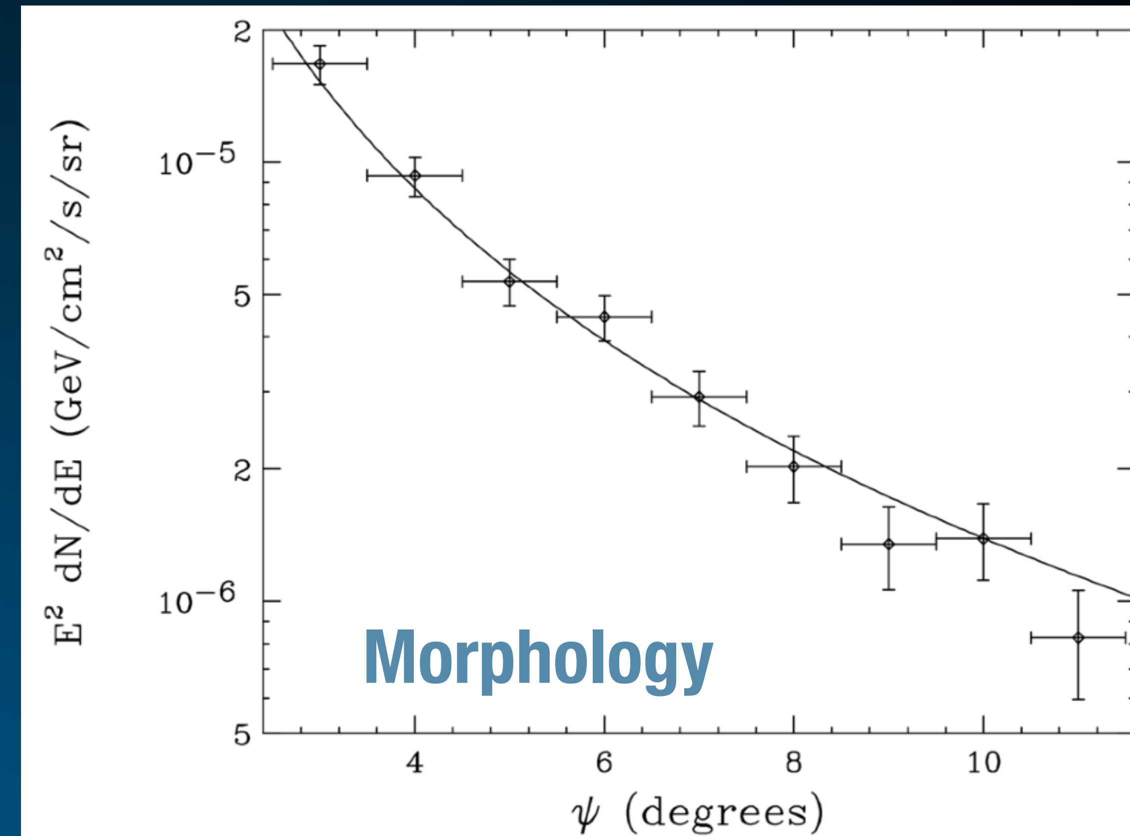

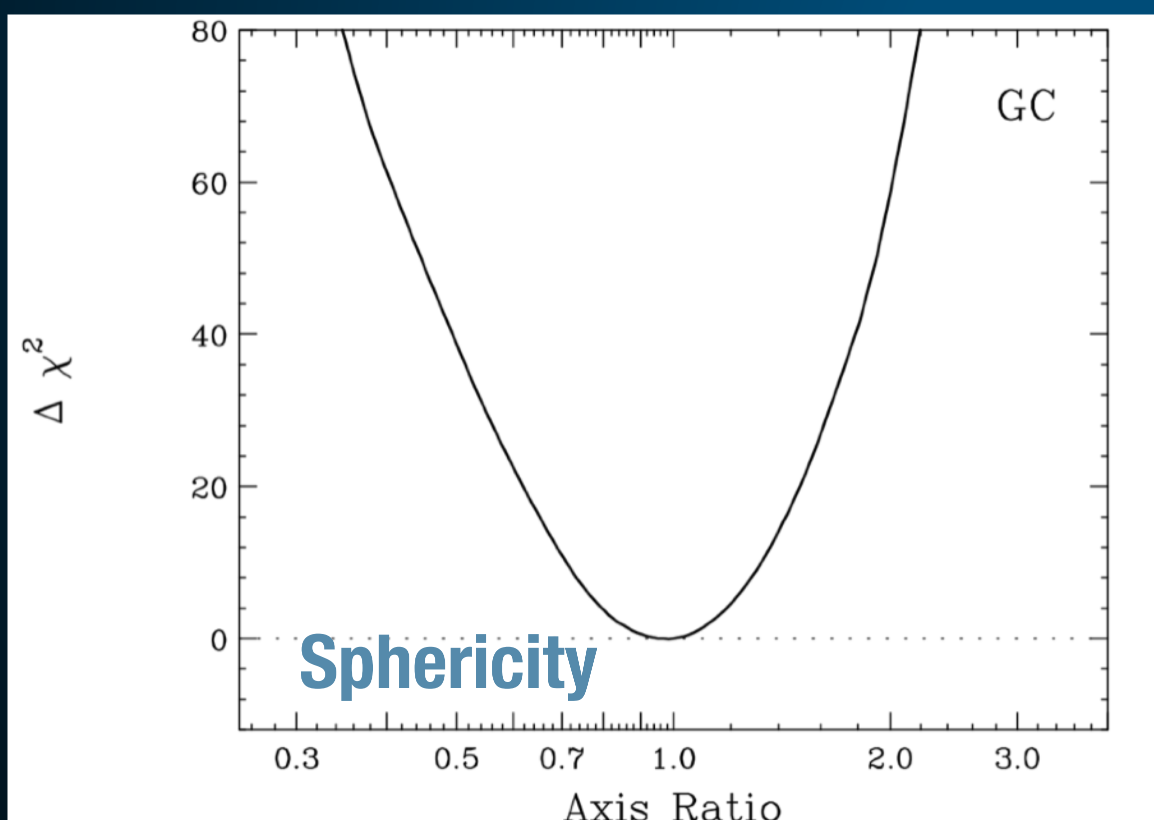

Constrained

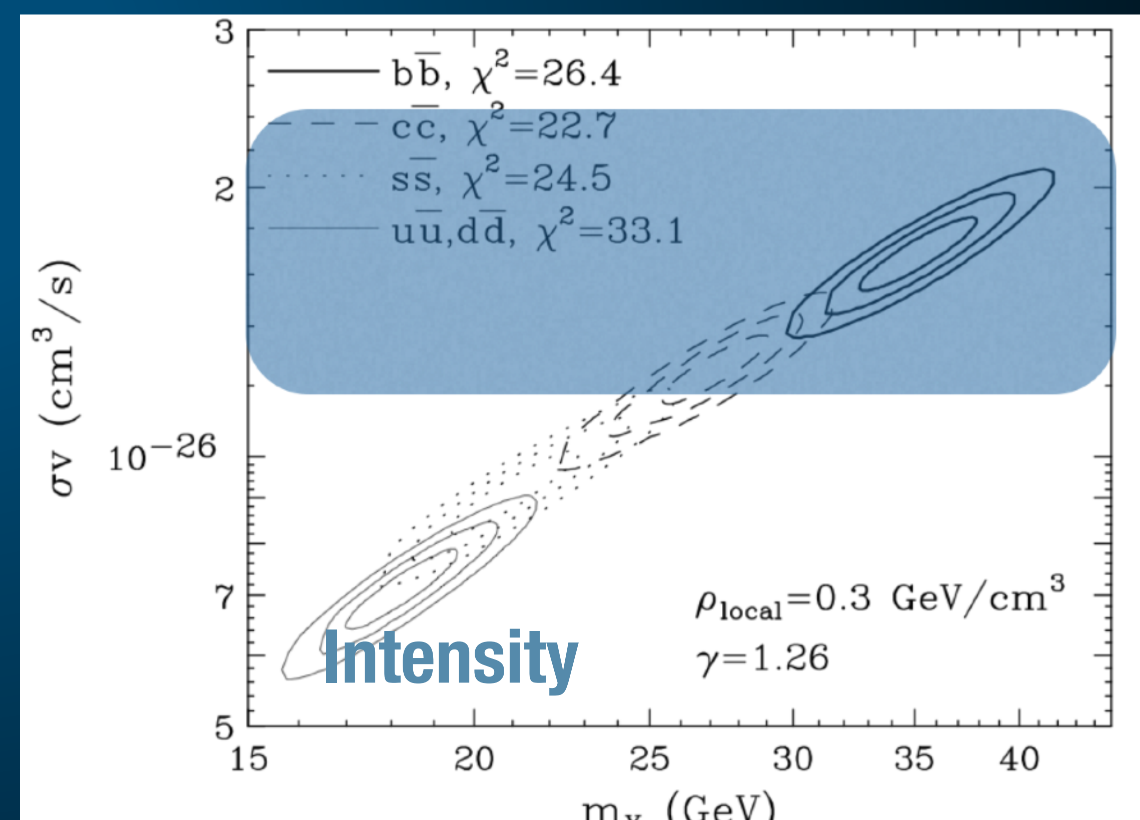

Constrained

Dark Matter Models Exist

Chan (1607.02246)
Jia (1607.00737)
Barrau et al. (1606.08031)
Huang et al. (1605.09018)
Cui et al. (1605.08138)
Krauss et al. (1605.05327)
Kumar et al. (1605.00611)
Biswas et al. (1604.06566)
Sage et al. (1604.04589)
Choquette et al. (1604.01039)
Cuoco et al. (1603.08228)
Chao et al. (1602.05192)
Horiuchi et al. (1602.04788)
Hektor et al. (1602.00004)
Freytsis et al. (1601.07556)
Kim et al. (1601.05089)
Huang et al. (1512.08992)
Kulkami et al. (1512.06836)
Tang et al. (1512.02899)
Cox et al. (1512.00471)
Cai et al. (1511.09247)
Agrawal et al. (1511.06293)
Duerr et al. (1510.07562)
Drozd et al. (1510.07053)
Arcadi et al. (1510.02297)
Williams (1510.00714)
Cai & Spray (1509.08481)
Freese et al. (1509.05076)
Bhattacharya et al. (1509.03665)
Algeri et al. (1509.01010)
Fox & Tucker-Smith (1509.00499)
Dutta et al. (1509.05989)
Liu et al. (1508.05716)
Berlin et al. (1508.05390)
Fan et al. (1507.06993)
Hektor et al. (1507.05096)
Achterbeg et al. (1507.04644)
Biswas et al. (1507.04543)

Butter et al. (1507.02288)
Mondal et al. (1507.01793)
Cao et al. (1506.06471)
Banik et al. (1506.05665)
Ipek (1505.07826)
Buchmueller et al. (1505.07826)
Balazs et al. (1505.06758)
Medina (1505.05565)
Kim et al. (1505.04620)
Ko et al. (1504.06944)
Ko & Tang (1504.03908)
Ghorbani & Ghorbani (1504.03610)
Fortes et al. (1503.08220)
Cline et al. (1503.08213)
Rajaraman et al. (1503.05919)
Bi et al. (1503.03749)
Kopp et al. (1503.02669)
Elor et al. (1503.01773)
Gherghetta et al. (1502.07173)
Berlin et al. (1502.06000)
Achterberg et al. (1502.05703)
Modak et al. (1502.05682)
Guo et al. (1502.00508)
Chen & Nomura (1501.07413)
Kozaczuk & Martin (1501.07275)
Berlin et al. (1501.03496)
Kaplinghat et al. (1501.03507)
Alves et al. (1501.03490)
Biswas et al. (1501.02666)
Biswas et al. (1501.02666)
Ghorbani & Ghorbani (1501.00206)
Cerdeno et al. (1501.01296)
Liu et al. (1412.1485)
Hooper (1411.4079)
Arcadi et al. (1411.2985)
Cheung et al. (1411.2619)
Agrawal et al. (1411.2592)
Kile et al. (1411.1407)

Buckley et al. (1410.6497)
Heikinheimo & Spethmann (1410.4842)
Freytsis et al. (1410.3818)
Yu et al. (1410.3347)
Cao et al. (1410.3239)
Guo et al. (1409.7864)
Yu (1409.3227)
Cahill-Rowley et al. (1409.1573)
Banik & Majumdar (1408.5795)
Bell et al. (1408.5142)
Ghorbani (1408.4929)
Okada & Seto (1408.2583)
Frank & Mondal (1408.2223)
Baek et al. (1407.6588)
Tang (1407.5492)
Balazs & Li (1407.0174)
Huang et al. (1407.0038)
McDermott (1406.6408)
Cheung et al. (1406.6372)
Arina et al. (1406.5542)
Chang & Ng (1406.4601)
Wang & Han (1406.3598)
Cline et al. (1405.7691)
Berlin et al. (1405.5204)
Mondal & Basak (1405.4877)
Martin et al. (1405.0272)
Ghosh et al. (1405.0206)
Abdullah et al. (1404.5503)
Park & Tang (1404.5257)
Cerdeno et al. (1404.2572)
Izaguirre et al. (1404.2018)
Agrawal et al. (1404.1373)
Berlin et al. (1404.0022)
Alves et al. (1403.5027)
Finkbeiner & Weiner (1402.6671)
Boehm et al. (1401.6458)
Kopp et al. (1401.6457)
Modak et al. (1312.7488)

Alves et al. (1312.5281)
Fortes et al. (1312.2837)
Banik et al. (1311.0126)
Arhrib et al. (1310.0358)
Kelso et al. (1308.6630)
Kozaczuk et al. (1308.5705)
Kumar (1308.4513)
Demir et al. (1308.1203)
Buckley et al. (1307.3561)
Cline et al. (1306.4710)
Cannoni et al. (1205.1709)
An et al. (1110.1366)
Buckley et al. (1106.3583)
Boucenna et al. (1106.3368)
Ellis et al. (1106.0768)
Cheung et al. (1104.5329)
Marshall et al. (1102.0492)
Abada et al. (1101.0365)
Tytgat (1012.0576)
Logan (1010.4214)
Barger et al. (1008.1796)
Raklev et al. (0911.1986)

Bayesian Lines of Evidence

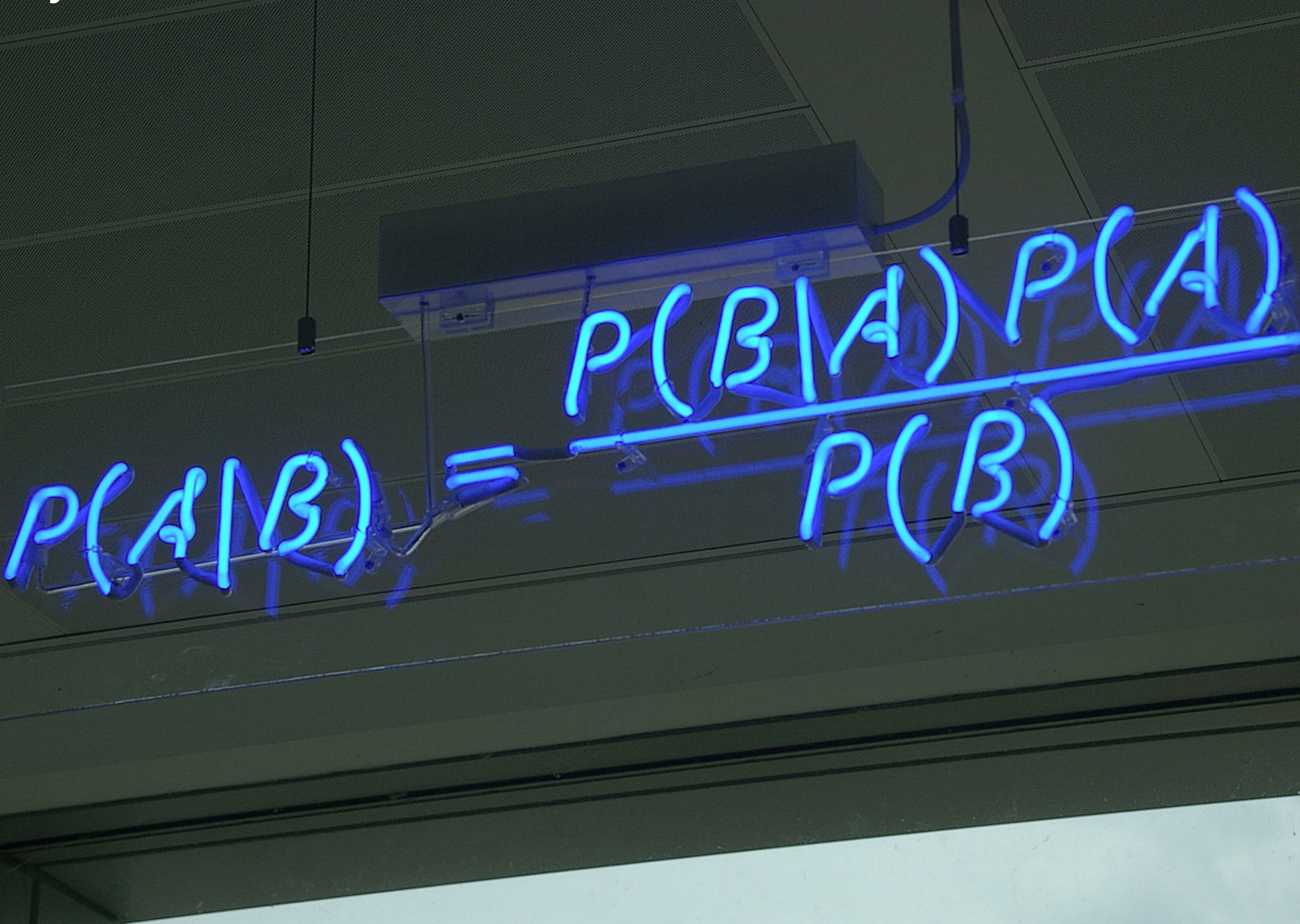

Pulsar Fits to the Data

These are the four resilient features of the GeV Excess:

2.) Hard Gamma-Ray Spectrum peaking at ~2 GeV

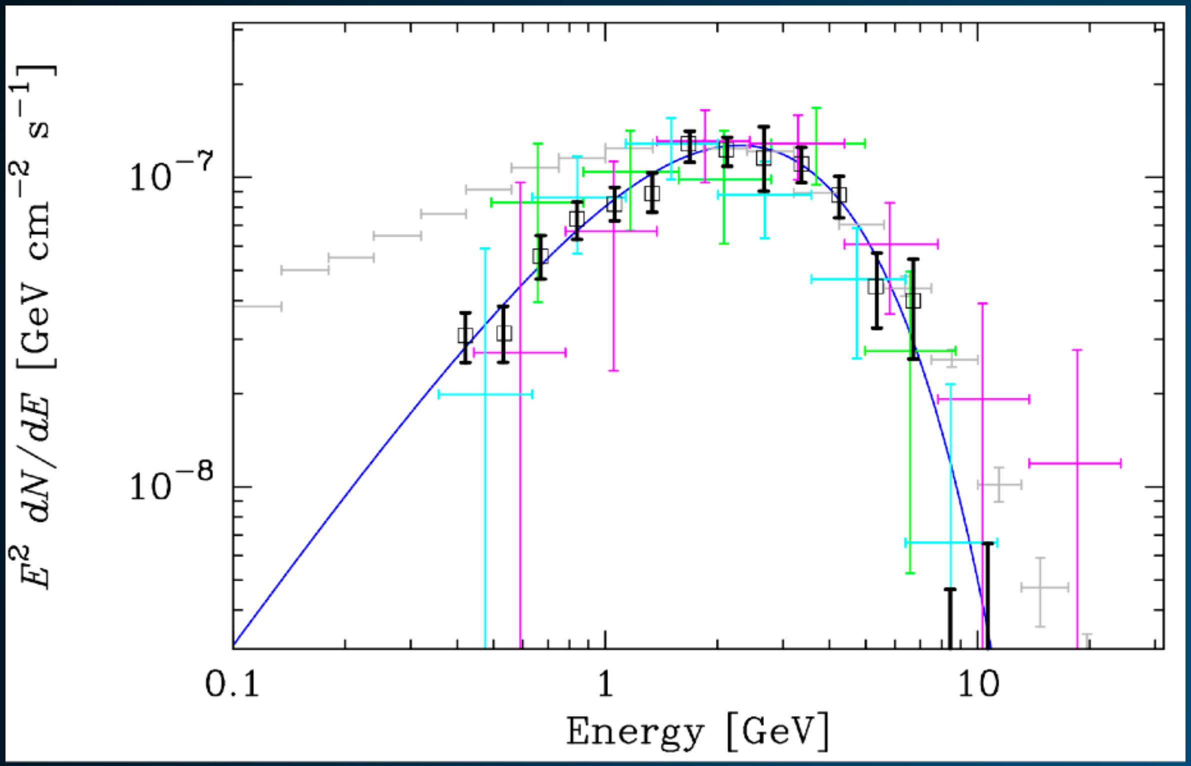

Pulsars match the spectral peak.

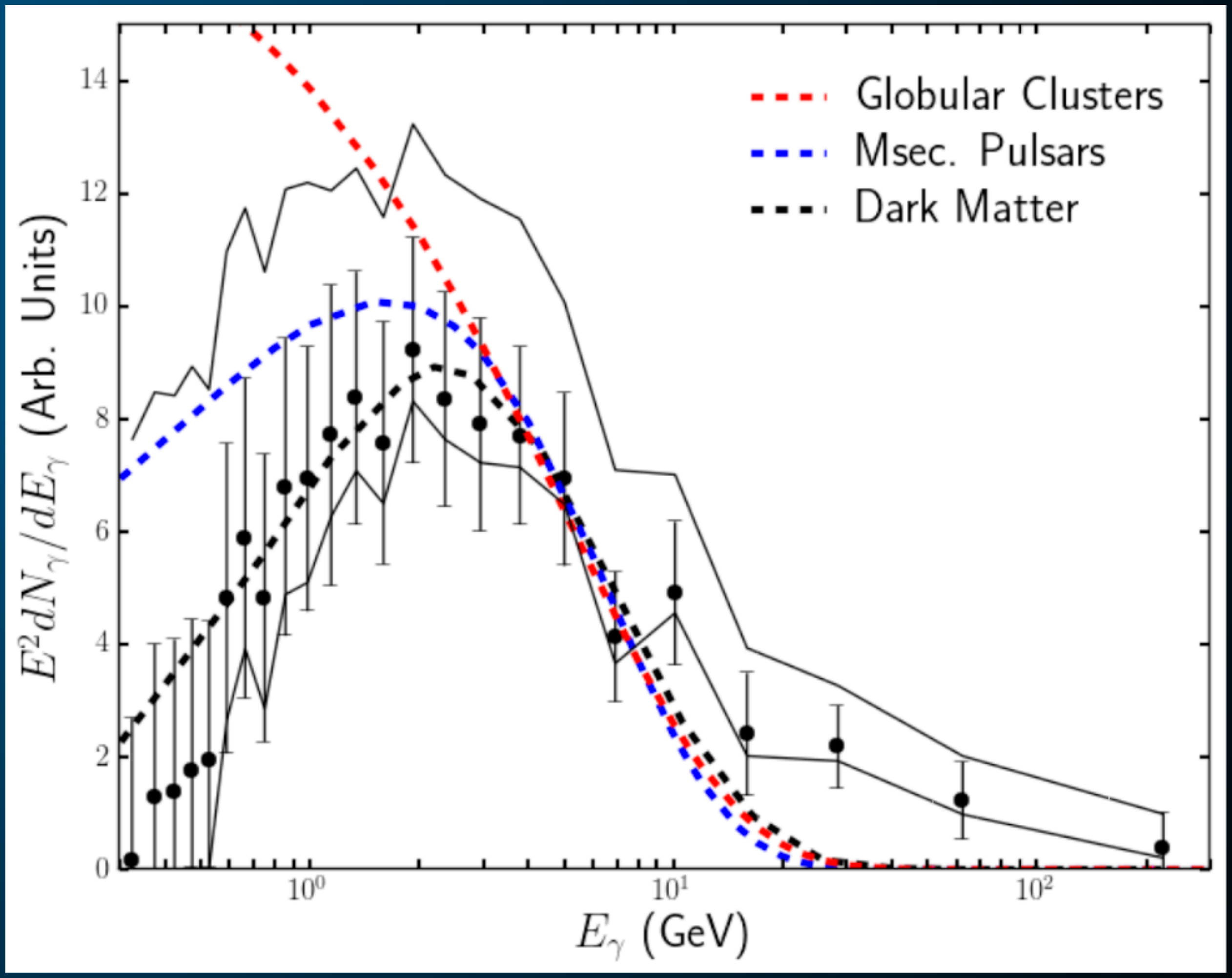

Fit of low-energy spectrum disputed.

Cholis et al. (2014)

Pulsar Fits to the Data

These are the four resilient features of the GeV Excess:

3.) Spherically Symmetric Emission Morphology

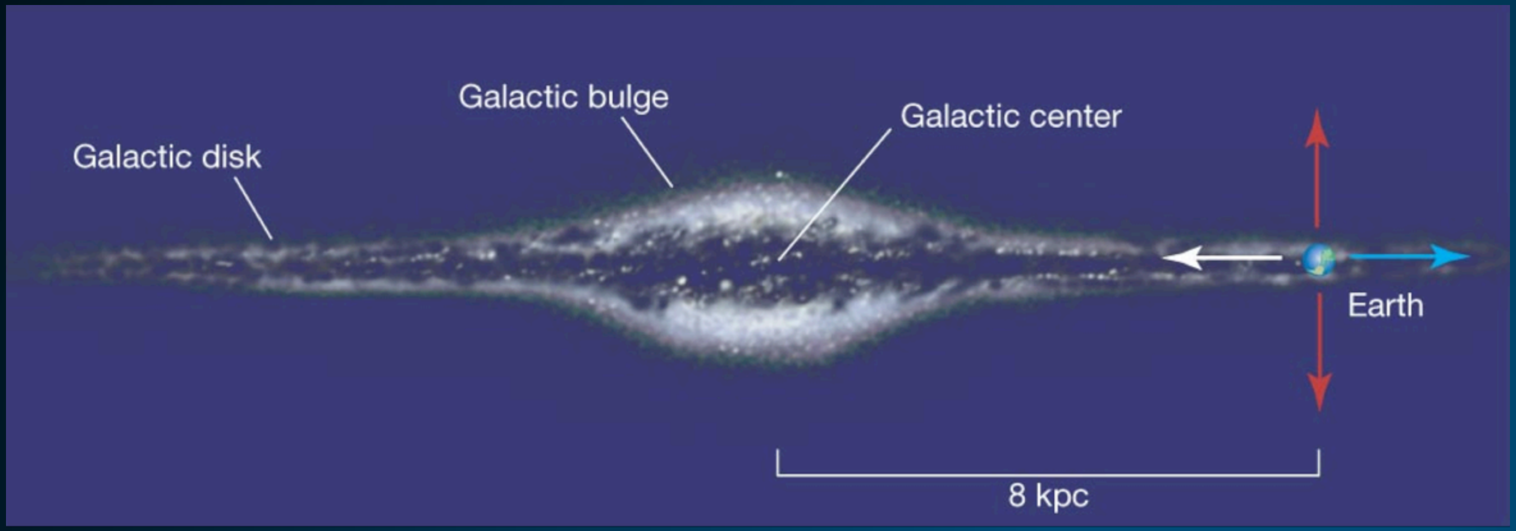

Pulsars in the Galactic bulge expected to have spherically symmetric morphology.

But could be X-shaped. Might be hard to distinguish.

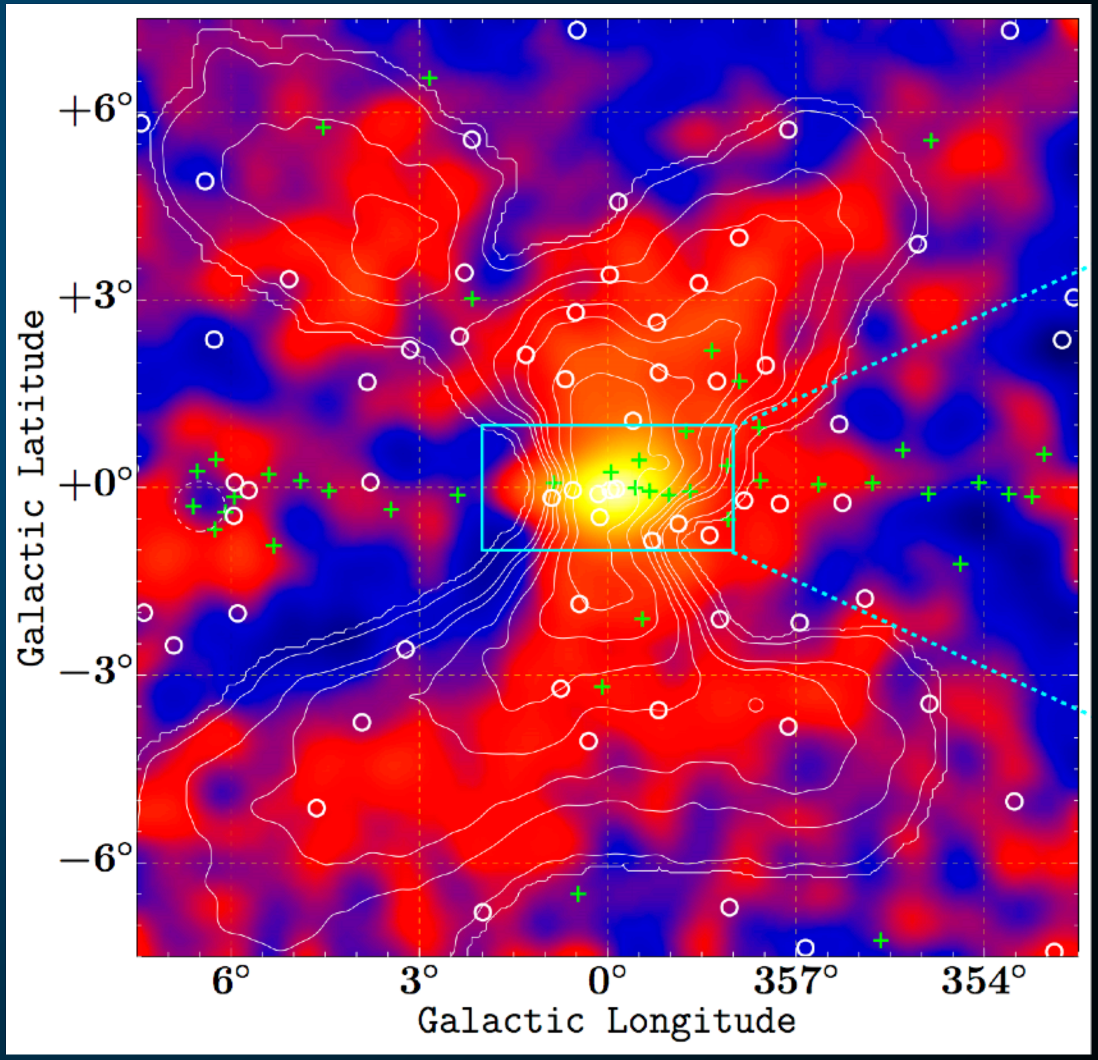

Macias et al. (2016)

Pulsar Fits to the Data

<u>These are the four resilient features of the GeV Excess:</u>

4.) Extension to >10° from the GC.

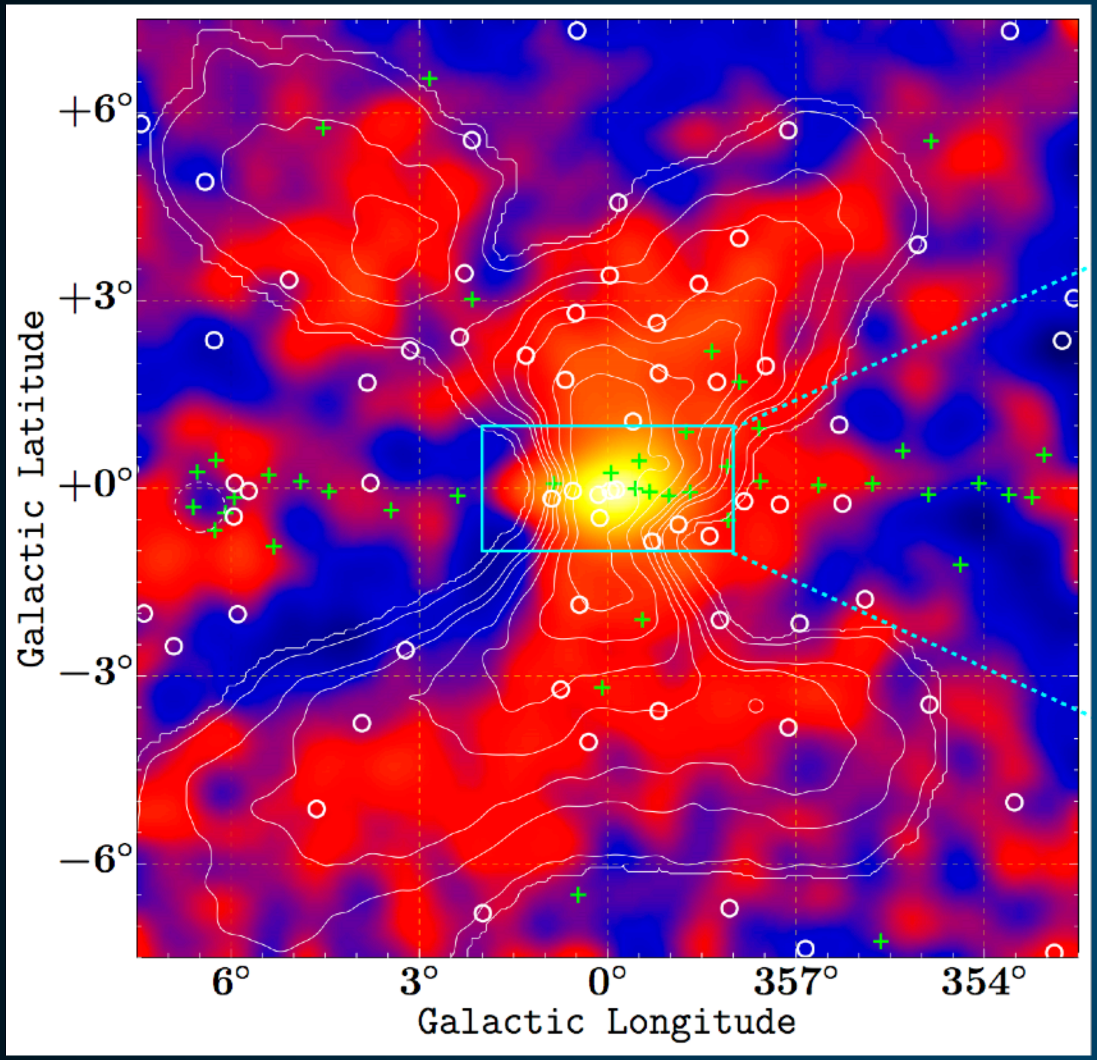

Bulge does not extend out to 10°.

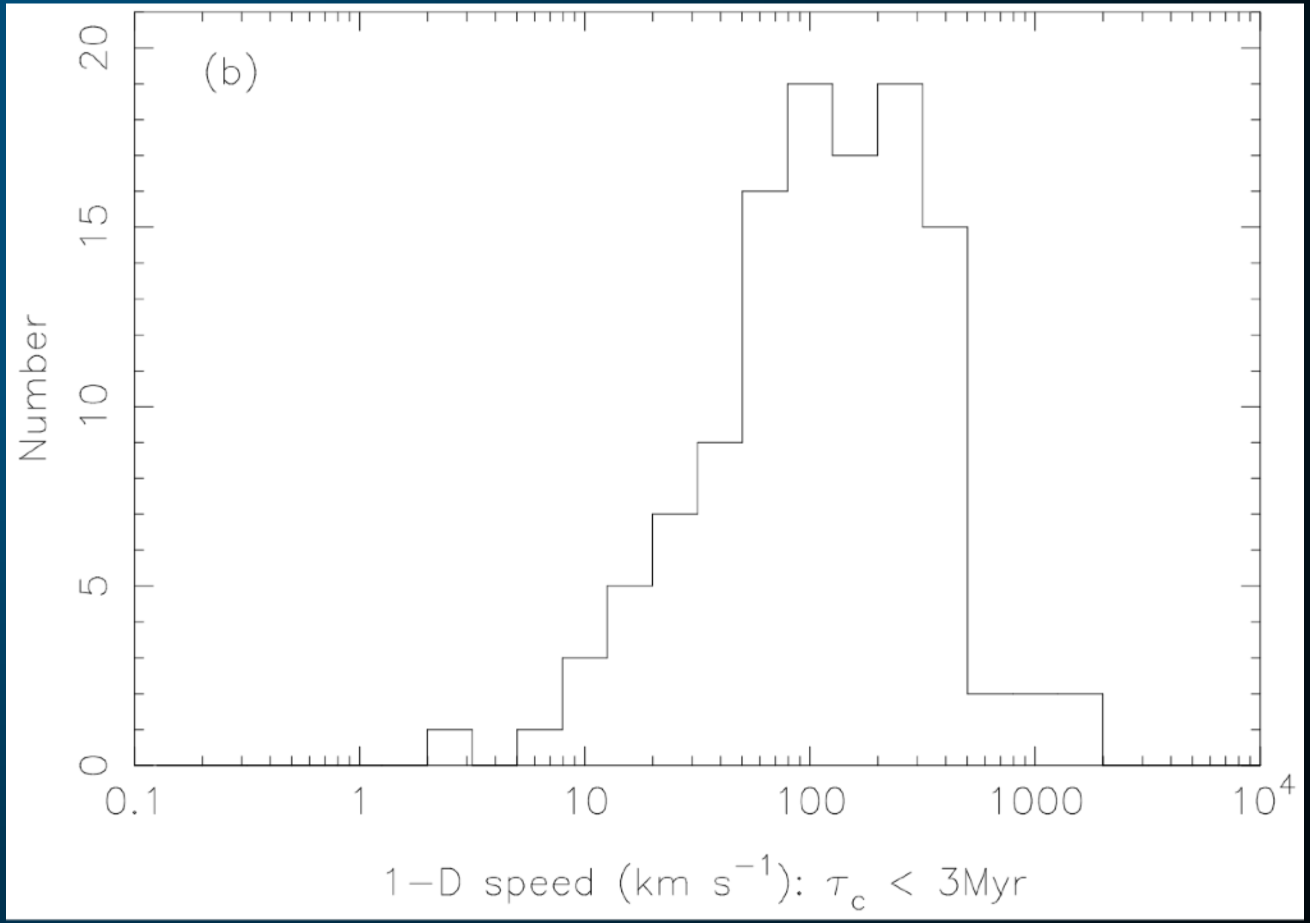

But pulsars get significant kicks (~500 pc/Myr)

Hobbs et al. (2005)

Part I:

Sub-Threshold Fluctuation Spectrum

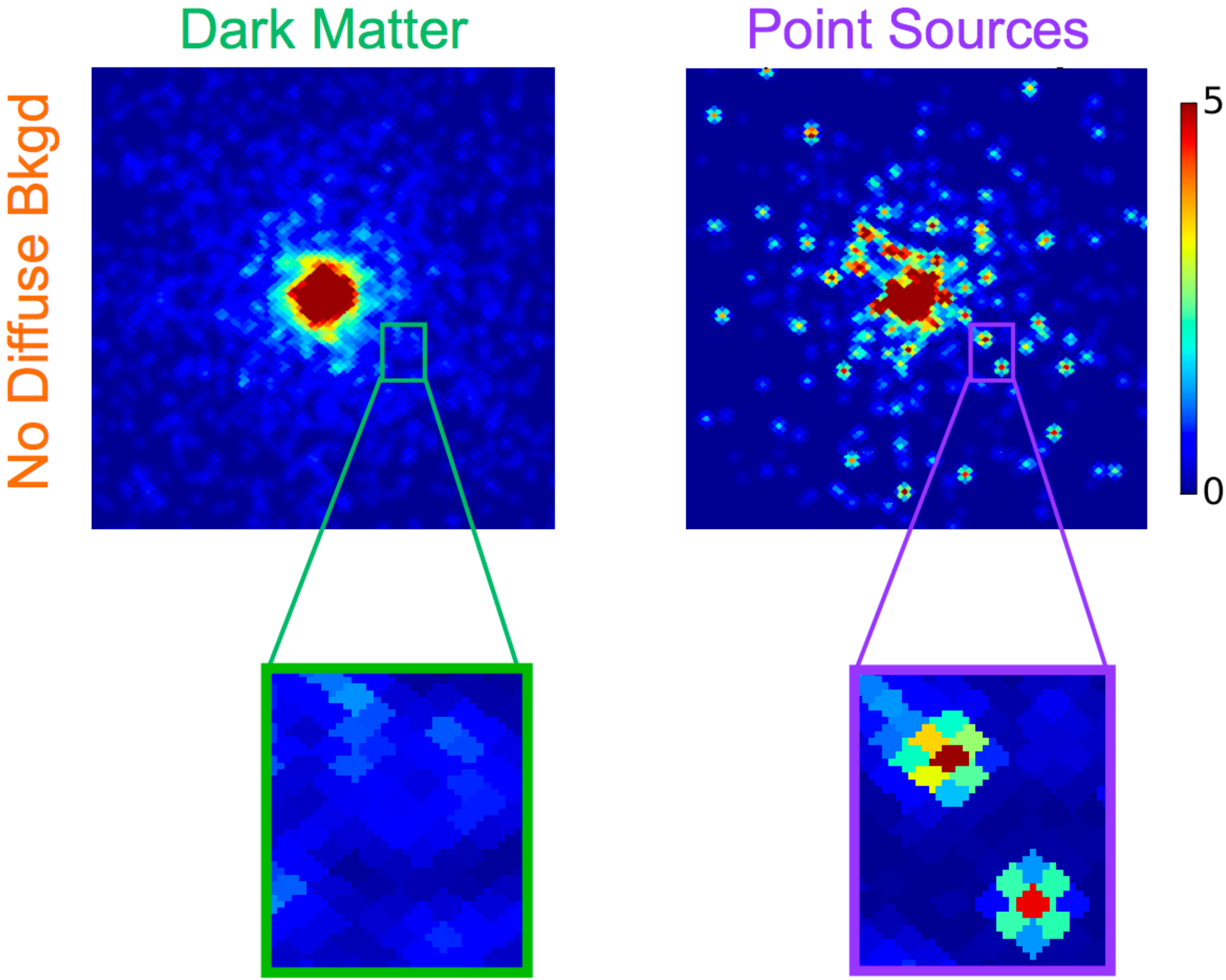

slide from Mariangela Lisanti

Evidence for Point Source Fluctuations?

Bartels et al. (2015)

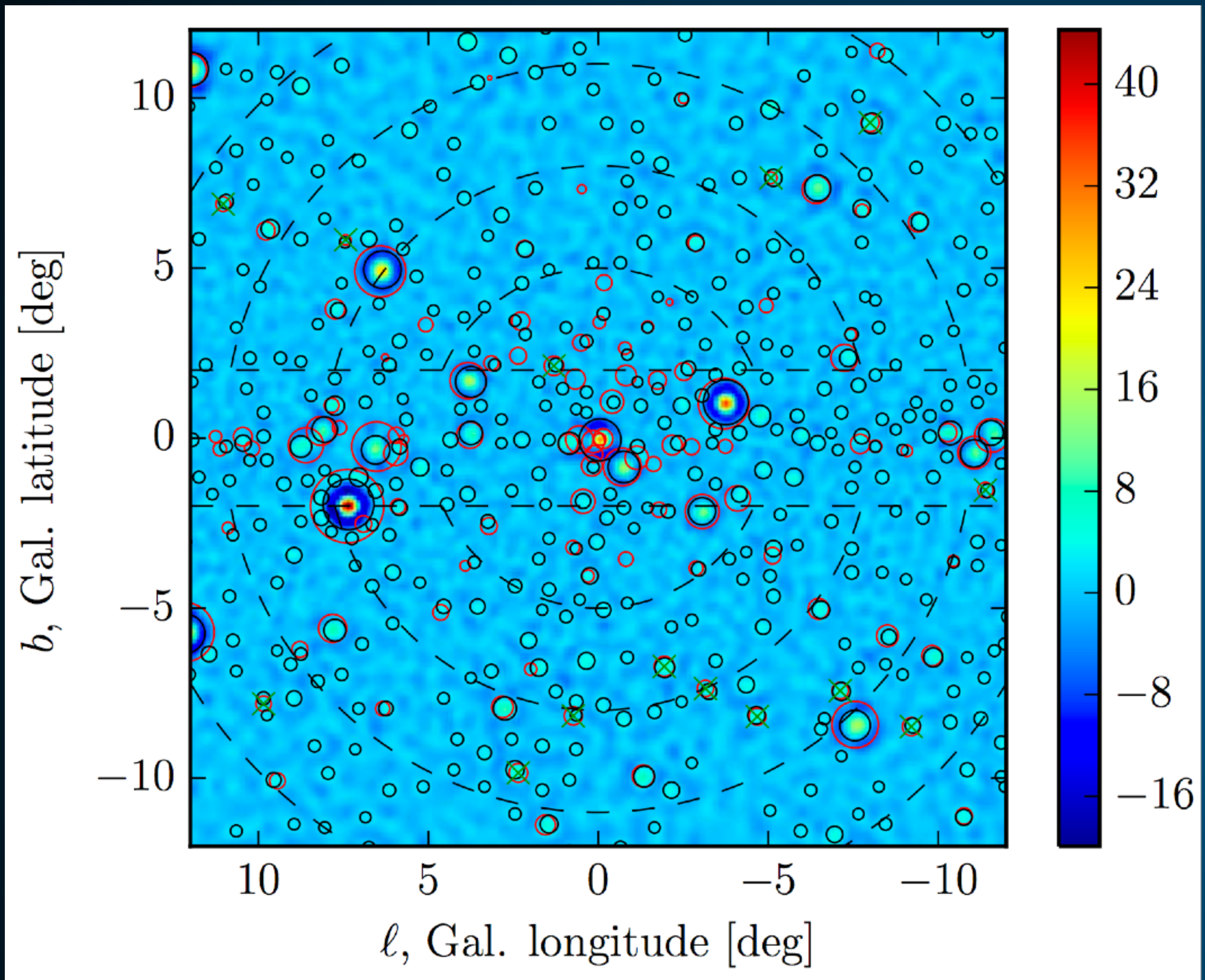

Lee et al. (2015)

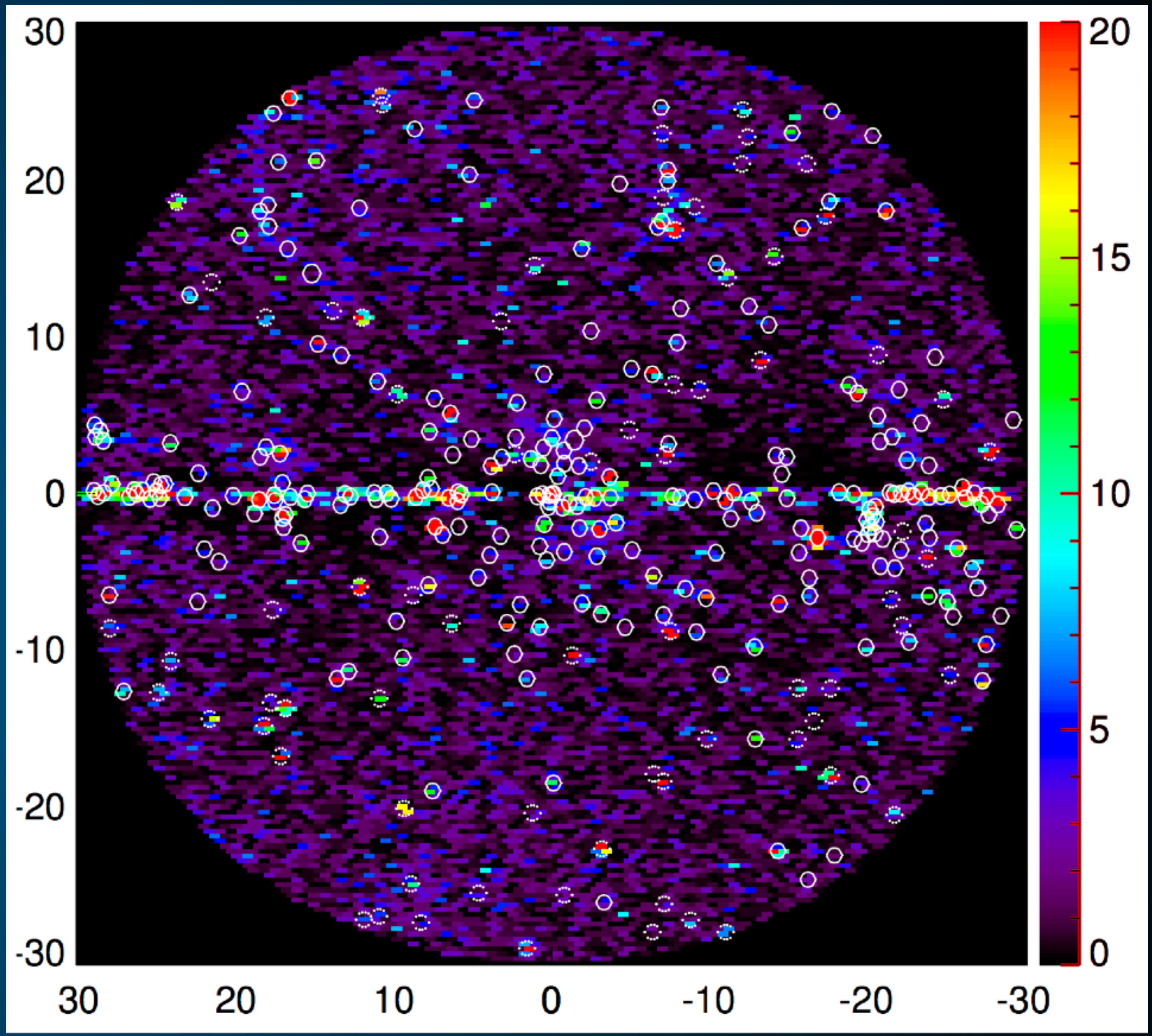

- **Recent analyses of hot-spots and cold spots in the GC region find evidence for the presence of a population of sub-threshold point sources.**

Evidence for Point Source Fluctuations?

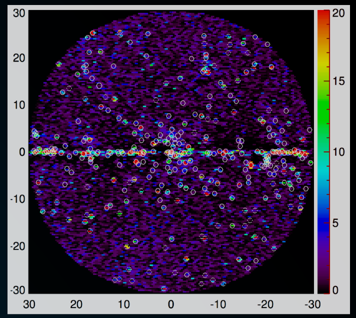

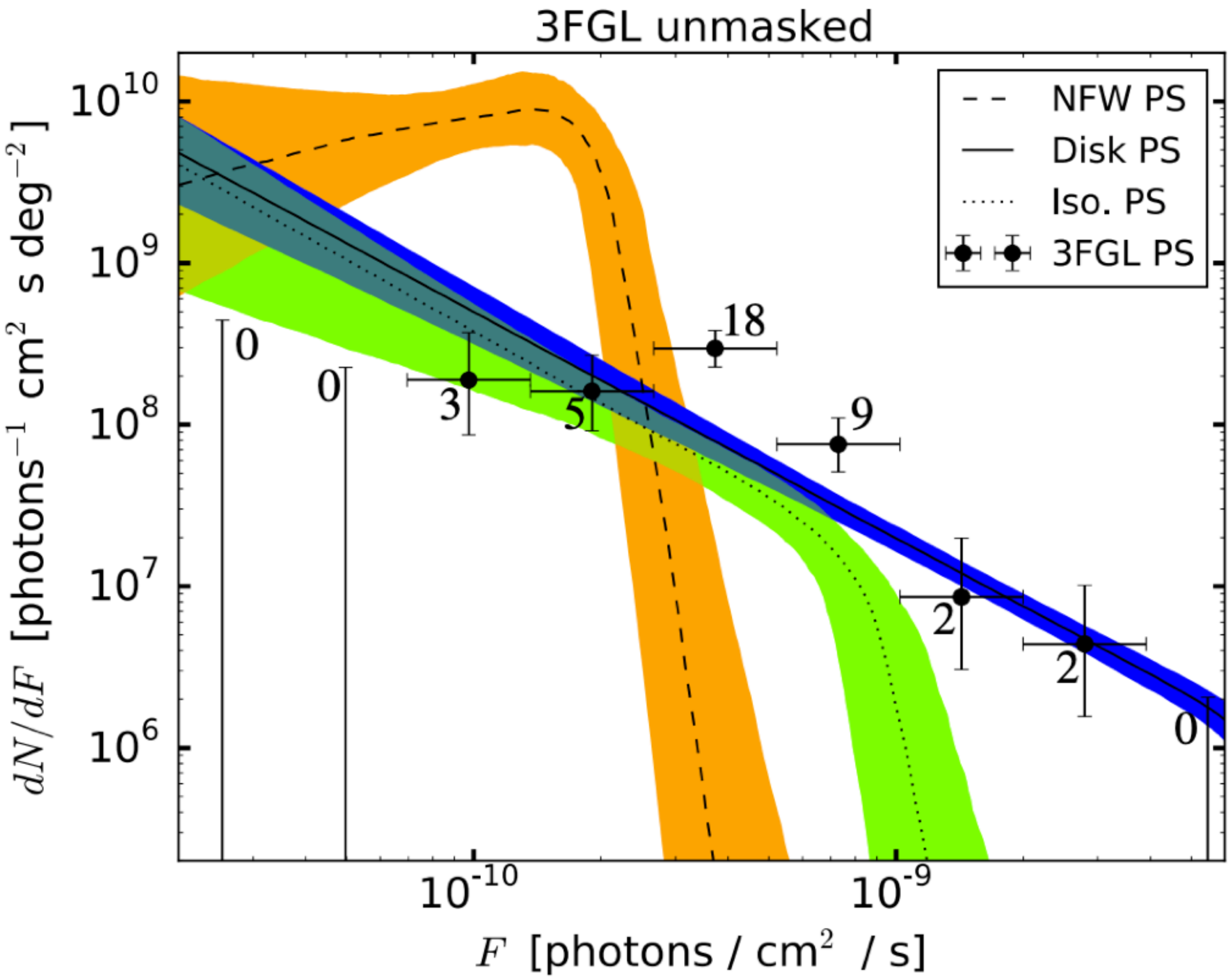

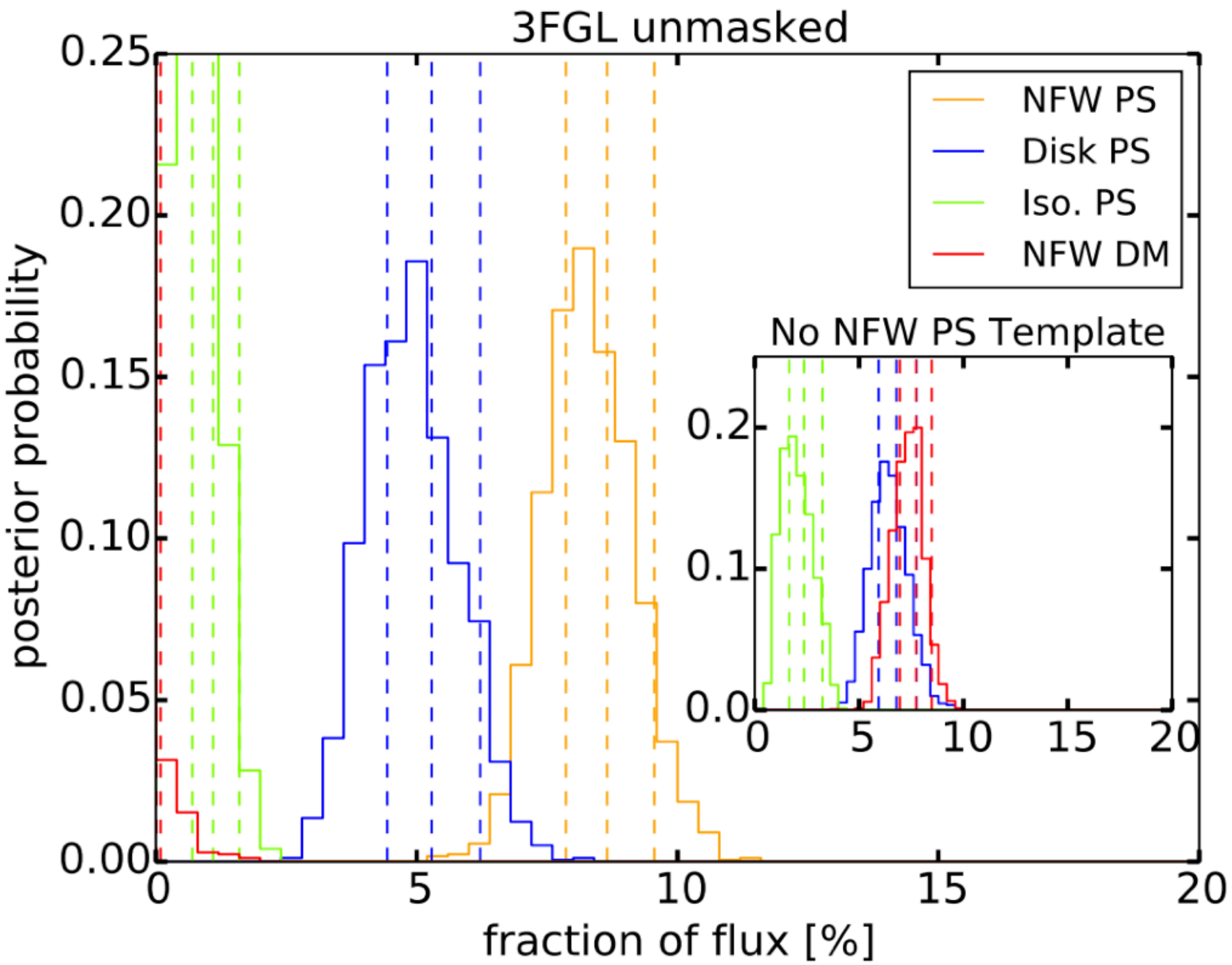

- Point sources effectively replace the smooth component of the excess (and this is preferred by the fit).

Evidence for Point Source Fluctuations?

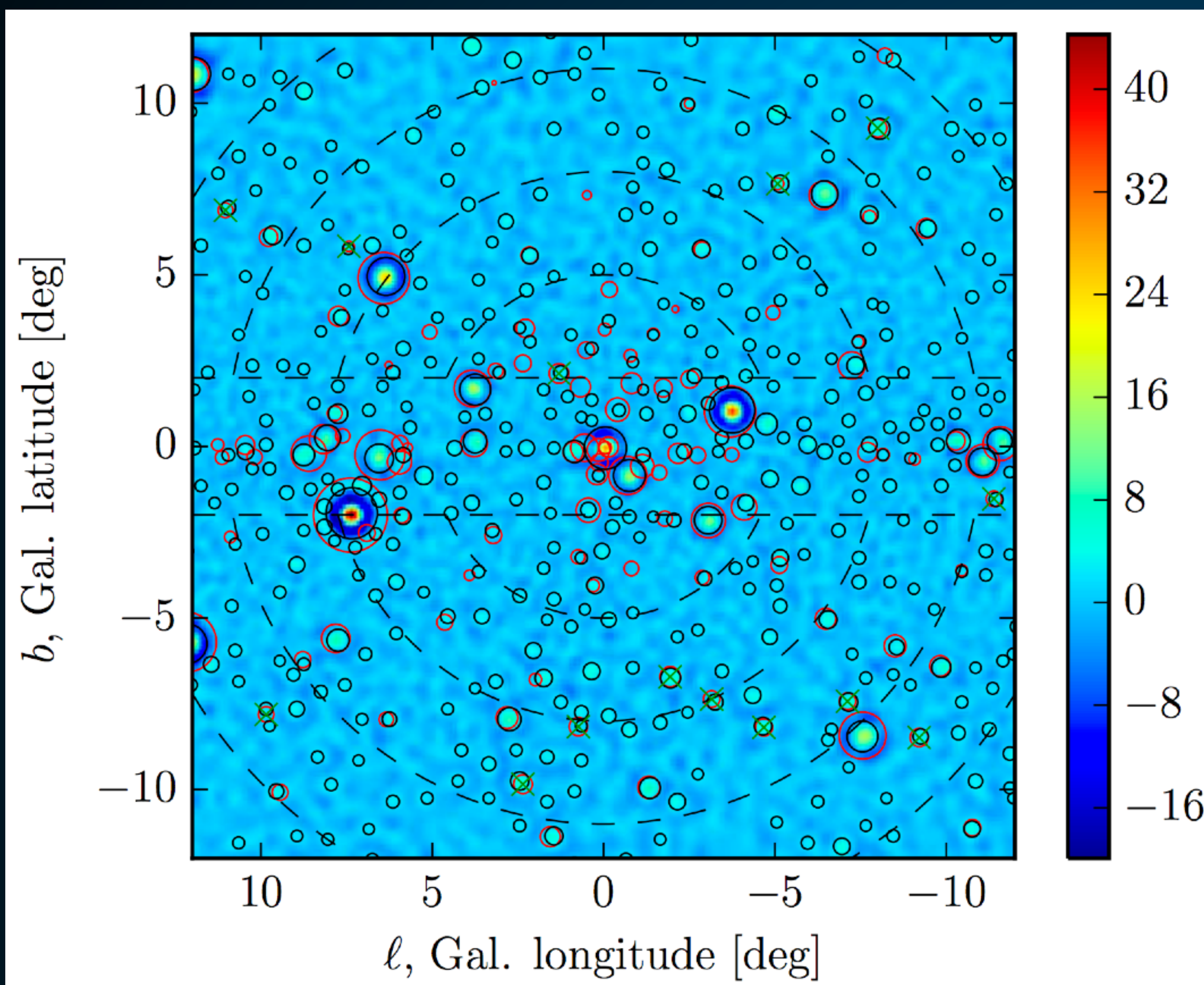

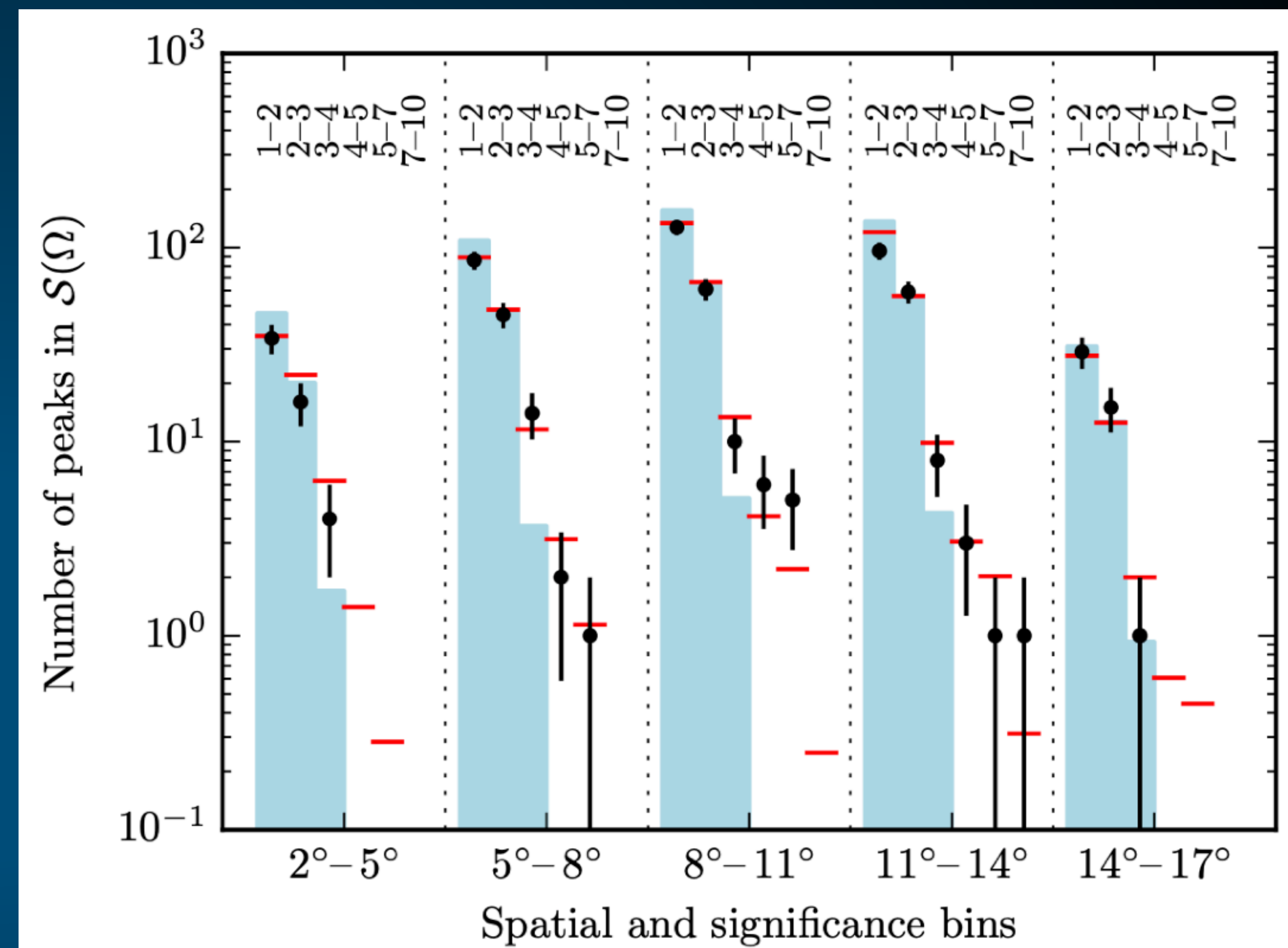

- Same result from a wavelet analysis — most emission is absorbed by a top-hat with a width determined by the PSF.

Part I:

Sub-Threshold Fluctuation Spectrum

Difficulties in Point Source Determinations

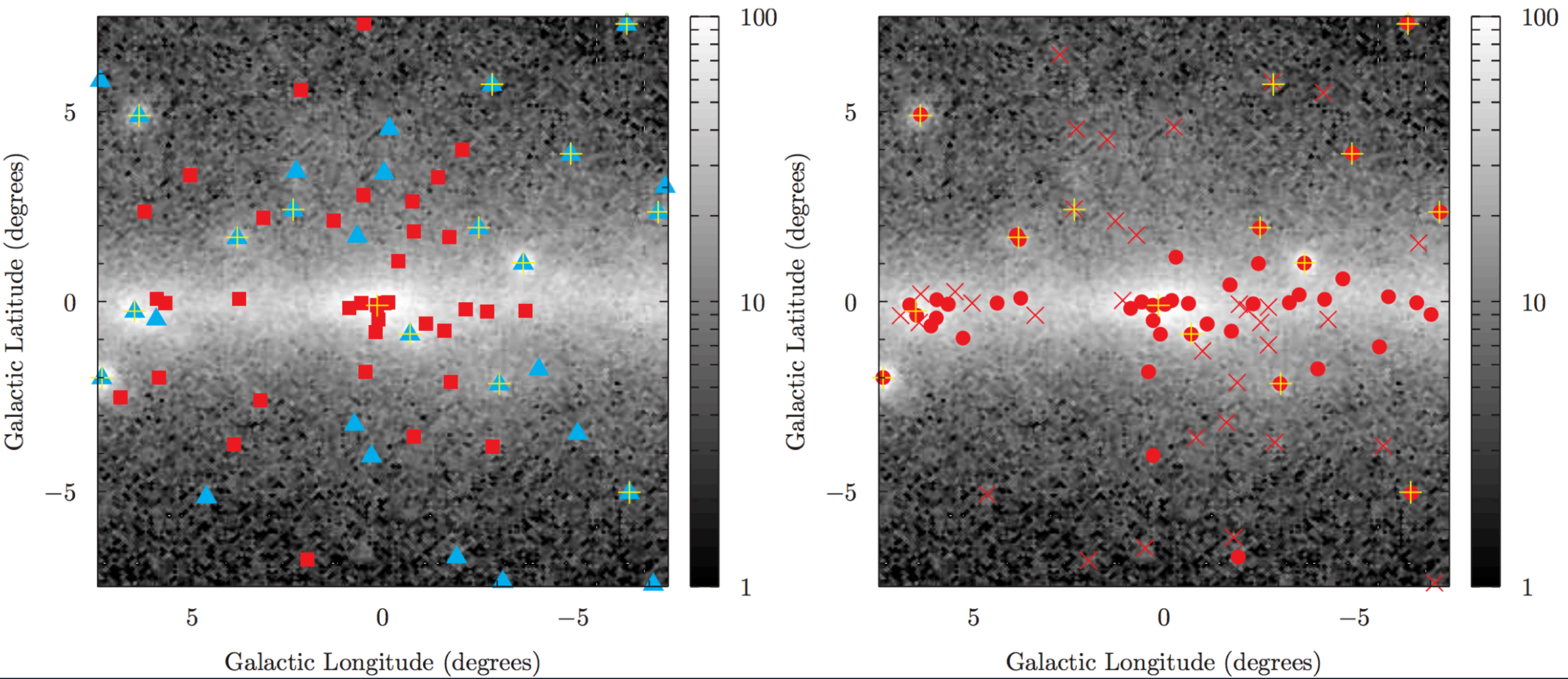

- Changing the diffuse model can significantly change the distribution of even 5σ point sources.

Alternative Models

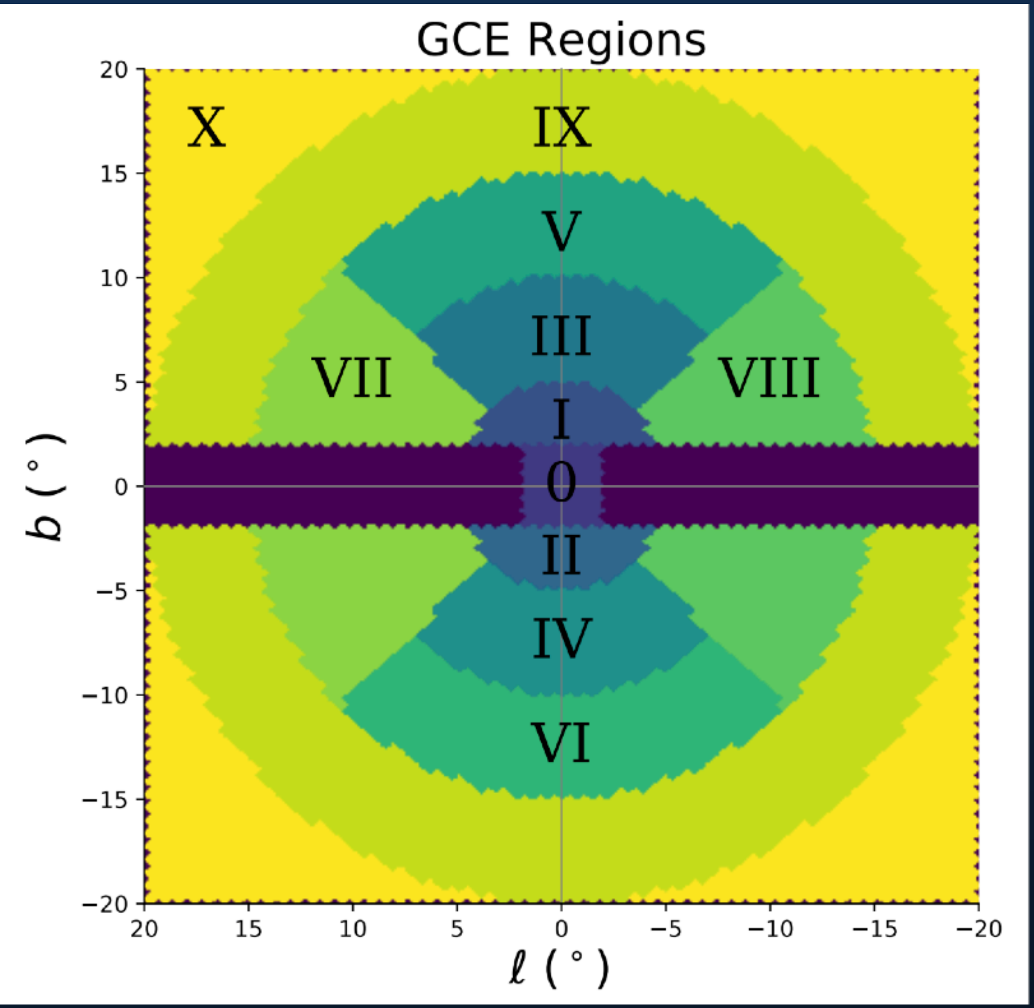

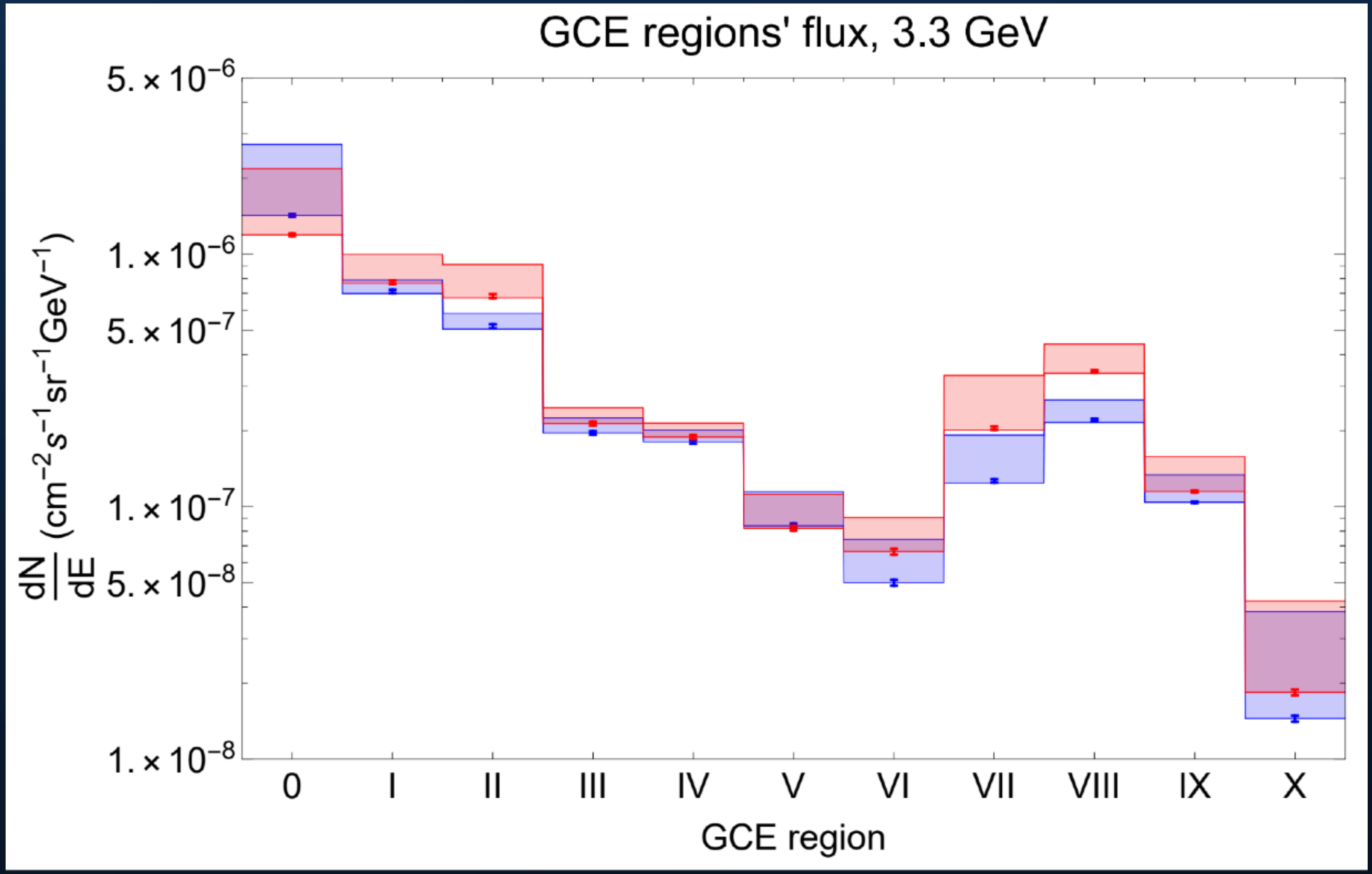

Blue (total power in GCE), Red (power in GCE at scales larger than 4°.

Significant negative point source power near the Galactic plane.

Balaji et al. (1803.01952)

Alternative Models

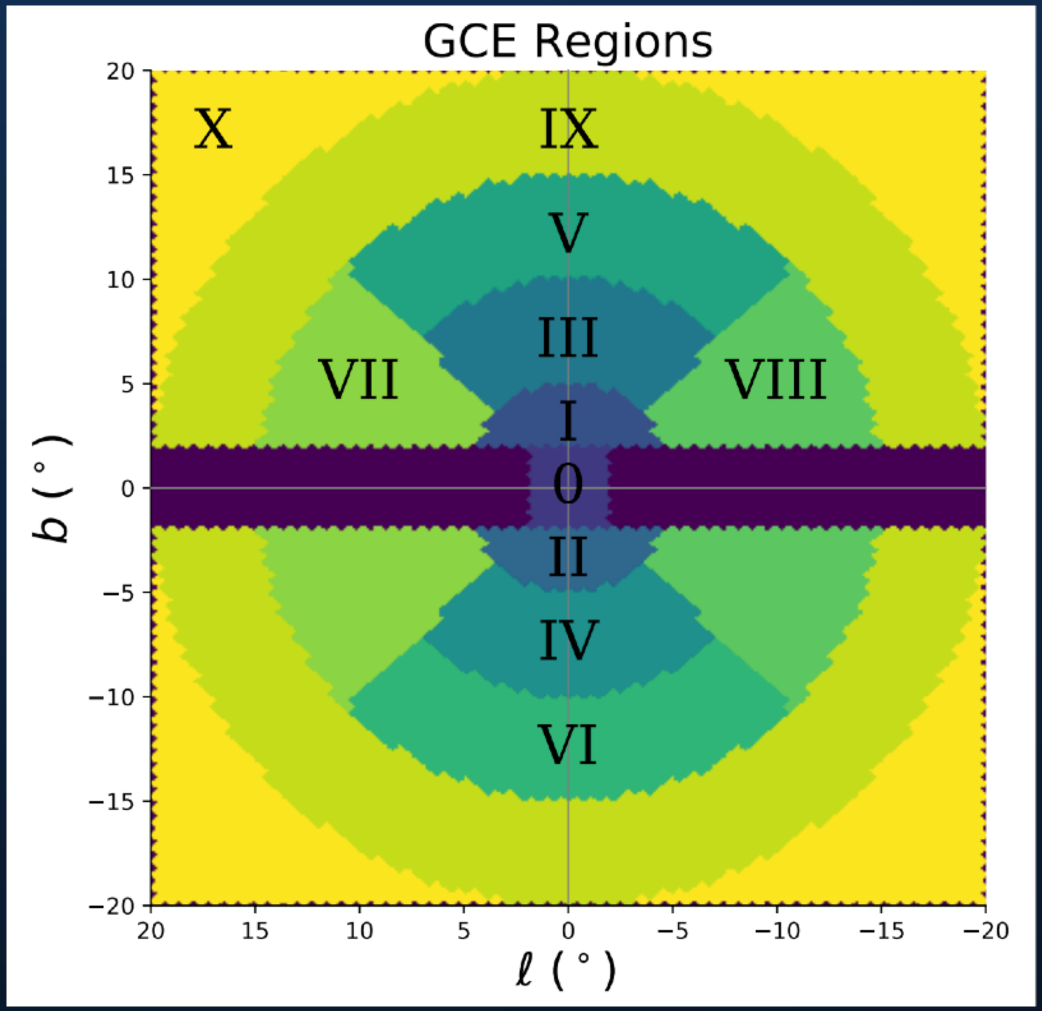

Regions VII and VIII are the easiest to understand and compare to, since they are removed from the center, far from the Bubbles, and in these parts of the sky point sources from the Galactic disk are expected to be relatively most dominant. At 1.5 GeV and above, in these two regions we find that ∼30–50% of the total ($1 \leq j \leq 9$) emission is in the first two wavelet scales, and moreover the first two wavelet scales contribute *negatively*. There

are 1.2 3FGL point sources per deg^2 on average in these two windows. This is still higher than the average of 1.02 3FGL point sources per deg^2 along the two stripes of $2° \leq |b| \leq 5°$ extending at all longitudes: Regions VII and VIII are rich in detected point sources. Only Regions II and VI have a similar ∼ 30% of their emission in the first two wavelet scales, which is also negative. The magnitude and the sign of this small scale contribution is intriguing. The negative sign in the first two wavelet levels for the regions near the Galactic center and Galactic disk means that unphysical flux has been imparted to the templates on small angular scales at intermediate angular distances from the Galactic center. This is suggestive either of mismodelled bremsstrahlung and pion emission or the inclusion of spurious point sources near the galactic center. We note that Region 0 does not suffer from a similarly large negative contribution at small angular scales. This may be an indication of the large positive contribution from the GCE, or an issue with the procedure to determine the point-source maps.

Balaji et al. (1803.01952)

Part II:

Global Morphology

Global Morphology of the Excess

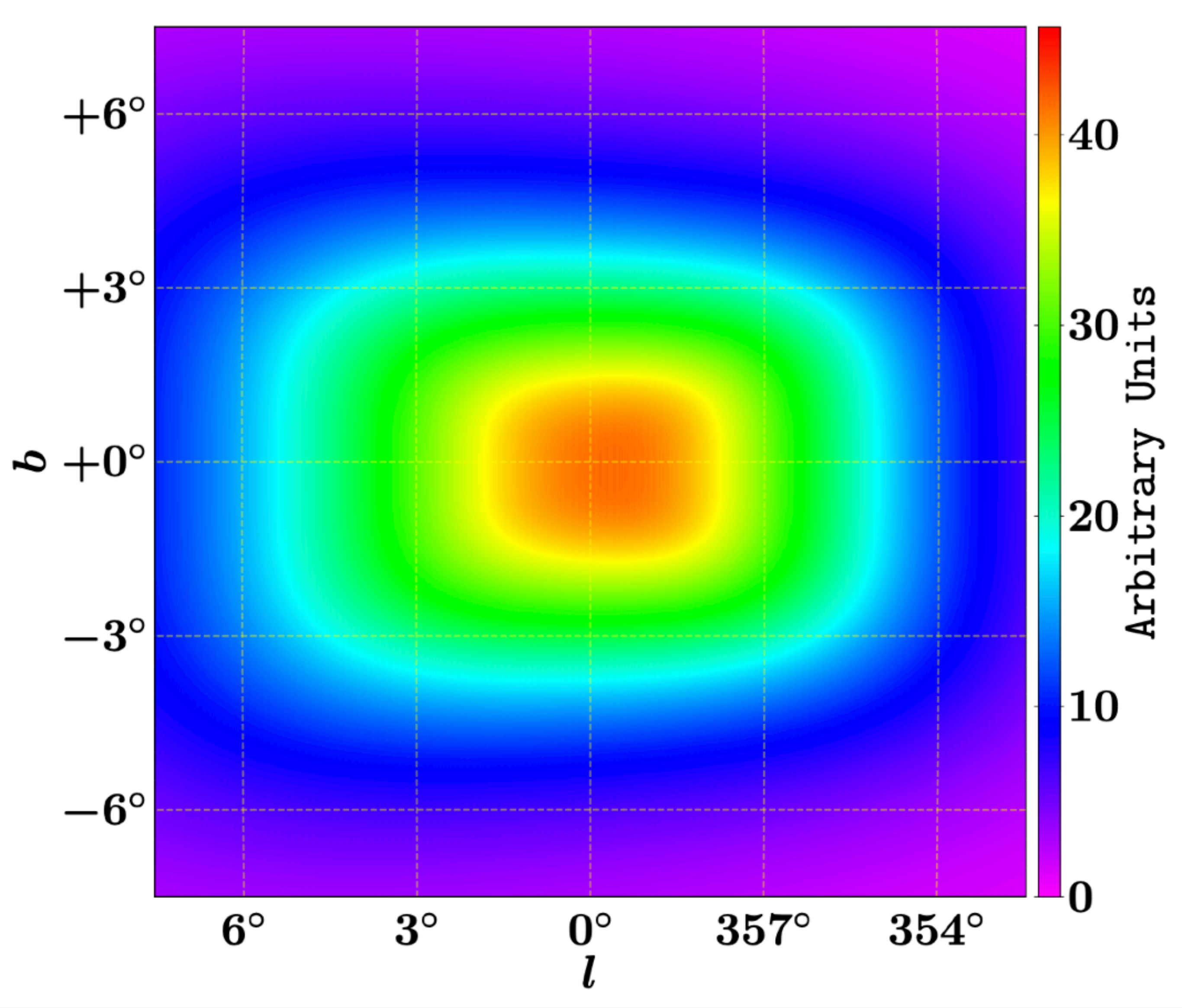

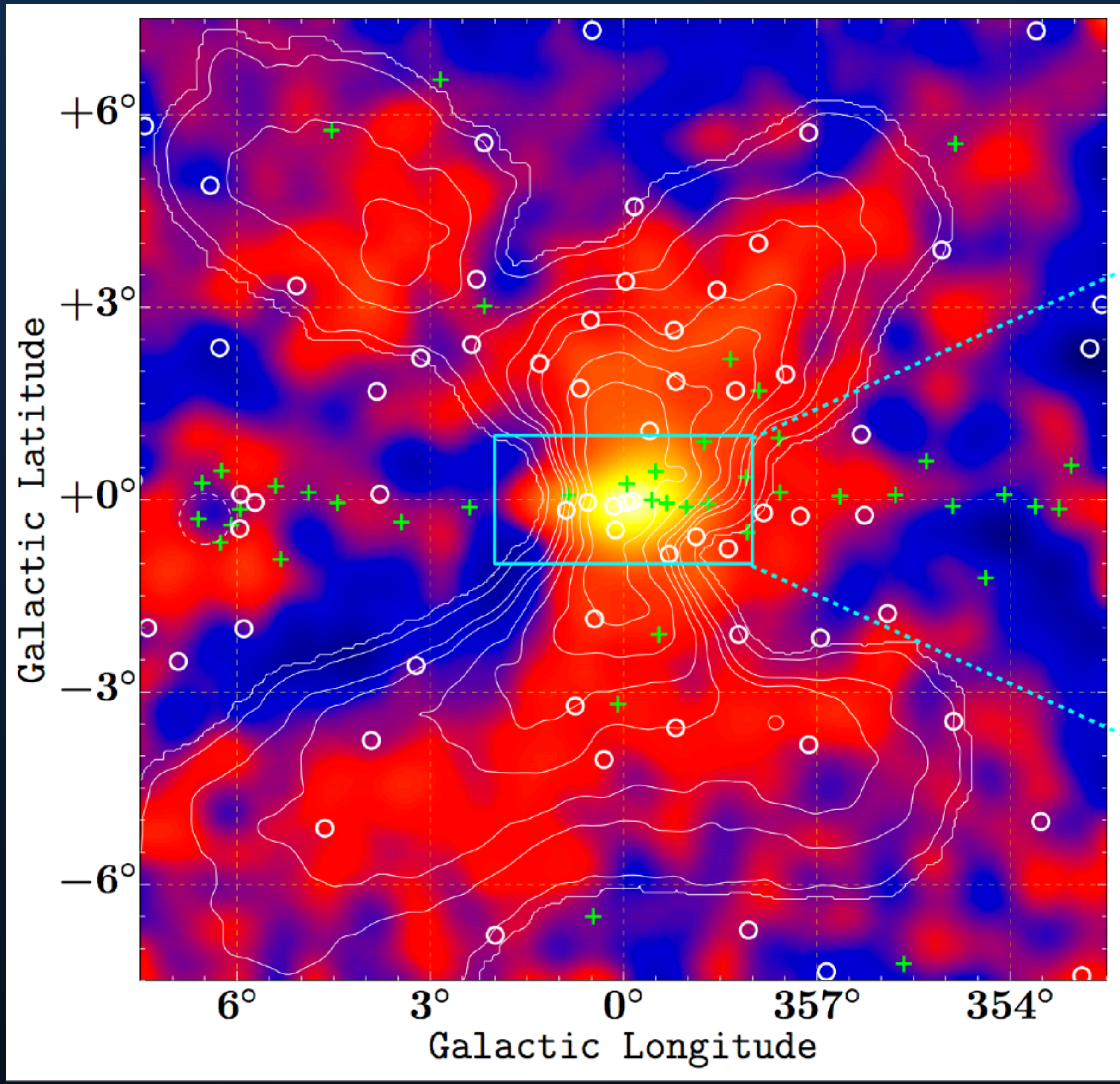

Can compare different models for the Galactic Bulge with the data.

Macias et al. (2016)

Global Morphology of the Excess

Base	Source	$\log(\mathcal{L}_{\mathrm{Base}})$	$\log(\mathcal{L}_{\mathrm{Base+Source}})$	$\mathrm{TS}_{\mathrm{Source}}$	σ	Number of source parameters
baseline	FB	-172461.4	-172422.3	78	6.9	19
baseline	NFW-s	-172461.4	-172265.3	392	18.4	19
baseline	Boxy bulge	-172461.4	-172238.7	445	19.7	19
baseline	X-bulge	-172461.4	-172224.1	475	20.5	19
baseline	NFW	-172461.4	-172167.9	587	23.0	19
baseline	NB	-172461.4	-171991.8	939	29.5	19
baseline	NP	-172461.4	-169804.1	5315	55.7	64×19
baseline+NP	FB	-169804.1	-169773.6	61	5.8	19
baseline+NP	NB	-169804.1	-169697.2	214	13.0	19
baseline+NP	Boxy bulge	-169804.1	-169663.7	281	15.3	19
baseline+NP	NFW	-169804.1	-169623.3	362	17.6	19
baseline+NP	X-bulge	-169804.1	-169616.2	376	18.0	19
baseline+NP+X-bulge	NFW	-169616.2	-169568.4	96	7.9	19
baseline+NP+X-bulge	NB	-169616.2	-169542.0	148	10.4	19
baseline+NP+X-bulge+NB	NFW	-169542.0	-169531.0	22	2.4	19
baseline+NP+X-bulge+NB	FB	-169542.0	-169525.5	33	3.5	19
baseline+NP+NB	X-bulge	-169697.2	-169542.0	310	16.1	19
baseline+NP+NB	Boxy bulge	-169697.2	-169566.0	262	14.6	19
baseline+NP+NFW	X-bulge+NB	-169623.3	-169531.0	185	10.8	2×19
baseline+NP+NFW+NB	X-bulge	-169598.9	-169531.0	136	9.9	19
baseline+NP+Boxy bulge+NB	NFW	-169566.0	-169553.3	25	2.7	19

Part II:

Global Morphology

Emission Extends Outside Bulge

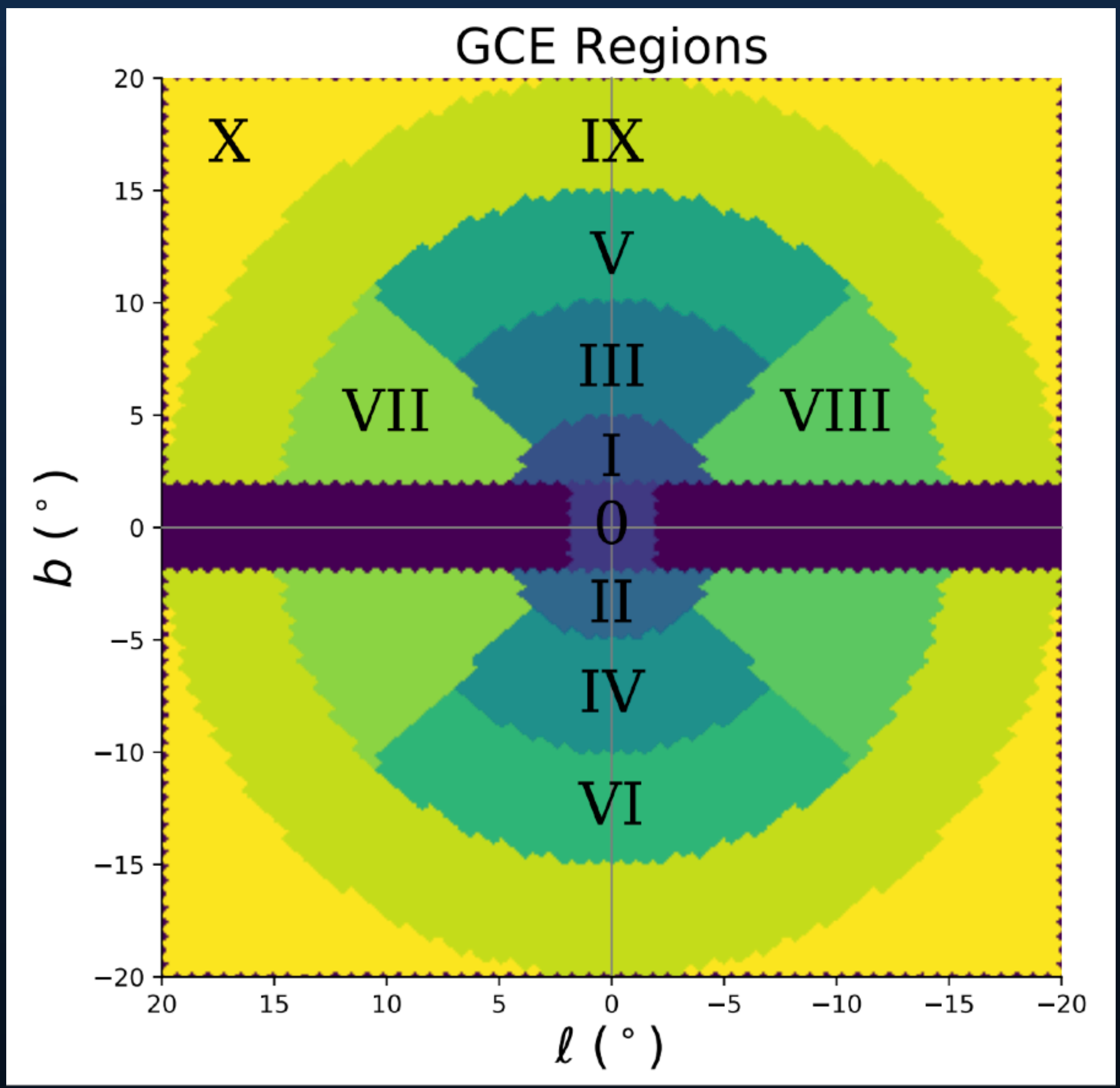

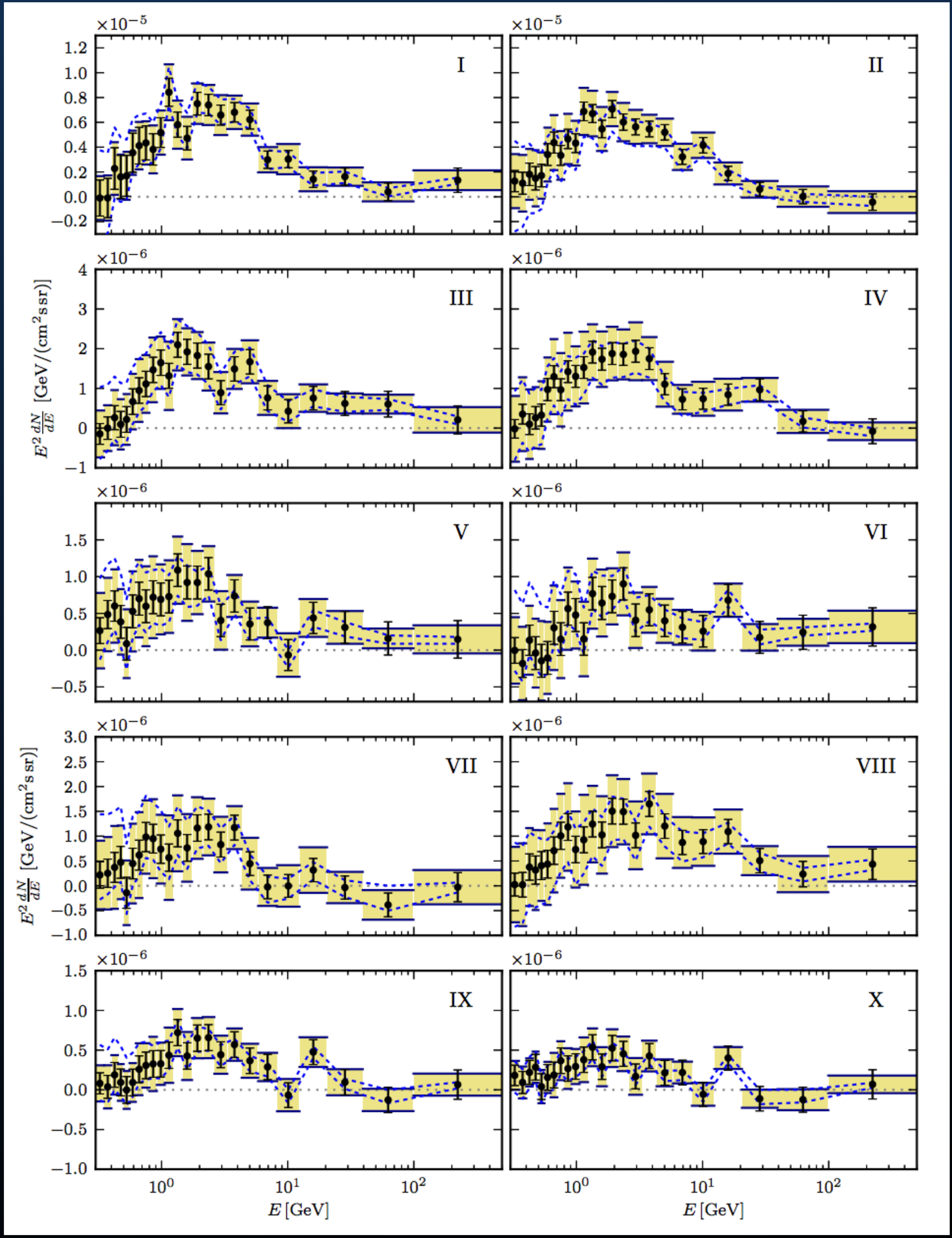

Cholis et al. (2014; 1409.0042)

Emission Extends Outside Bulge

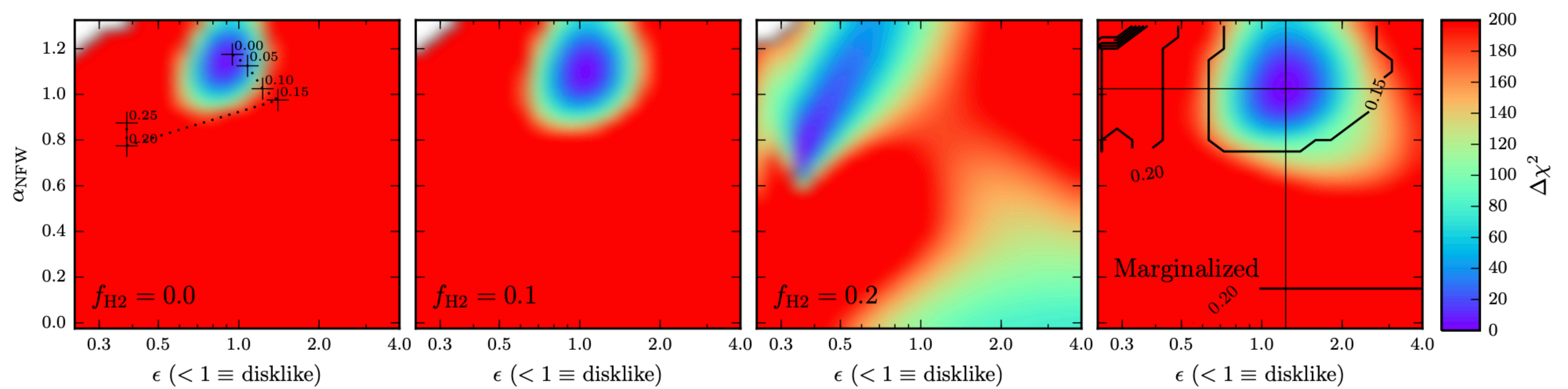

Changes in the diffuse model can lead to very different fits.

Carlson, TL, Profumo (1603.06584)

Multi-Wavelength Lines of Evidence

Part I:

MSP Luminosity Function

Arguments Against the Pulsar Interpretation

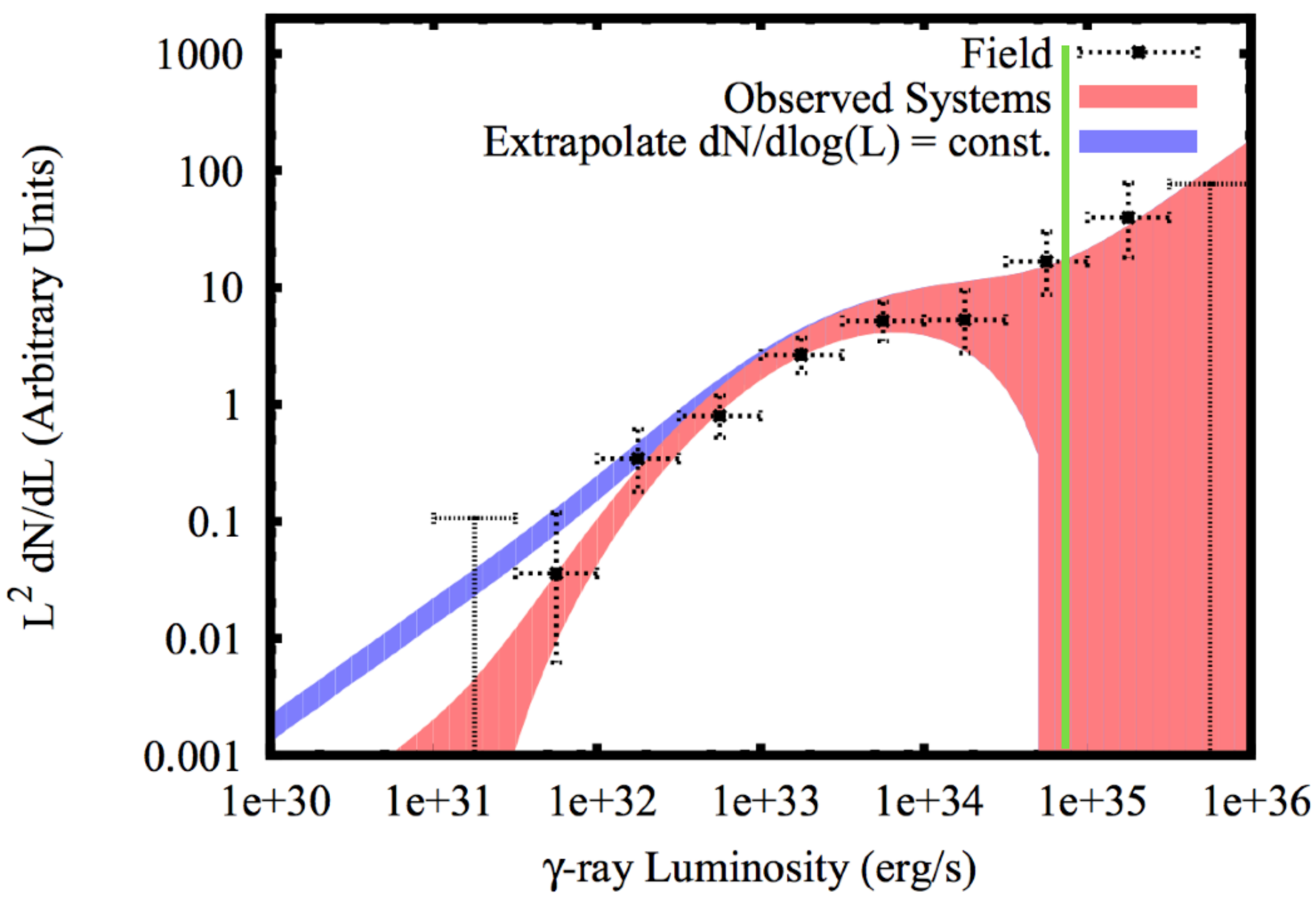

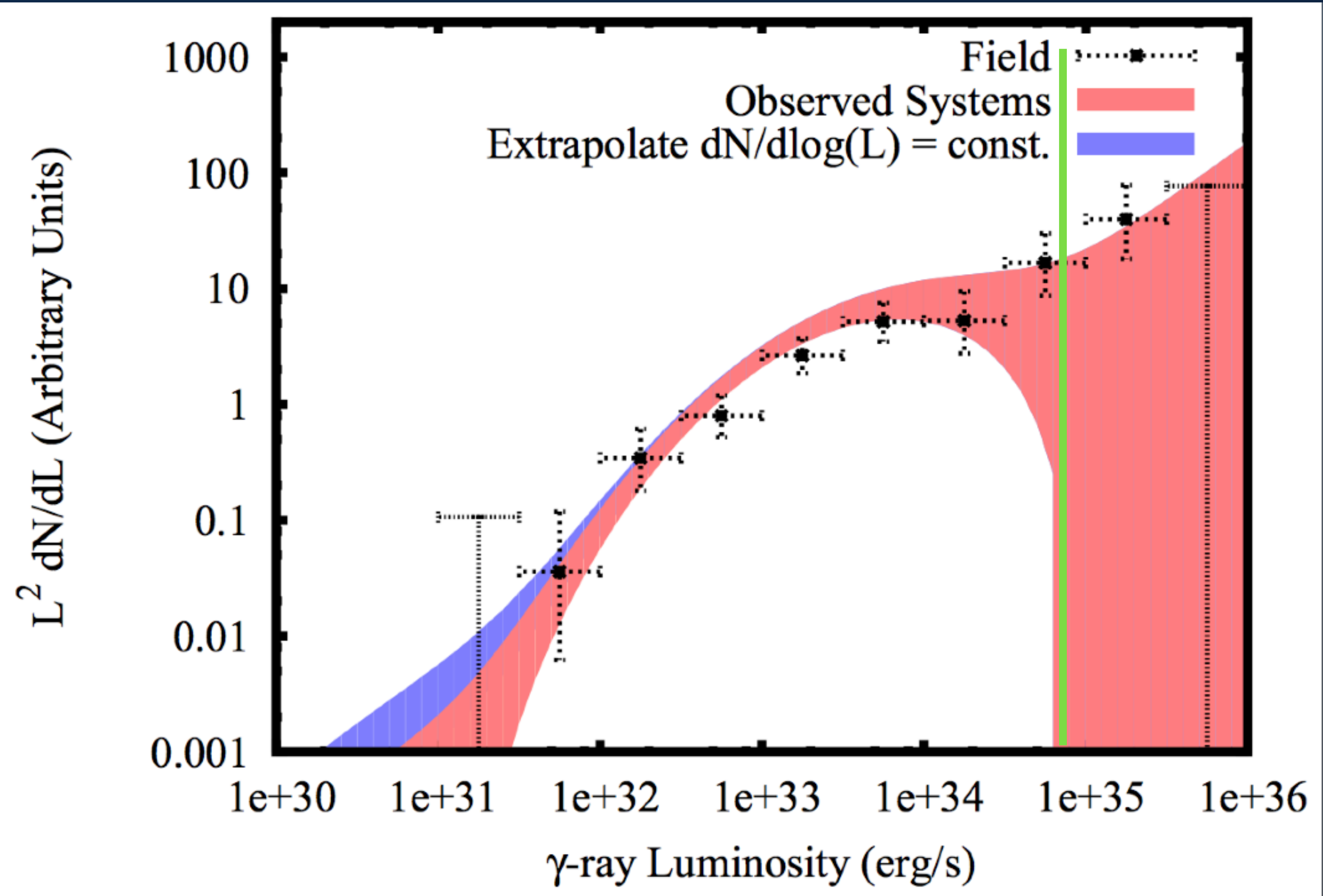

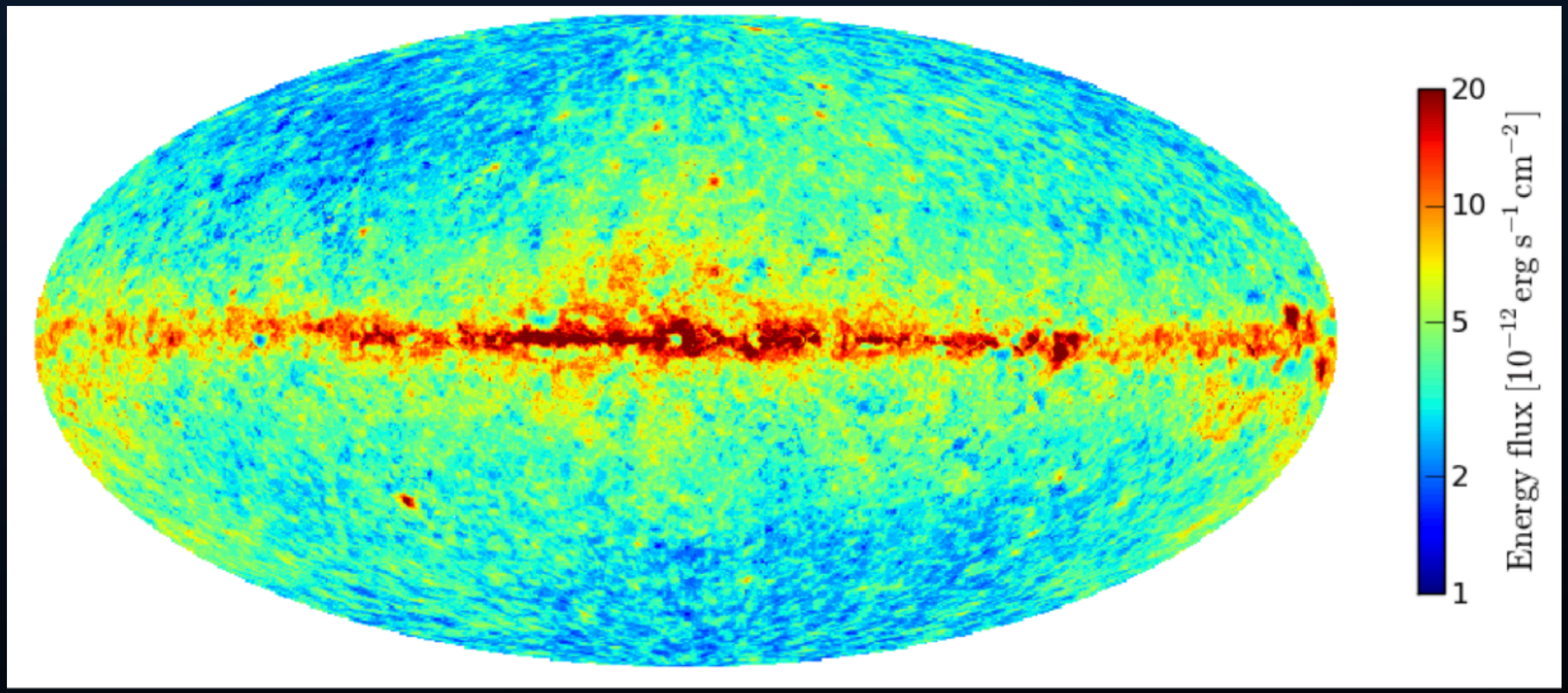

Cholis et al. (2014; 1407.5583)

Fermi-LAT Collaboration (2013; 1305.4385)

Arguments Against the Pulsar Interpretation

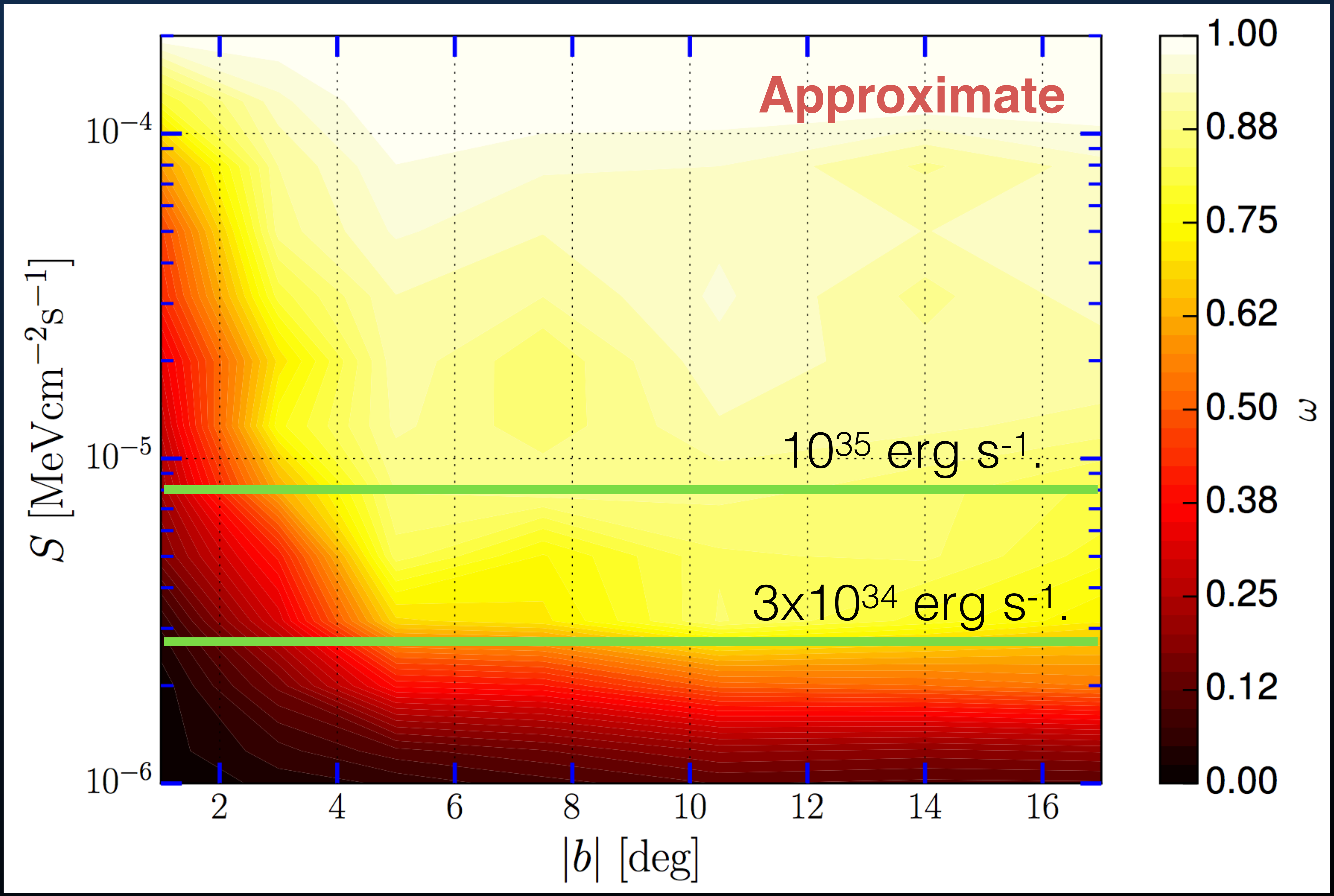

Fermi-LAT Collaboration (2017; 1705.00009v1)

Arguments Against the Pulsar Interpretation

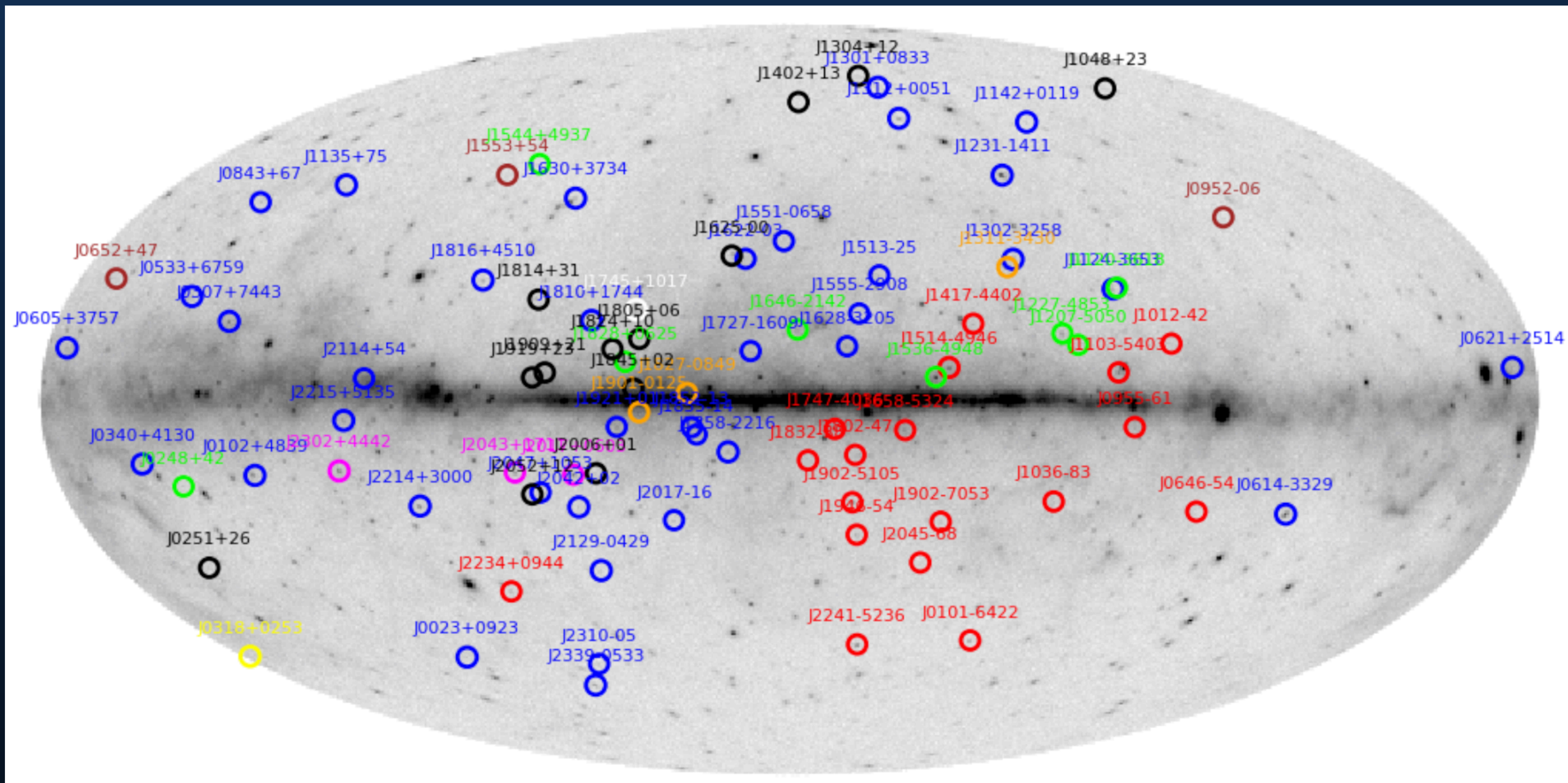

The distribution of observed pulsars does not show a bulge component.

Paul Ray (Private Communication; see also 1205.3089)

Part I:

MSP Luminosity Function

Arguments for the Pulsar Interpretation

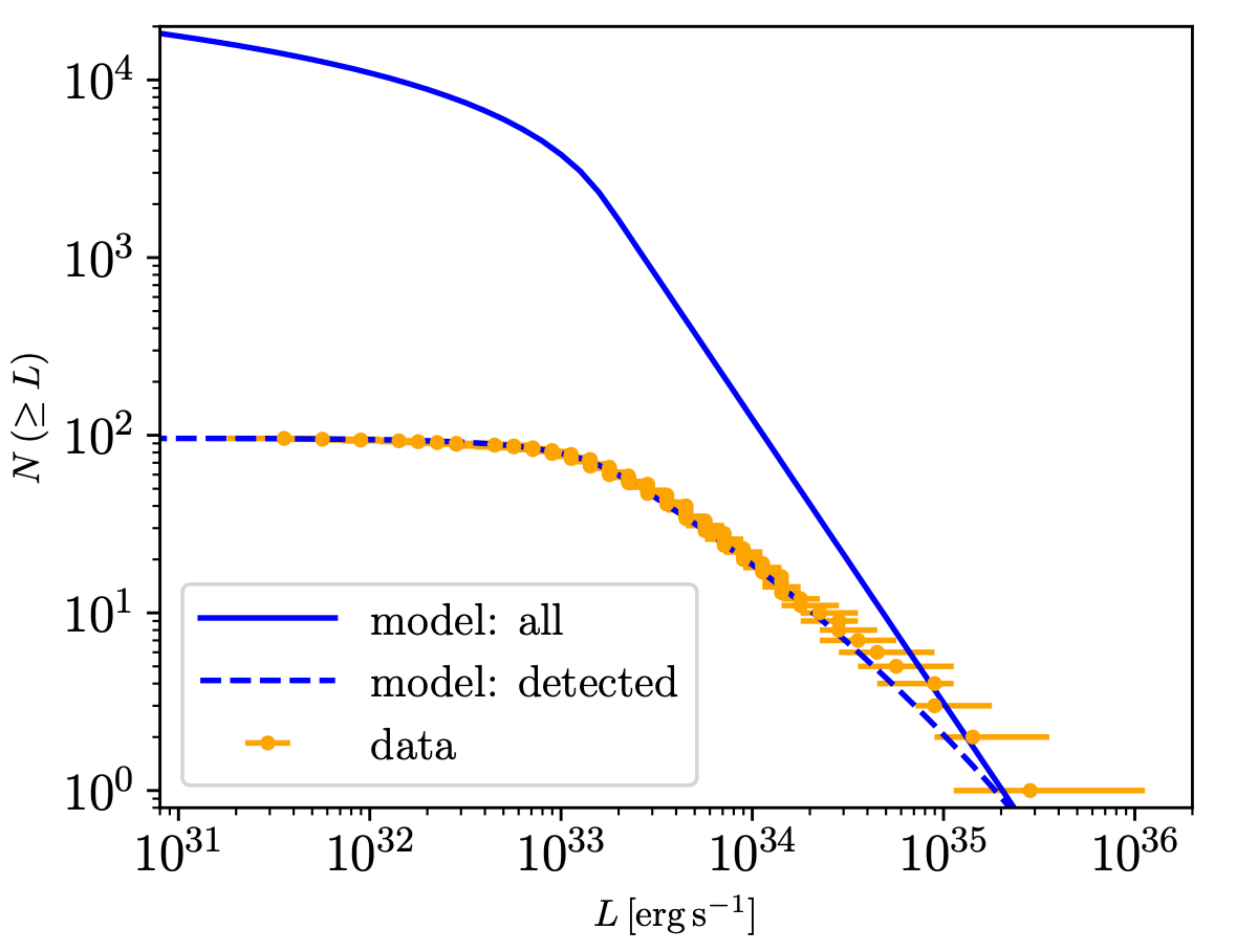

Other groups have found different luminosity distributions - can avoid this problem.

Bartels et al. (1805.11097)

Arguments for the Pulsar Interpretation

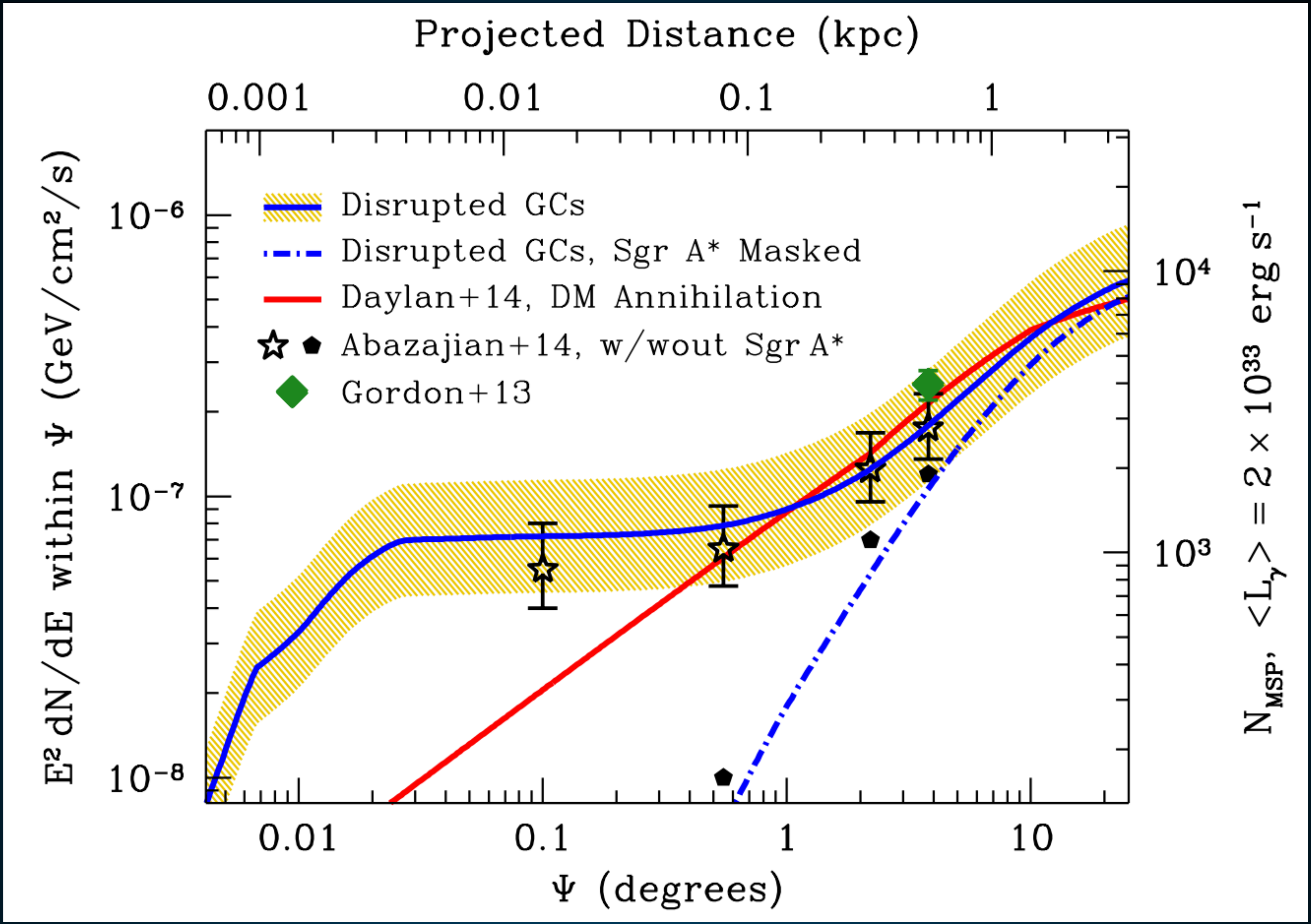

Dynamical Models involving disrupted globular clusters have been proposed.

Brandt & Kocsis (1507.05616)

Part II:

LMXB Density

The Low-Mass X-Ray Binary Connection

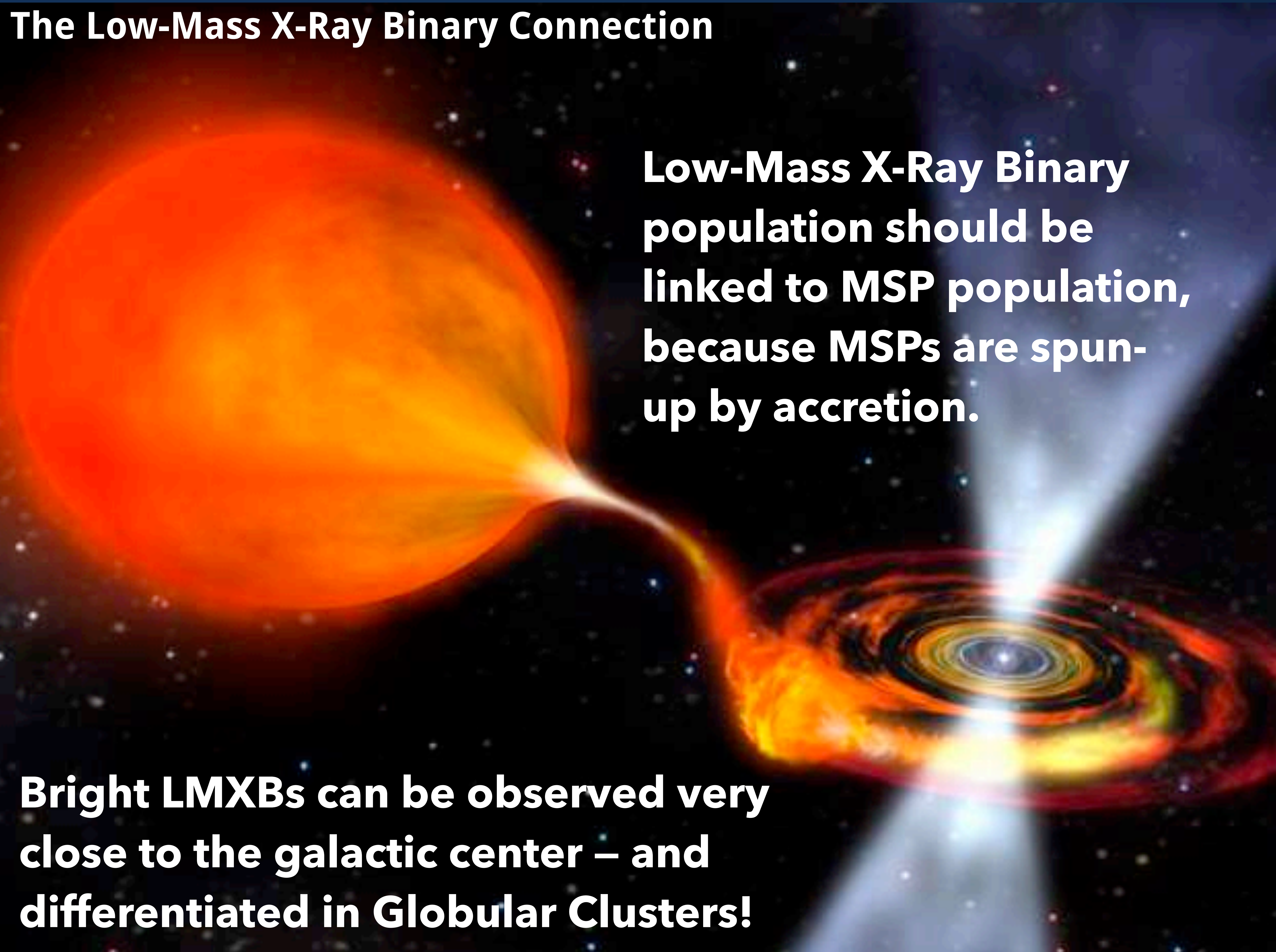

Low-Mass X-Ray Binary population should be linked to MSP population, because MSPs are spun-up by accretion.

Bright LMXBs can be observed very close to the galactic center – and differentiated in Globular Clusters!

The Low-Mass X-Ray Binary Connection

$$L_\gamma^{\mathrm{IG}} = L_\gamma^{\mathrm{clusters}} \times \left(\frac{N_{\mathrm{LMXB}}^{\mathrm{IG}}}{N_{\mathrm{LMXB}}} \right)$$

Globular Cluster	Flux (erg/cm^2/s)	Distance (kpc)	Stellar Encounter Rate	TS
NGC 104	$2.51^{+0.05}_{-0.06} \times 10^{-11}$	4.46	1.00	3995.9
NGC 362	$6.74^{+2.63}_{-2.46} \times 10^{-13}$	8.61	0.74	9.69
Palomar 2	$< 2.69 \times 10^{-13}$	27.11	0.93	0.0
NGC 6624	$1.14^{+0.10}_{-0.10} \times 10^{-11}$	7.91	1.15	455.8
NGC 1851	$9.05^{+2.92}_{-2.67} \times 10^{-13}$	12.1	1.53	14.4
NGC 5824	$< 4.78 \times 10^{-13}$	32.17	0.98	0.0
NGC 6093	$4.32^{+0.57}_{-0.53} \times 10^{-12}$	10.01	0.53	91.9
NGC 6266	$1.84^{+0.07}_{-0.10} \times 10^{-11}$	6.83	1.67	850.7
NGC 6284	$< 2.85 \times 10^{-13}$	15.29	0.67	0.0
NGC 6441	$1.00^{+0.09}_{-0.07} \times 10^{-11}$	11.6	2.30	210.9
NGC 6652	$4.84^{+0.51}_{-0.52} \times 10^{-12}$	10.0	0.70	128.3
NGC 7078/M15	$1.81^{+0.40}_{-0.39} \times 10^{-12}$	10.4	4.51	29.7
NGC 6440	$1.57^{+0.10}_{-0.11} \times 10^{-11}$	8.45	1.40	311.2
Terzan 6	$2.18^{+1.20}_{-0.90} \times 10^{-12}$	6.78	2.47	5.1
NGC 6388	$1.77^{+0.06}_{-0.09} \times 10^{-11}$	9.92	0.90	778.4
NGC 6626/M28	$1.95^{+0.13}_{-0.13} \times 10^{-11}$	5.52	0.65	749.8
Terzan 5	$6.61^{+0.17}_{-0.13} \times 10^{-11}$	5.98	6.80	2707.1
NGC 6293	$9.39^{+5.69}_{-5.45} \times 10^{-13}$	9.48	0.85	3.98
NGC 6681	$9.91^{+4.14}_{-3.86} \times 10^{-13}$	9.01	1.04	7.2
NGC 2808	$3.77^{+0.48}_{-0.48} \times 10^{-11}$	9.59	0.92	96.7
NGC 6715	$6.02^{+4.15}_{-3.77} \times 10^{-13}$	26.49	2.52	2.6
NGC 7089	$< 4.50 \times 10^{-13}$	11.56	0.52	0.0

LMXB	Notes	Globular Cluster	References
4U 1820-30	P	NGC 6624	[69–71]
4U 0513-40	P	NGC 1851	[72–74]
4U 1746-37	P	NGC 6441	[69, 75, 76]
XB 1832-330	P	NGC 6652	[75, 77, 78]
M15 X-2	P	NGC 7078/M15	[79–81]
AC 211	P	NGC 7078/M15	[69, 80, 82]
SAX J1748.9-2021	T, XP	NGC 6440	[75, 83, 84]
GRS 1747-312	T	Terzan 6	[85–87]
Terzan 6 X-2	T	Terzan 6	[88]
IGR J17361-4441	T	NGC 6388	[89, 90]
IGR J18245-2542	T, XP	NGC 6626/M28	[91, 92]
EXO 1745-248	T	Terzan 5	[93, 94]
IGR J17480-2446	T	Terzan 5	[95–97]
Terzan 5 X-3	T	Terzan 5	[98]
MAXI J0911-635	T	NGC 2808	[99]

Haggard et al. (2017; 1701.02726)

The Low-Mass X-Ray Binary Connection

$$L_\gamma^{\mathrm{IG}} = L_\gamma^{\mathrm{clusters}} \times \left(\frac{N_{\mathrm{LMXB}}^{\mathrm{IG}}}{N_{\mathrm{LMXB}}} \right)$$

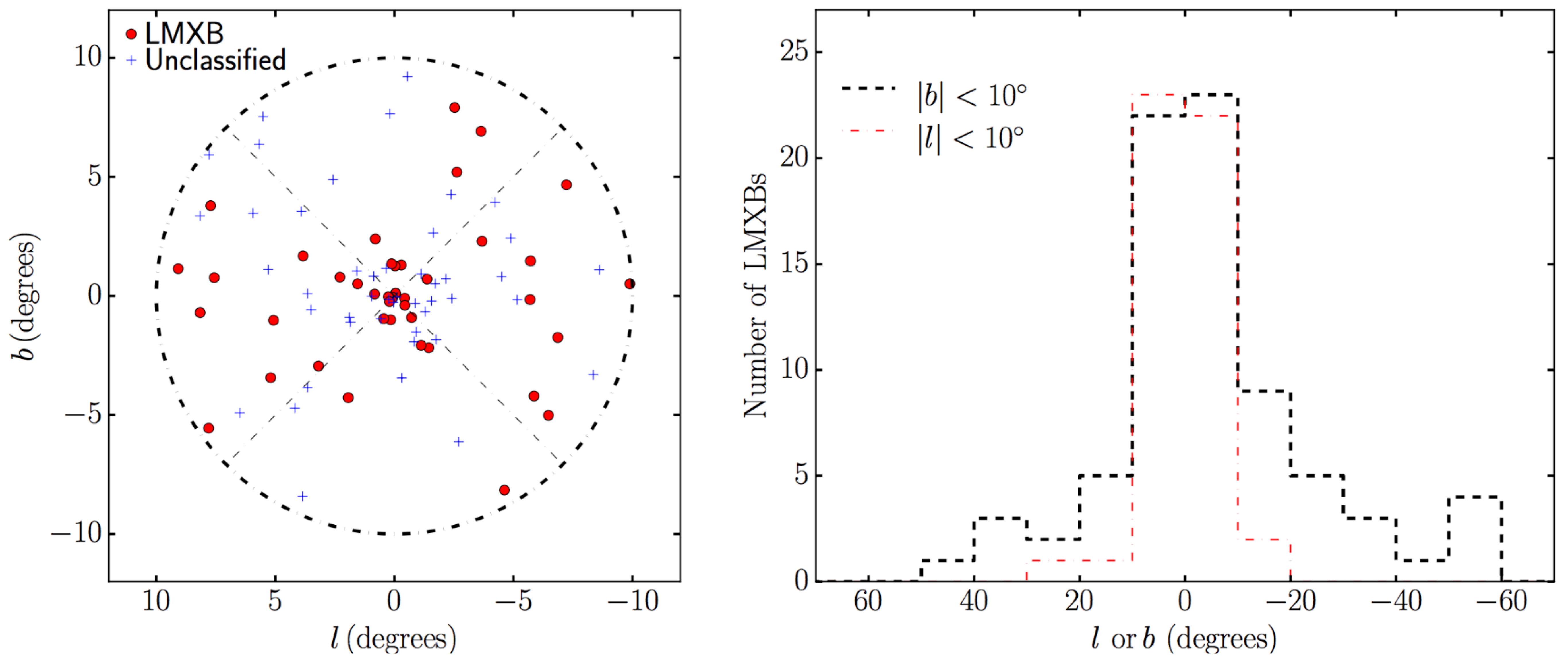

Haggard et al. (2017; 1701.02726)

The Low-Mass X-Ray Binary Connection

$$L_\gamma^{\rm IG} = L_\gamma^{\rm clusters} \times \left(\frac{N_{\rm LMXB}^{\rm IG}}{N_{\rm LMXB}} \right)$$

$$\begin{aligned}
L_\gamma^{\rm IG} &= (2.09^{+0.86}_{-0.71}) \times 10^{36}\,{\rm erg/s}, && \text{Only Sources Classified as LMXBs} \\
L_\gamma^{\rm IG} &= (4.38^{+1.79}_{-1.48}) \times 10^{36}\,{\rm erg/s}, && \text{Including All Unclassified Sources} \qquad (4.2)
\end{aligned}$$

Comparing this result with the measured gamma-ray luminosity of gamma-ray excess, $L_\gamma = (2.0 \pm 0.4) \times 10^{37}$ erg/s integrated within 10° of the Galactic Center [8, 113], we estimate that $10.5^{+4.7}_{-4.1}\%$ (only LMXBs) or $21.9^{+9.9}_{-8.6}\%$ (LMXBs and unclassified) of the excess emission can be potentially attributed to an underlying MSP population. As mentioned above, however, this calculation almost certainly overestimates the fraction of the Galactic Center excess that arises from MSPs.

Haggard et al. (2017; 1701.02726)

Are Dark Matter Models Ruled Out?

Ackermann et al. (2015; 1503.02641)

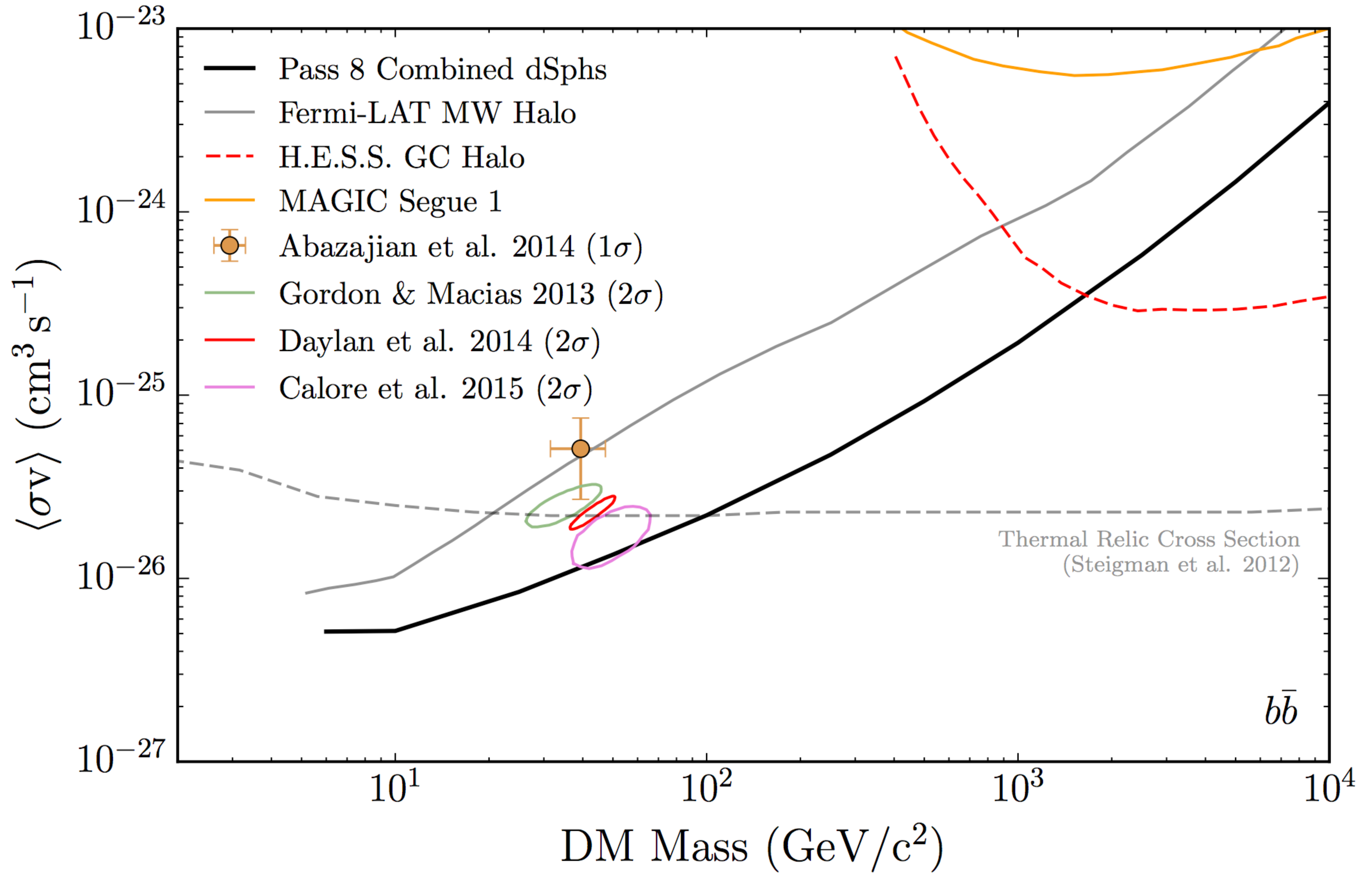

Multi-Wavelength Lines of Evidence

Part II:

LMXB Density

Multi-Wavelength Lines of Evidence

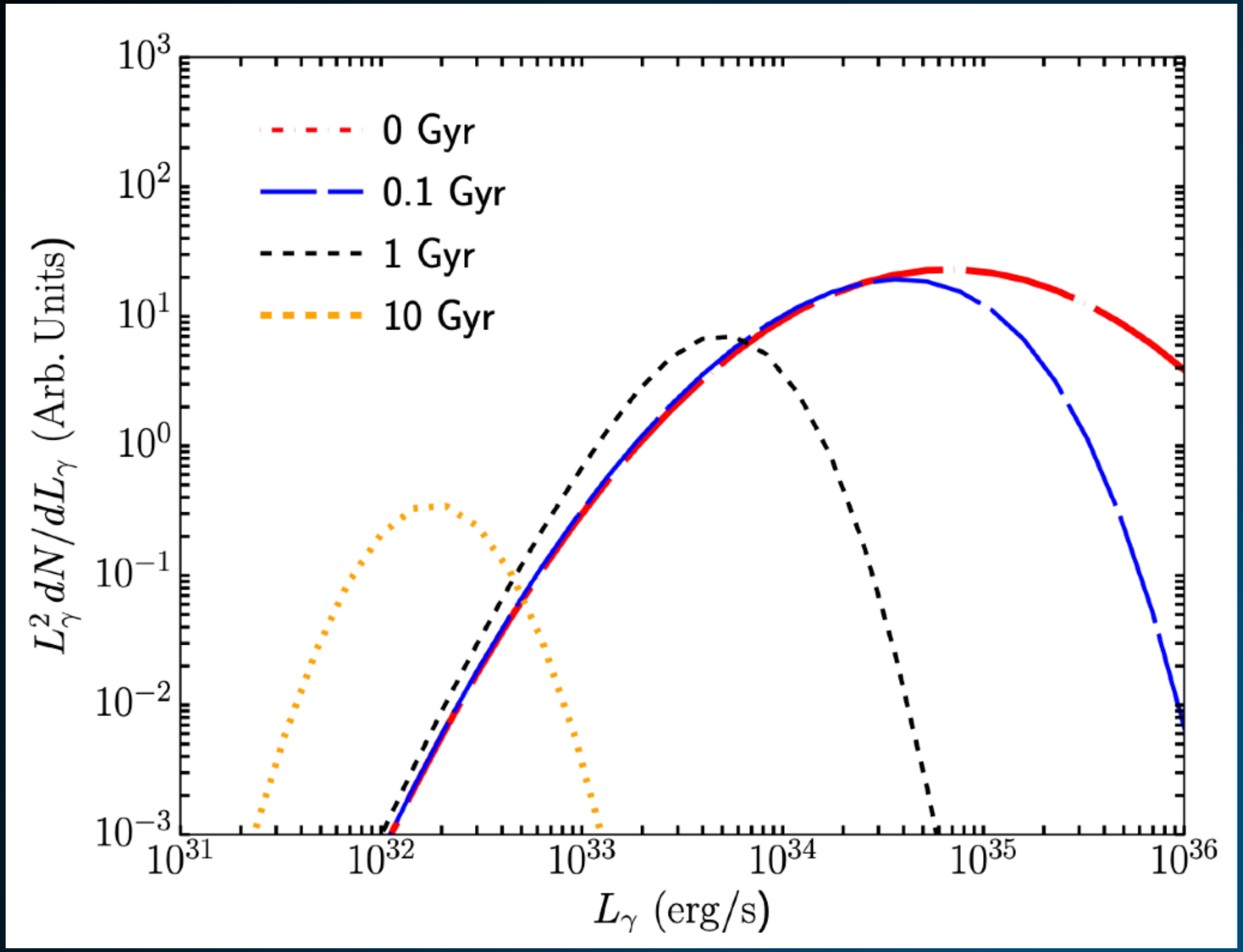

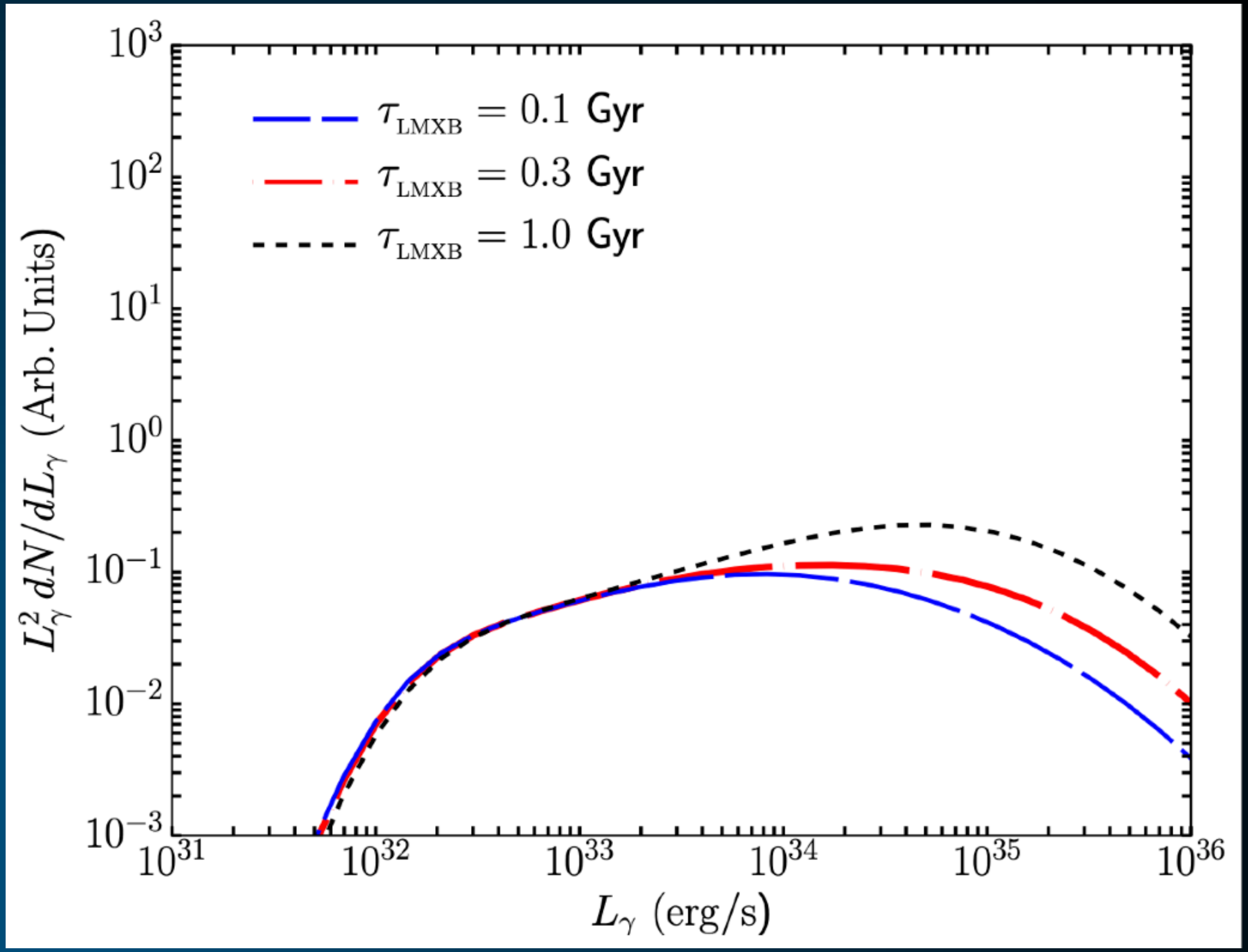

Comparative normalization depends on the spin-down of both parameters.

Hooper & Linden (1606.09250)

Are Dark Matter Models Ruled Out?

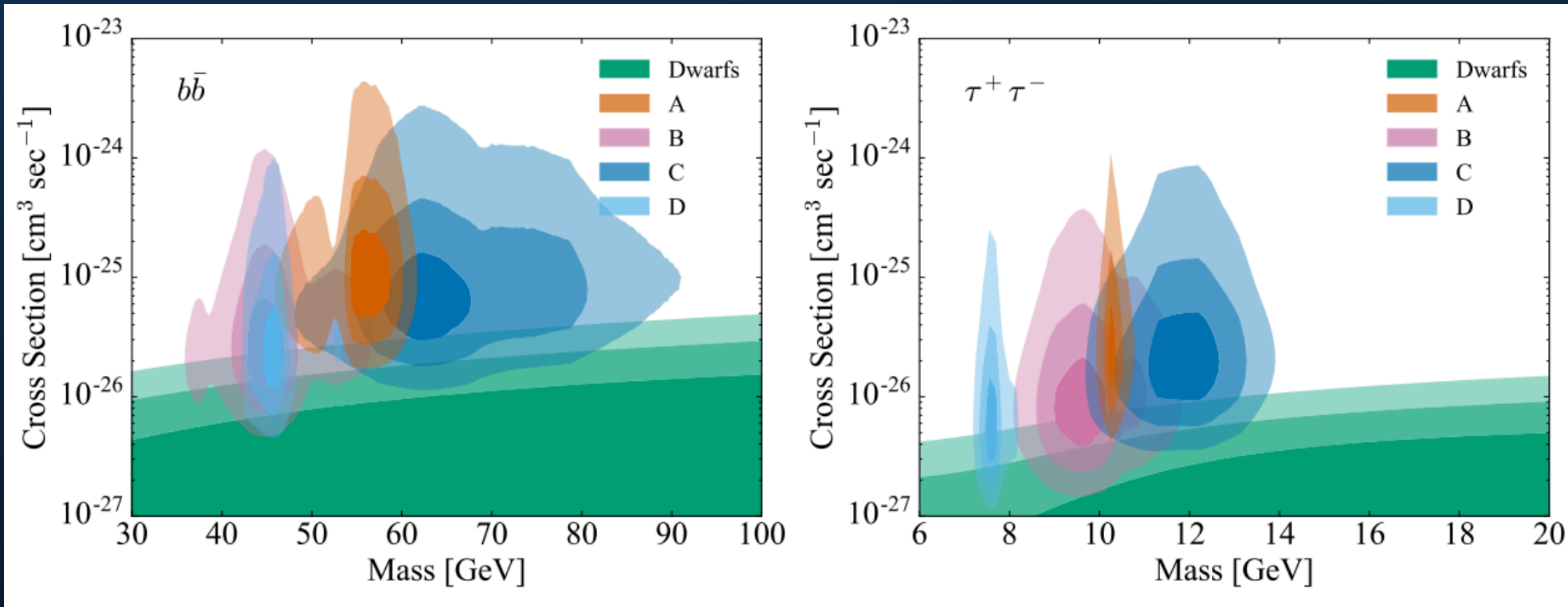

For the local density, we use the value determined by Zhang et al. (2012) [59]: $\rho_\odot = 0.28 \pm 0.08$ GeV cm^{-3}. This robust determination of the local DM density is derived from modeling the spatial and velocity distributions for a sample of 9000 K-Dwarf stars from the Sloan Digital Sky Survey (SDSS). The velocity distribution of these stars directly measures the local gravitational potential and, when combined with stellar density constraints, provides a measure of the local DM density.

		α-young Tilt	α-young No Tilt	α-old Tilt	α-old No Tilt	Combined analysis Tilt
95% CR upper	GeV cm^{-3}	**0.59**	0.57	0.85	0.51	0.48
	M$_\odot$ pc^{-3}	**0.016**	0.015	0.022	0.013	0.013
68% CR upper	GeV cm^{-3}	**0.53**	0.53	0.79	0.48	0.43
	M$_\odot$ pc^{-3}	**0.013**	0.014	0.021	0.013	0.012
Median	GeV cm^{-3}	**0.46**	0.48	0.73	0.46	0.40
	M$_\odot$ pc^{-3}	**0.012**	0.013	0.019	0.012	0.011
68% CR lower	GeV cm^{-3}	**0.37**	0.42	0.68	0.44	0.37
	M$_\odot$ pc^{-3}	**0.0098**	0.011	0.017	0.012	0.0097
95% CR lower	GeV cm^{-3}	**0.30**	0.35	0.60	0.42	0.34
	M$_\odot$ pc^{-3}	**0.0078**	0.0092	0.016	0.011	0.0091

Keeley et al. (2017; 1710.03215)

Sivertsson et al. (2017; 1708.07836)

Hints of Dark Matter Detections

Cuoco et al. (2017, 1711.06460)

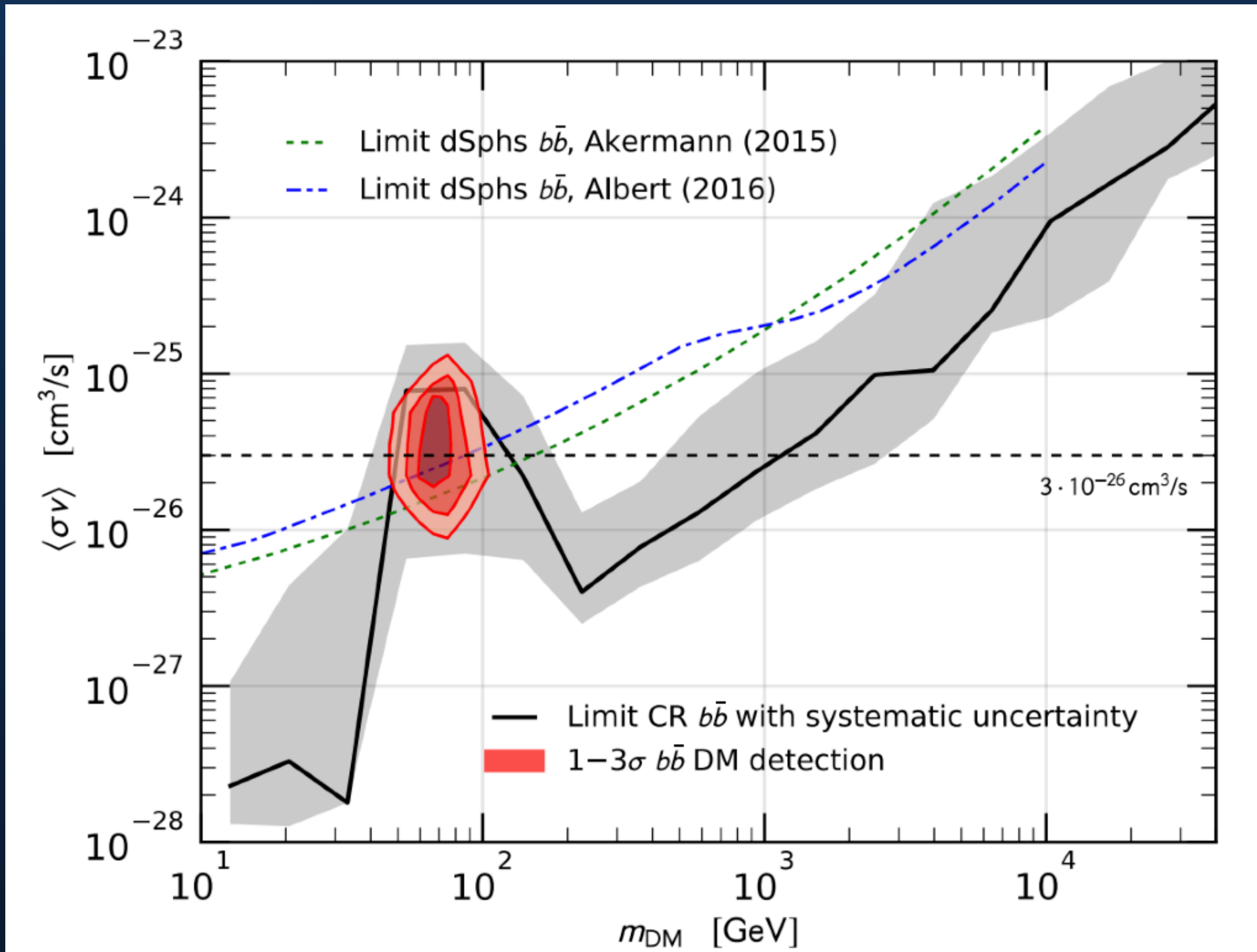

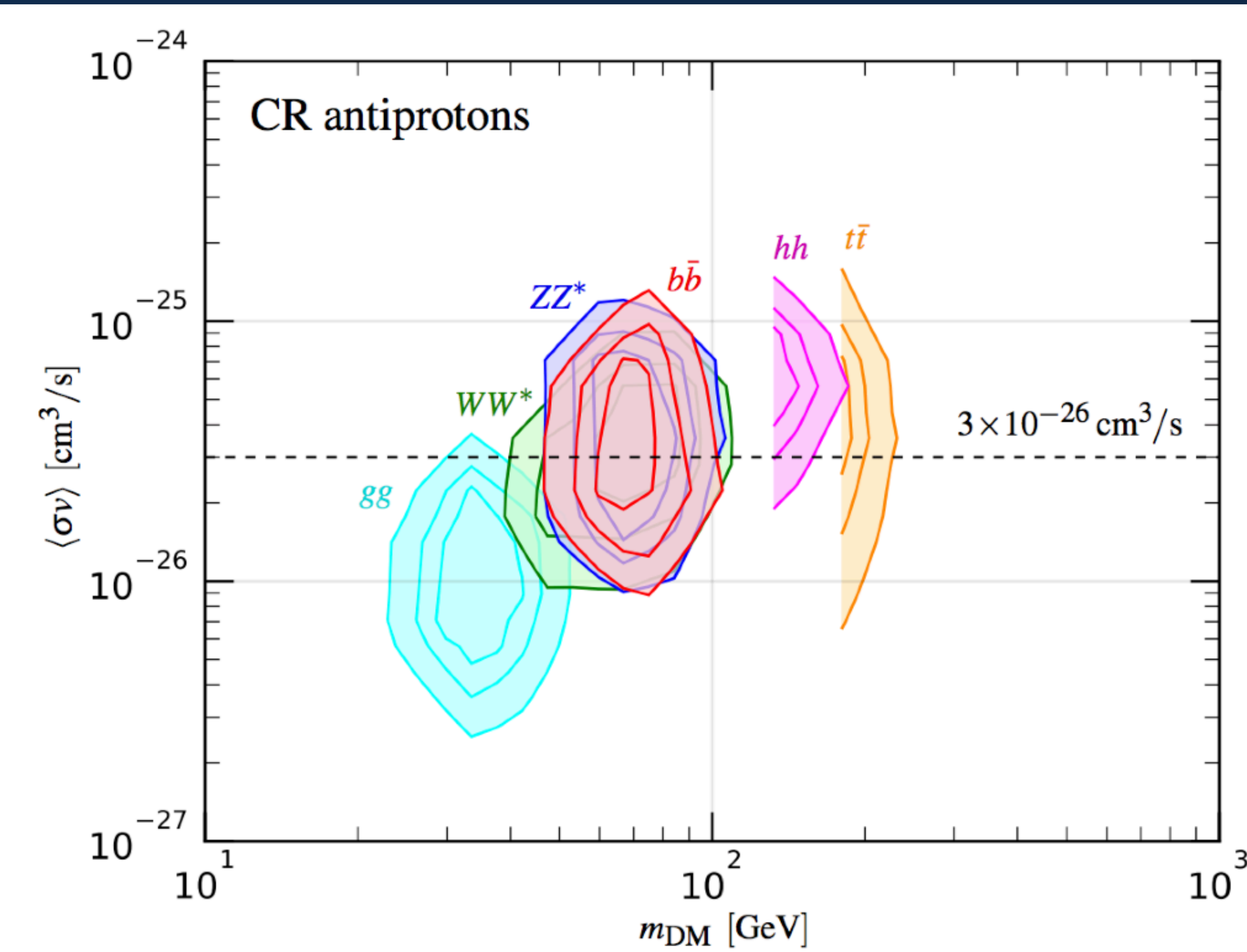

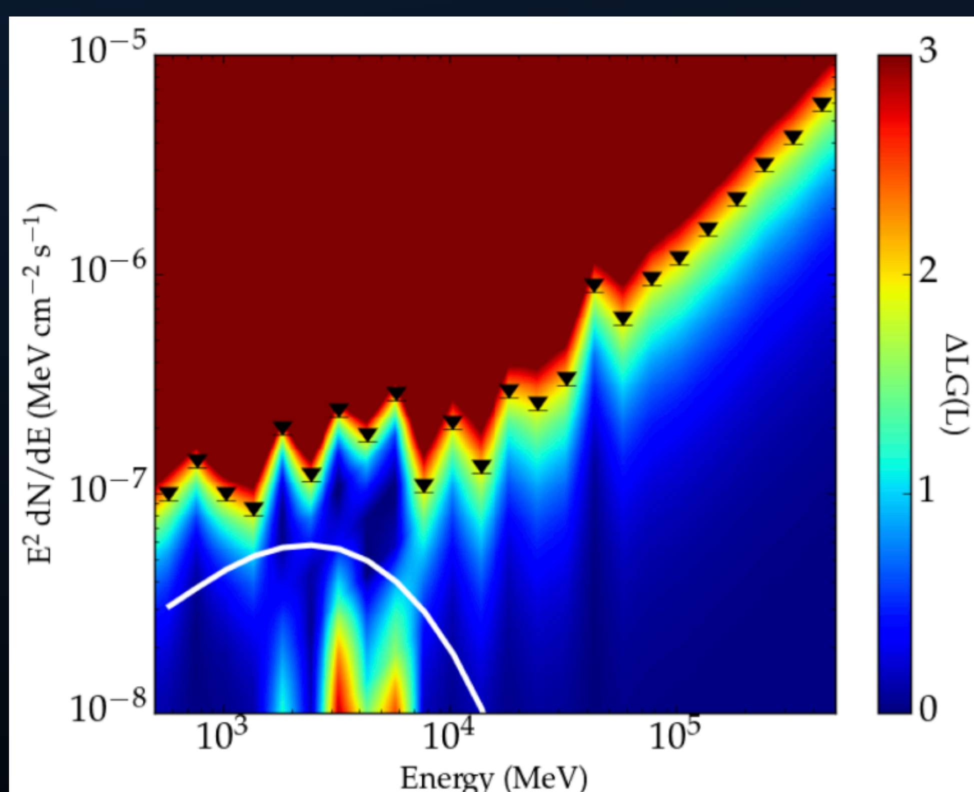

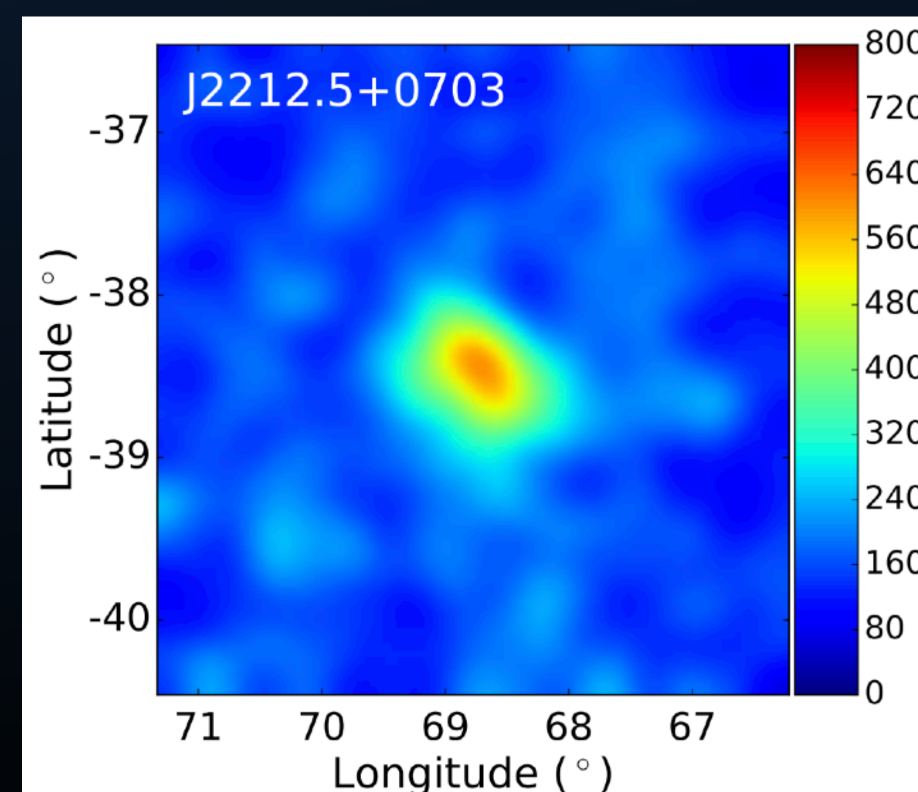

Hooper & Linden (2015, 1503.06029)

Bertoni et al. (2016; 1602.07303)

To date, we have observed eight events in the mass region from 0 to 10 GeV with Z= –2. All eight events are in the helium mass region.

Currently (having used 50 million core hours to generate 7 times more simulated events than measured events and having found no background events from the simulation), our best evaluation of the probability of the background origin for the eight $\overline{He}$ events is less than 3×10^{-8}. For the two $^{4}\overline{He}$ events our best evaluation of the probability (upon completion of the current 100 million core hours of simulation) will be less than 3×10^{-3}.

Note that for $^{4}\overline{He}$, projecting based on the statistics we have today, by using an additional 400 million core hours for simulation the background probability would be 10^{-4}. Simultaneously, continuing to run until 2023, which doubles the data sample, the background probability for $^{4}\overline{He}$ would be 2×10^{-7}, i.e., greater than 5-sigma significance.

Looking Forward

How to End a Talk When You Don't Have a Conclusion

REVIEW

https://doi.org/10.1038/s41586-018-0542-z

A new era in the search for dark matter

Gianfranco Bertone[1]* & Tim M. P. Tait[1,2]*

There is a growing sense of 'crisis' in the dark-matter particle community, which arises from the absence of evidence for the most popular candidates for dark-matter particles—such as weakly interacting massive particles, axions and sterile neutrinos—despite the enormous effort that has gone into searching for these particles. Here we discuss what we have learned about the nature of dark matter from past experiments and the implications for planned dark-matter searches in the next decade. We argue that diversifying the experimental effort and incorporating astronomical surveys and gravitational-wave observations is our best hope of making progress on the dark-matter problem.

The fall of natural weakly interacting massive particles

The existence of dark matter has been discussed for more than a century[1,2]. In the 1970s, astronomers and cosmologists began to build what is today a compelling body of evidence for this elusive component of the Universe, based on a variety of observations, including temperature anisotropies of the cosmic microwave background, baryonic acoustic oscillations, type Ia supernovae, gravitational lensing of galaxy clusters and rotation curves of galaxies[3,4]. The standard model of particle physics contains no suitable particle to explain these observations, and

the observed Higgs mass at the weak scale appears highly unnatural, requiring an incredibly fine-tuned cancellation between the individually much larger intrinsic contribution and the correction terms, such that their sum is the value observed at the Large Hadron Collider (LHC). Natural theories introduce additional particles and symmetries, which are arranged so that these large corrections cancel each other out, protecting the Higgs mass from the influence of heavy mass scales.

The prototypical natural theory is the minimal supersymmetric (SUSY) standard model, which introduces an additional partner for

Looking Forward

How to End a Talk When You Don't Have a Conclusion

MIT-CTP/5020

GeV-Scale Thermal WIMPs: Not Even Slightly Dead

Rebecca K. Leane,[1,*] Tracy R. Slatyer,[1,†] John F. Beacom,[2,3,4,‡] and Kenny C. Y. Ng[5,§]

[1]*Center for Theoretical Physics, Massachusetts Institute of Technology, Cambridge, MA 02139, USA*
[2]*Center for Cosmology and AstroParticle Physics (CCAPP), Ohio State University, Columbus, OH 43210, USA*
[3]*Department of Physics, Ohio State University, Columbus, OH 43210, USA*
[4]*Department of Astronomy, Ohio State University, Columbus, OH 43210, USA*
[5]*Department of Particle Physics and Astrophysics, Weizmann Institute of Science, Rehovot 76100, Israel*

(Dated: July 13, 2018)

Weakly Interacting Massive Particles (WIMPs) have long reigned as one of the leading classes of dark matter candidates. The observed dark matter abundance can be naturally obtained by freeze-out of weak-scale dark matter annihilations in the early universe. This "thermal WIMP" scenario makes direct predictions for the total annihilation cross section that can be tested in present-day experiments. While the dark matter mass constraint can be as high as $m_\chi \gtrsim 100$ GeV for particular annihilation channels, the constraint on the *total* cross section has not been determined. We construct the first model-independent limit on the WIMP total annihilation cross section, showing that allowed combinations of the annihilation-channel branching ratios considerably weaken the sensitivity. For thermal WIMPs with s-wave $2 \to 2$ annihilation to visible final states, we find the dark matter mass is only known to be $m_\chi \gtrsim 20$ GeV. This is the strongest largely model-independent lower limit on the mass of thermal-relic WIMPs; together with the upper limit on the mass from the unitarity bound ($m_\chi \lesssim 100$ TeV), it defines what we call the "WIMP window". To probe the remaining mass range, we outline ways forward.

I. INTRODUCTION

A leading candidate for dark matter (DM) is a Weakly Interacting Massive Particle (WIMP) that is a thermal

scenarios. The branching ratios, coupling types and signals are model-dependent, and so the lack of observations may just be due to such features. For example, there can be interference effects, momentum suppression, or

Looking Forward

Leane et al. (2018; 1805.10305)

How to End a Talk When You Don't Have a Conclusion

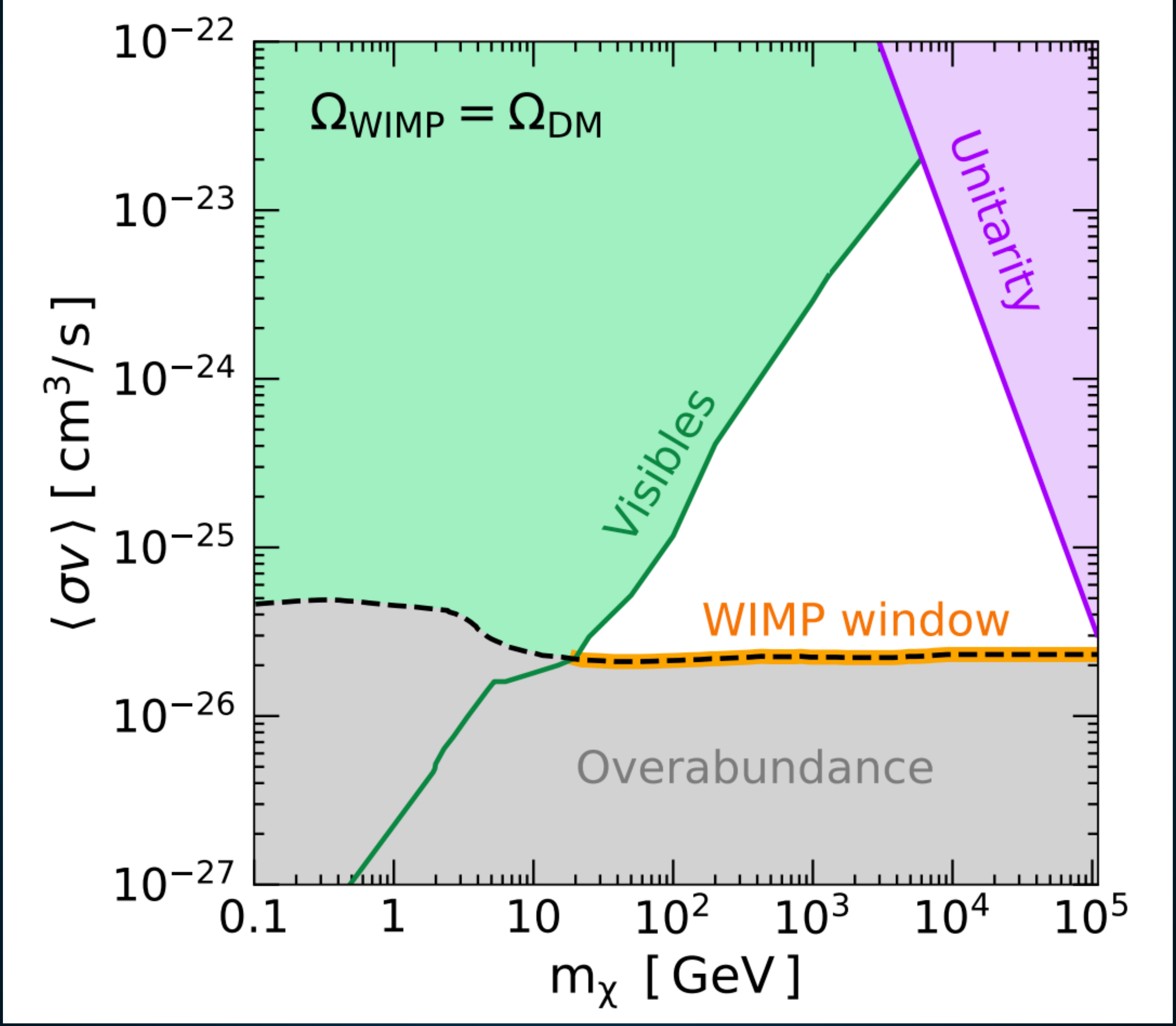

Looking Forward

How to End a Talk When You Don't Have a Conclusion

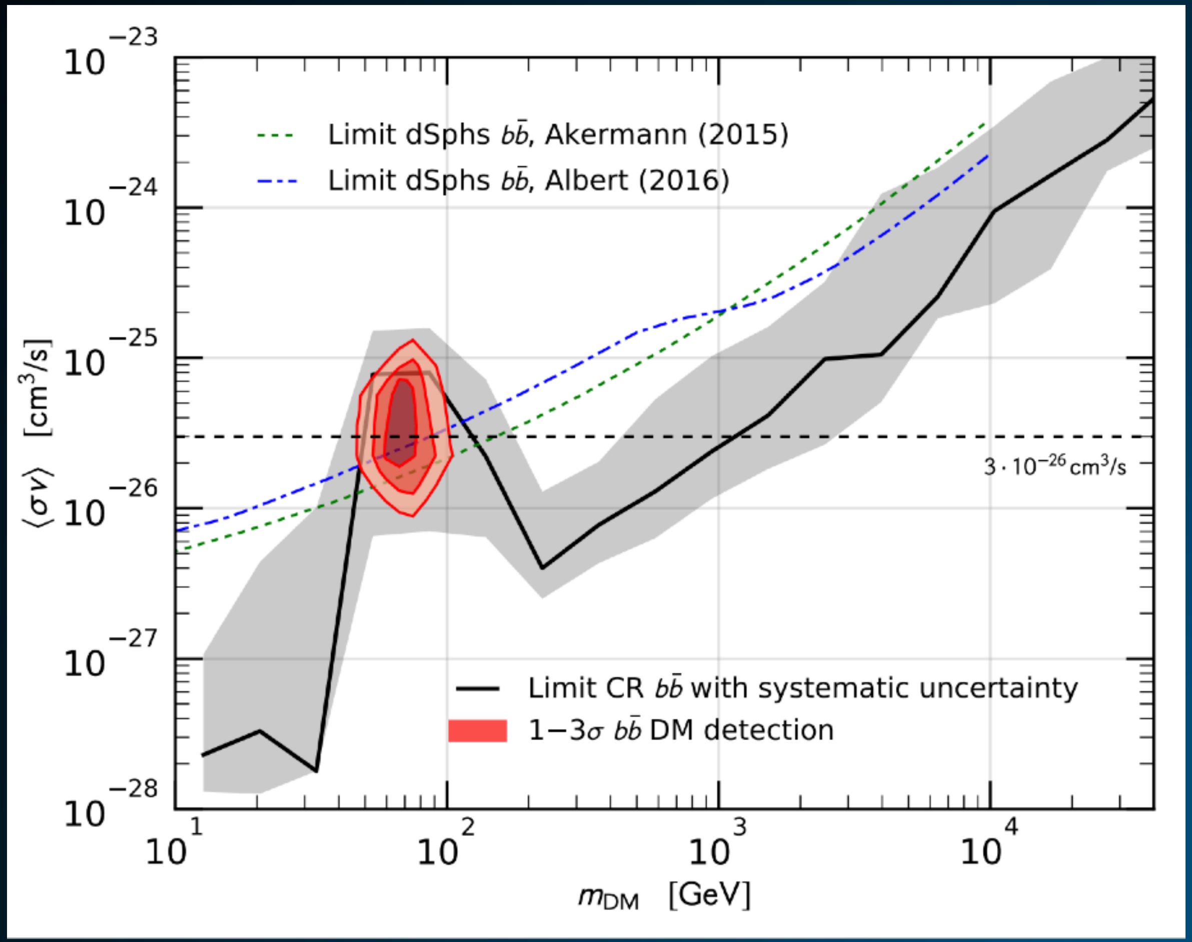

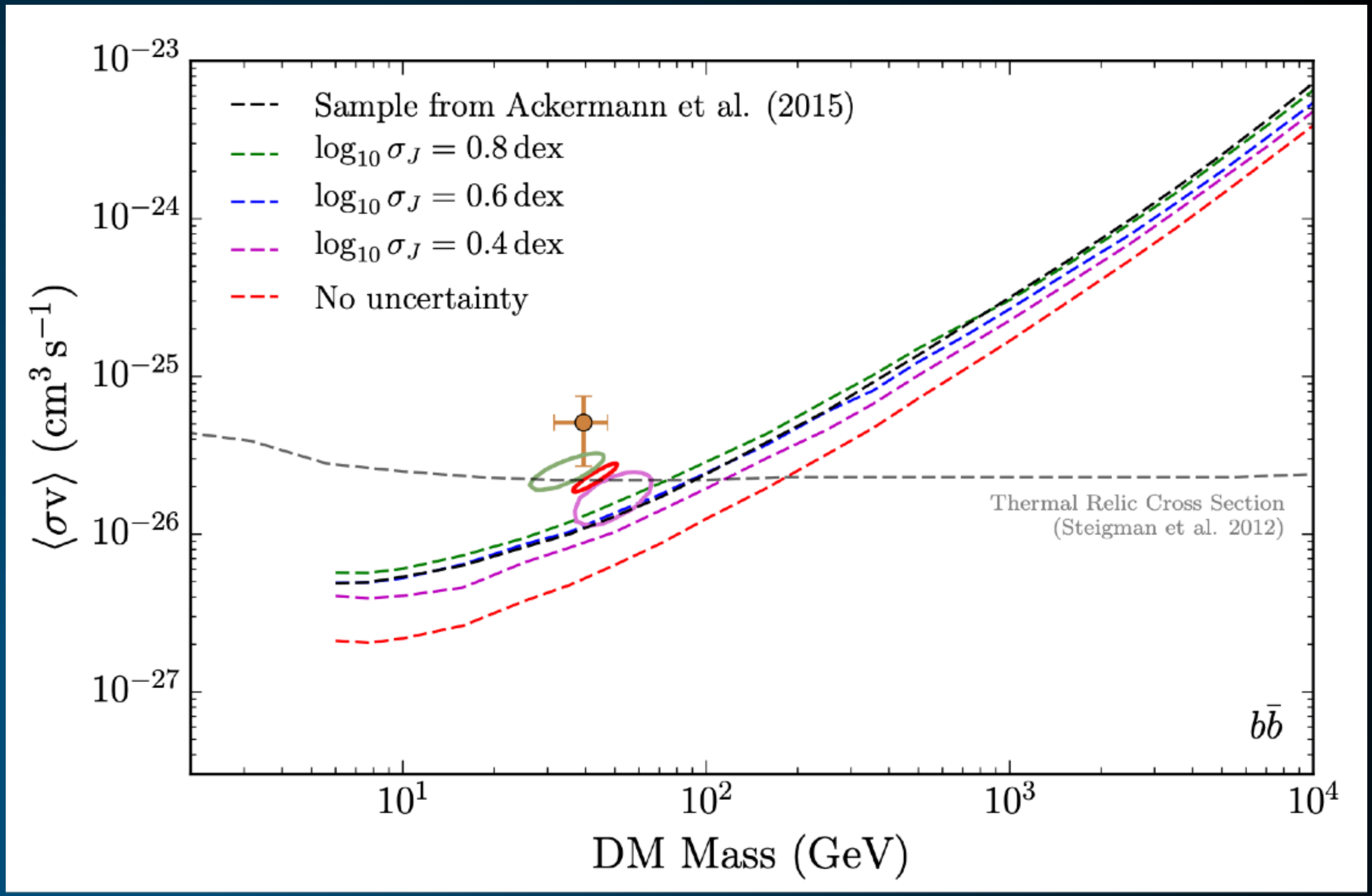

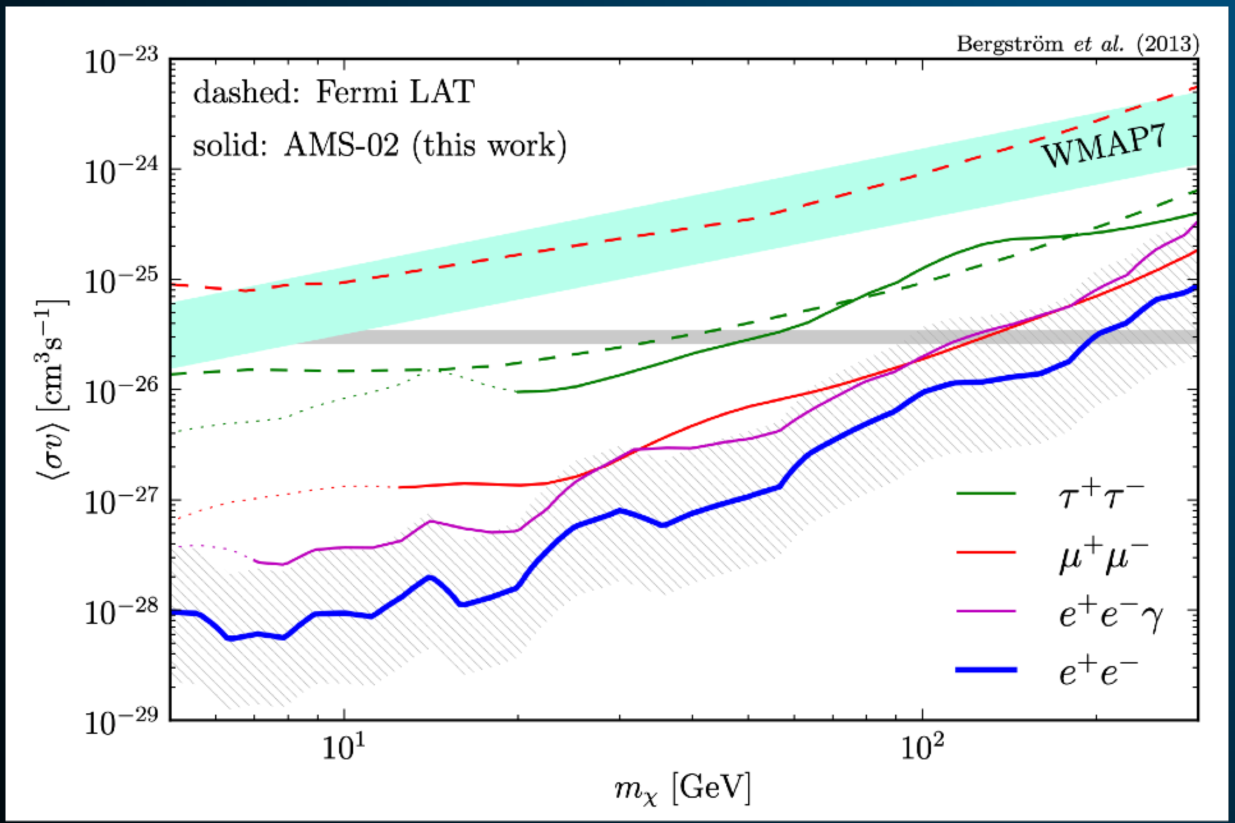

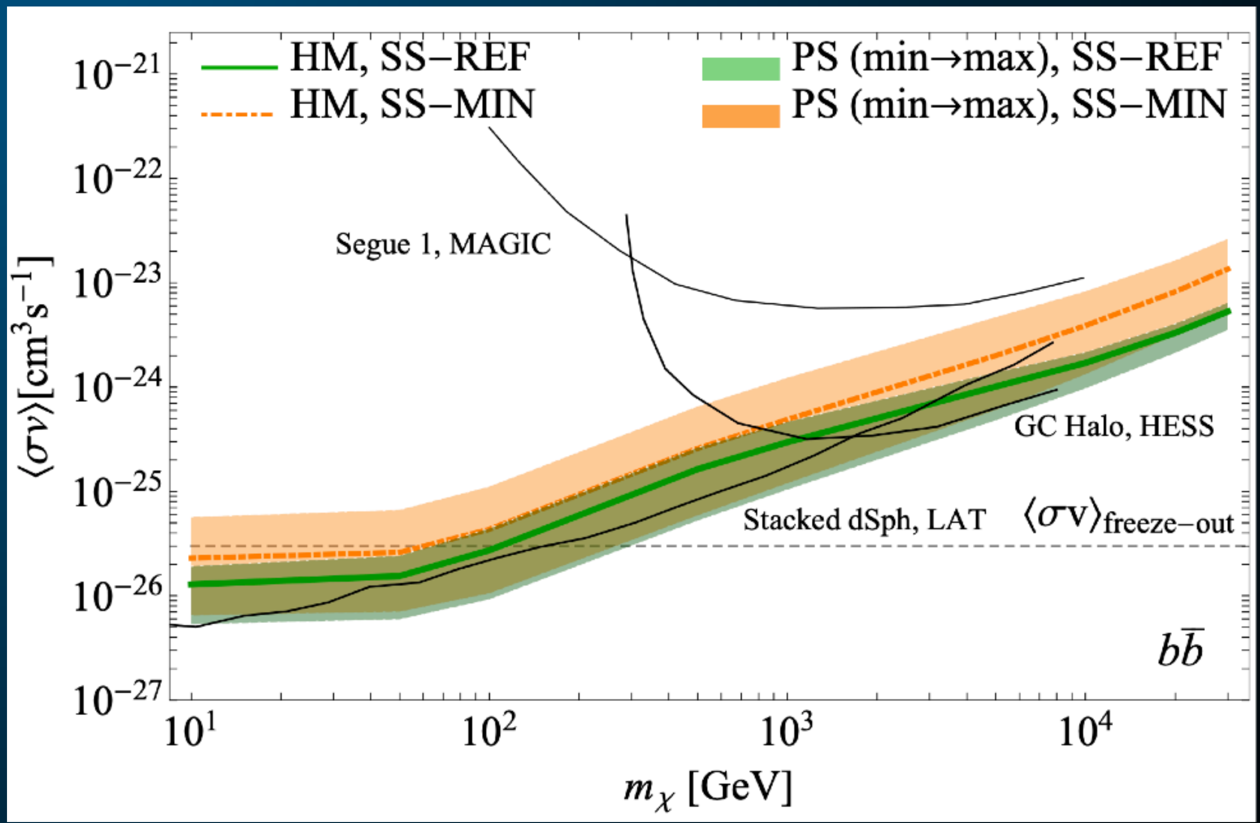

Looking Forward

How to End a Talk When You Don't Have a Conclusion

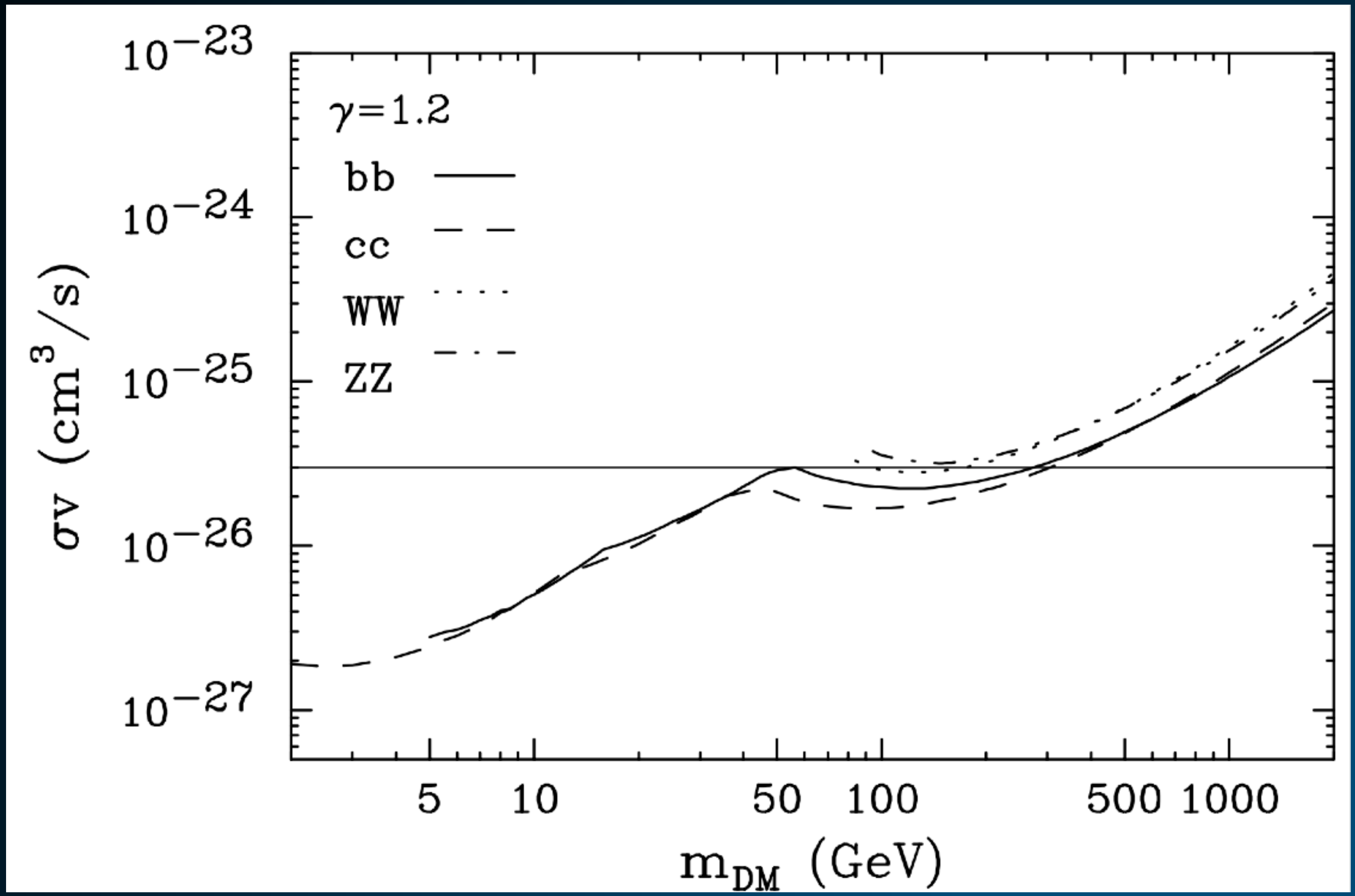

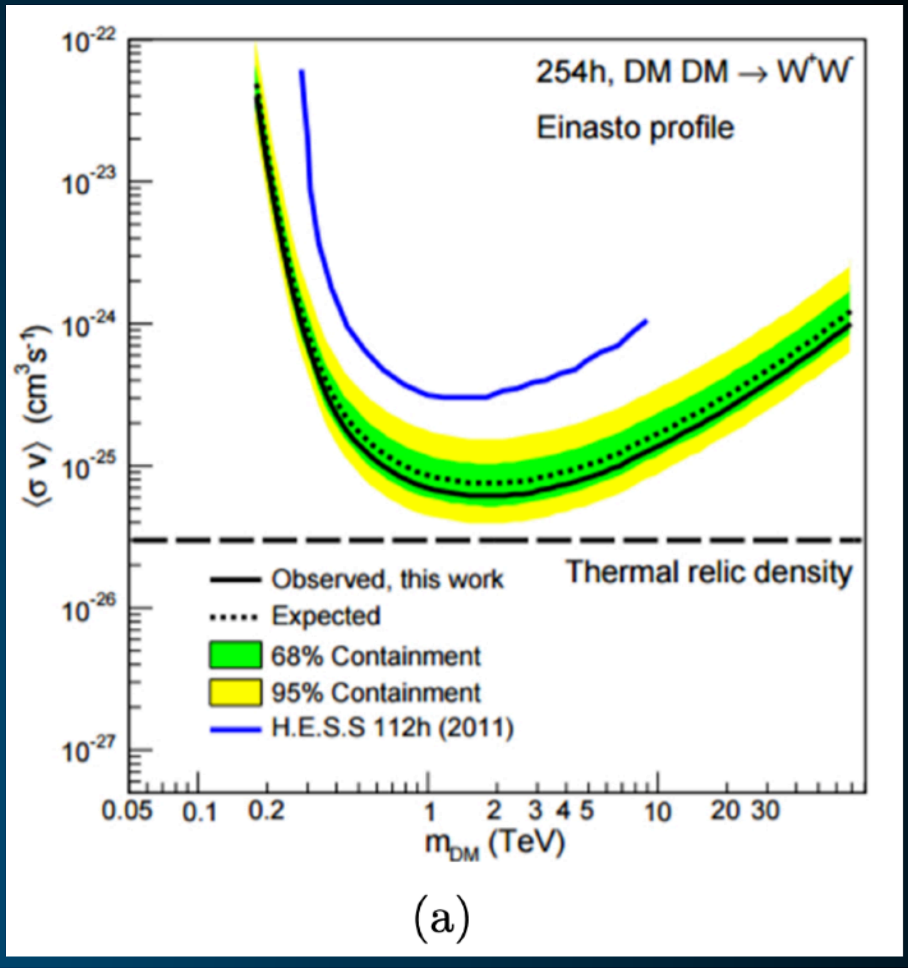

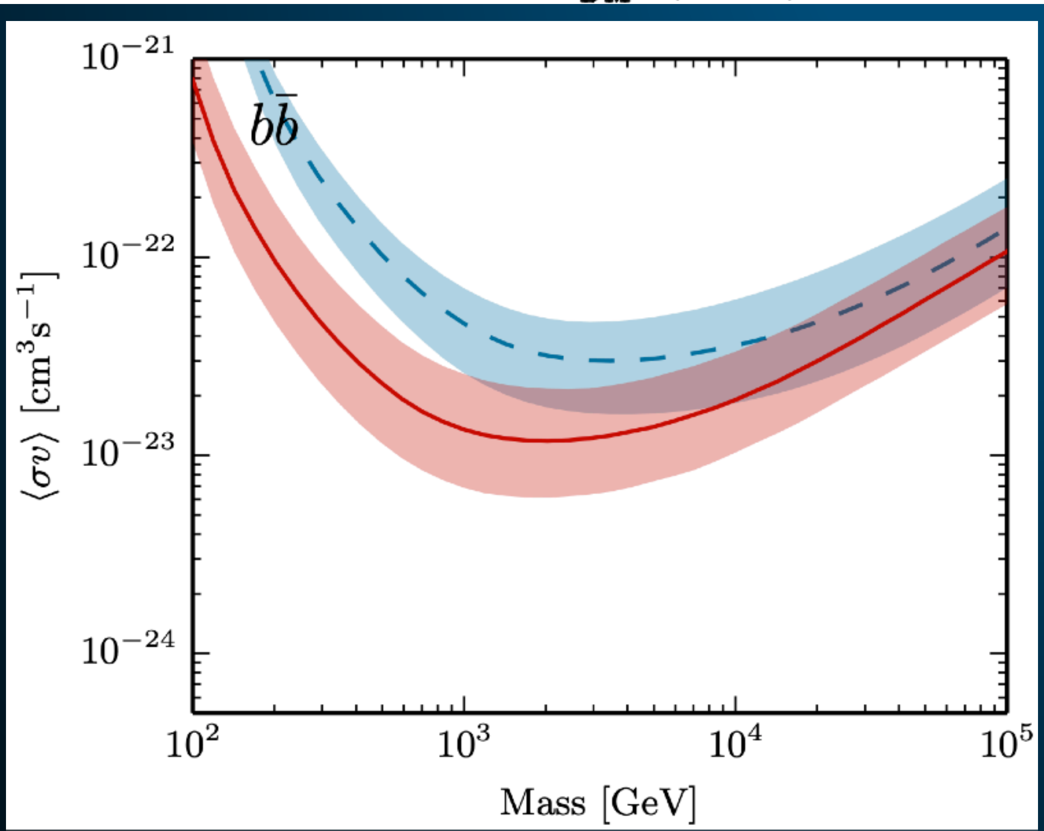

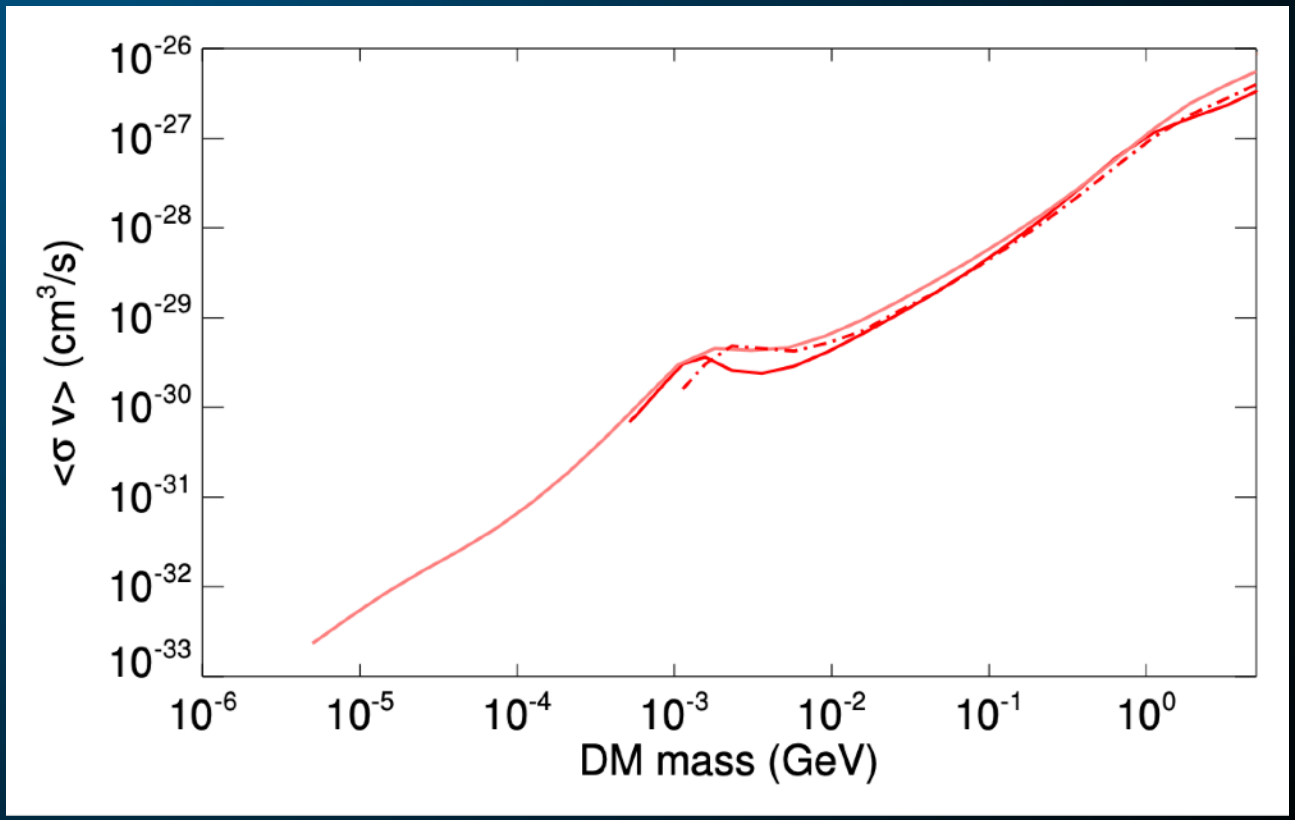

Looking Forward

How to End a Talk When You Don't Have a Conclusion

1.) Finding MSPs

2.) Constraining the Dark Matter Density

3.) Understanding Cosmic-Ray Propagation in the CMZ.

4.) New Constraints on Indirect Detection

Future Radio Surveys

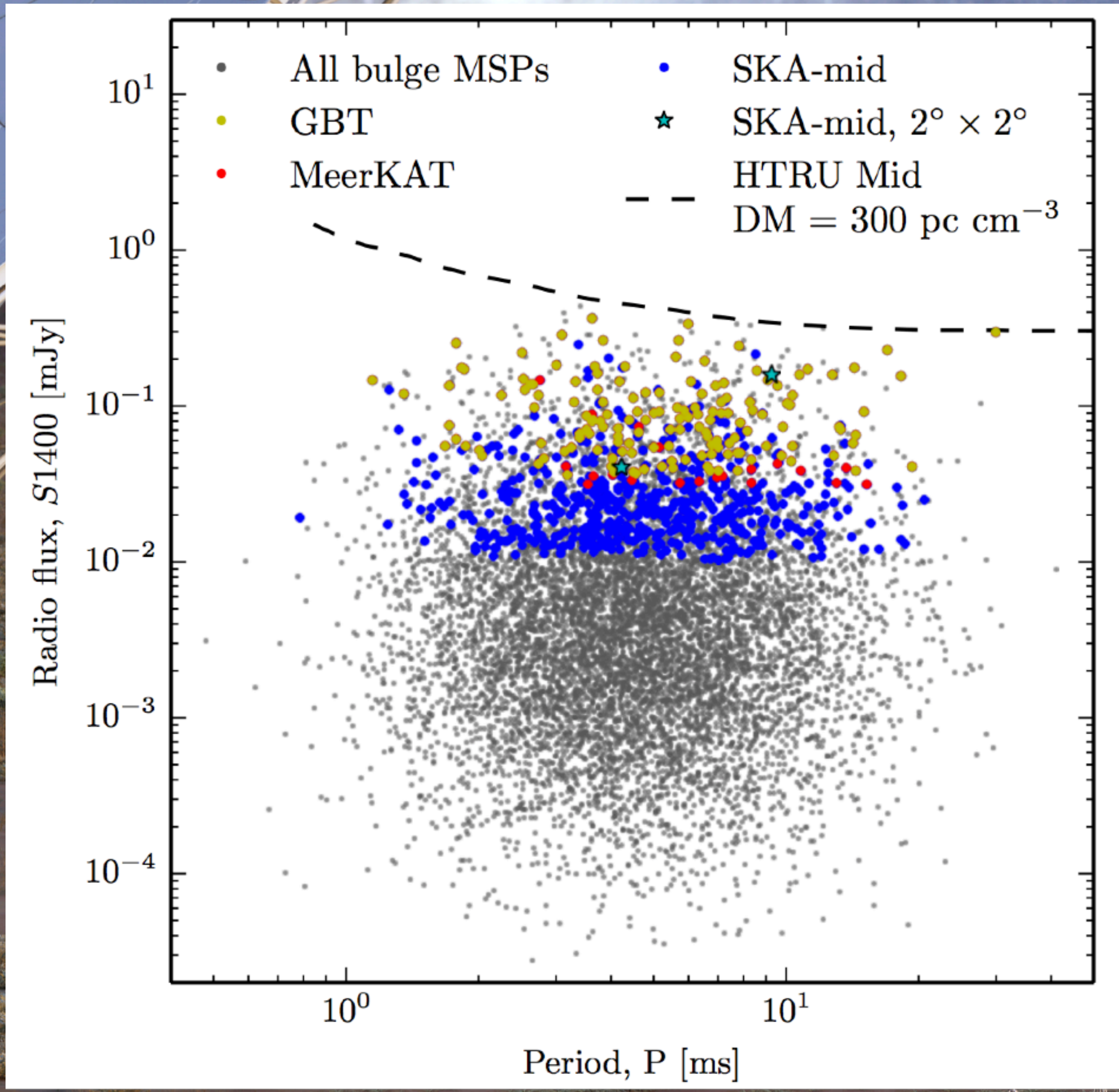

MeerKat and SKA will be extremely sensitive to Galactic center radio pulsars.

Calore et al. (2016; 1512.06825)

Future Radio Surveys

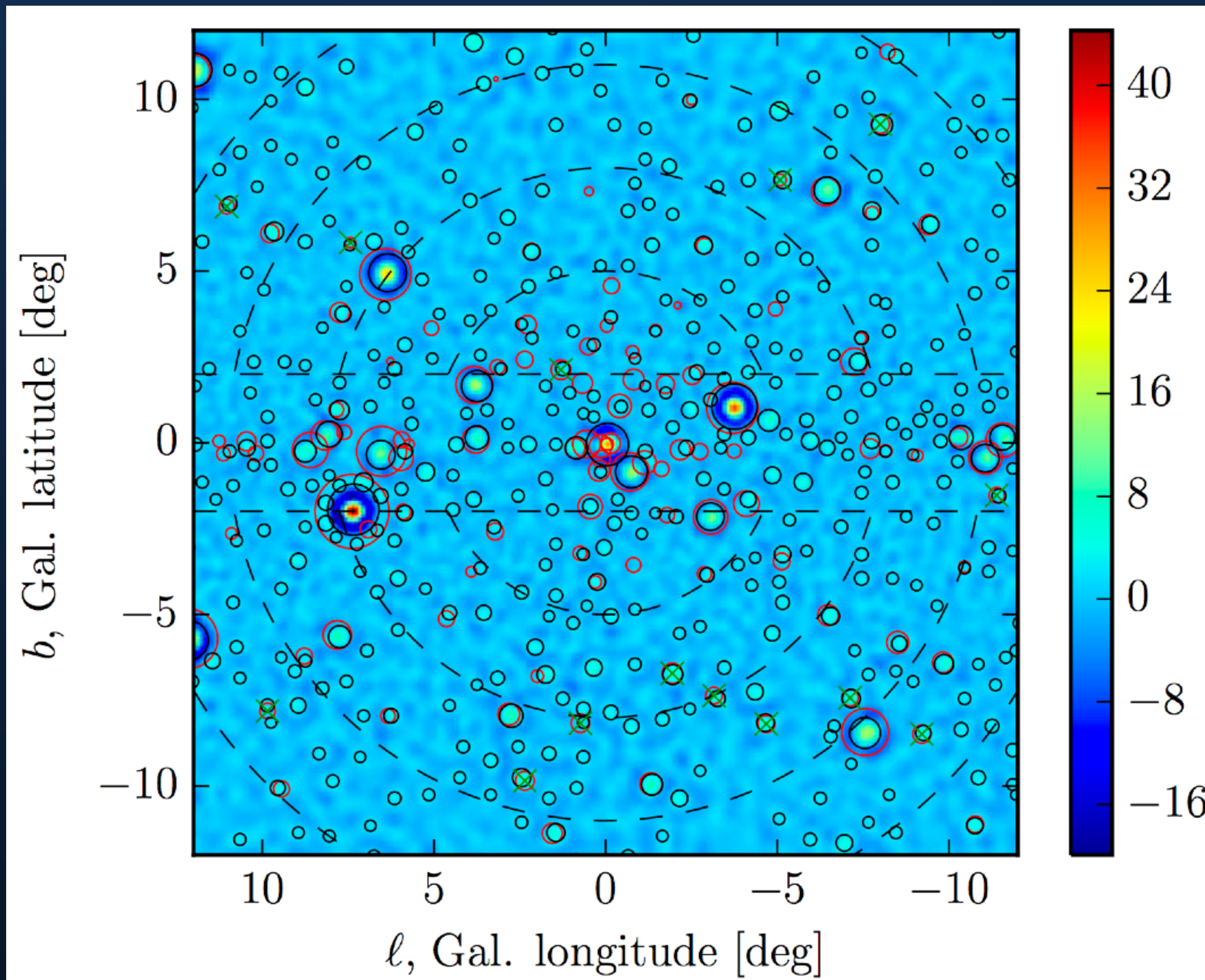

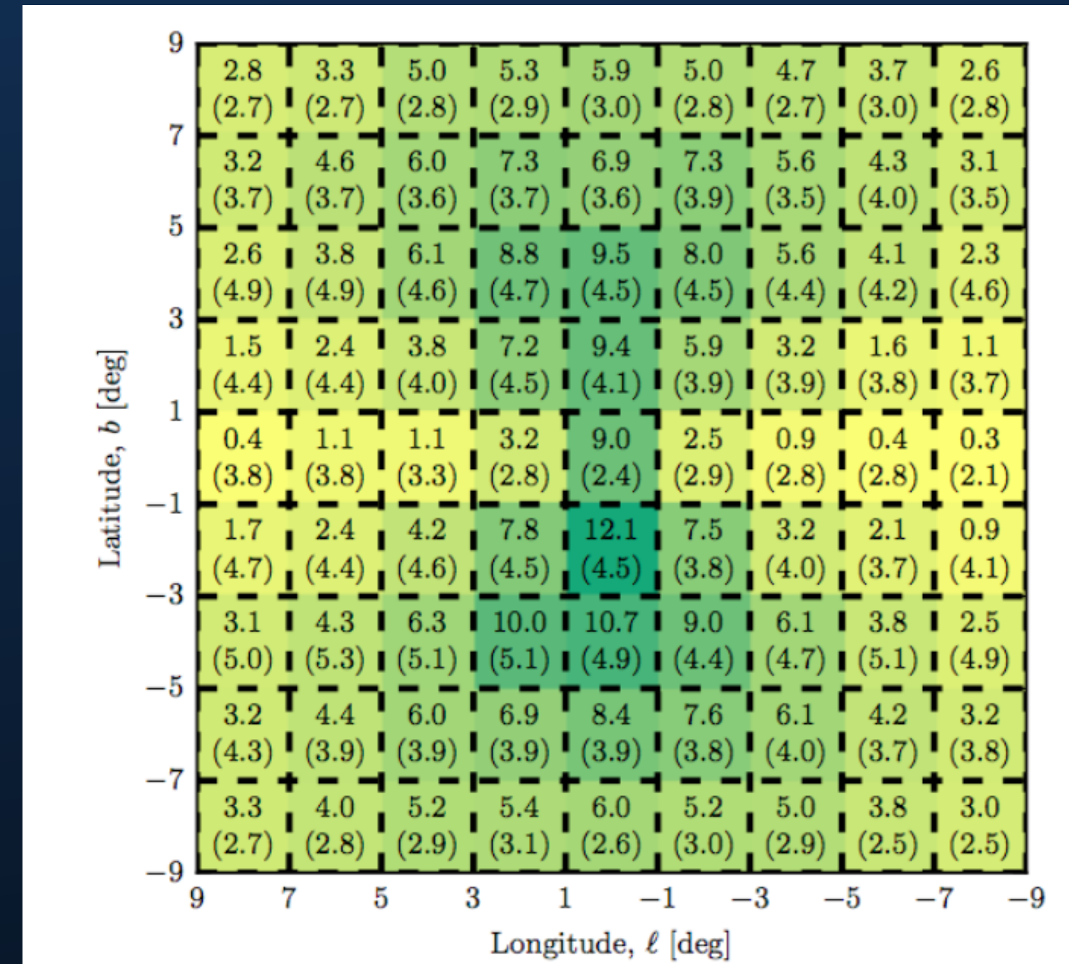

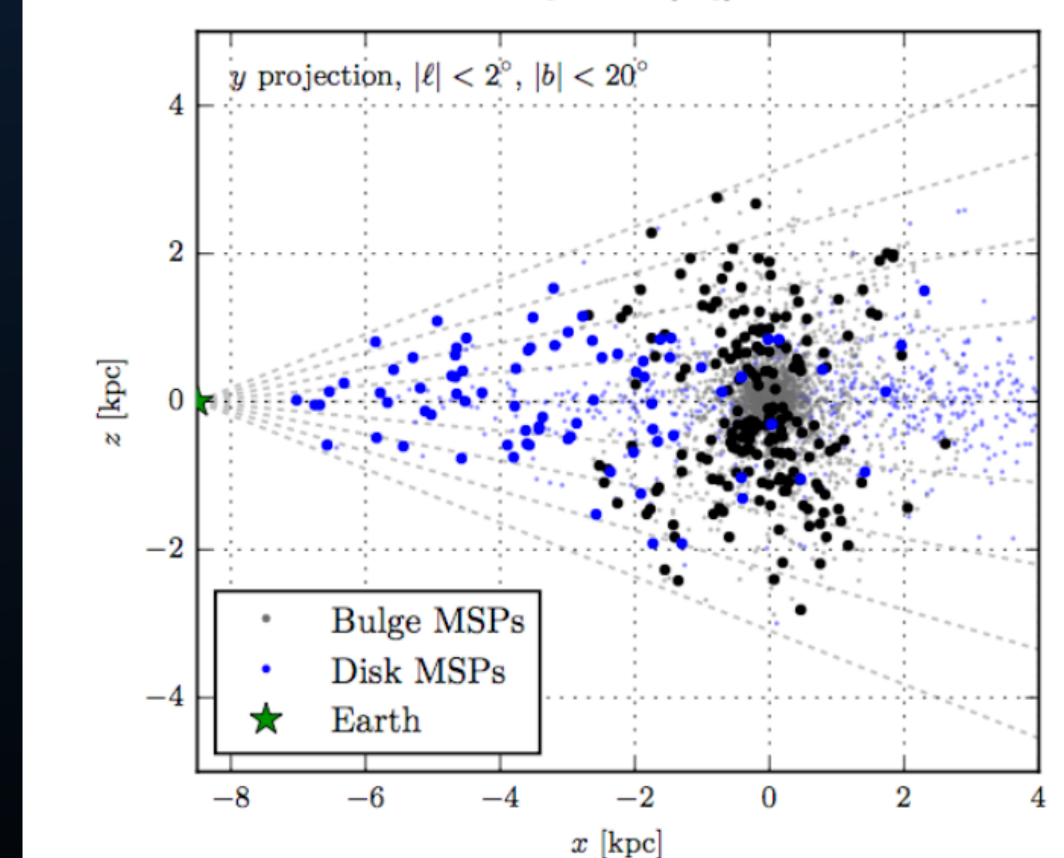

Radio surveys can find pulsars coincident with the positions of known gamma-ray hotspots.

Only a handful of sources necessary to provide definitive evidence.

Calore et al. (2016; 1512.06825)

New Observations of the Local Dark Matter Density

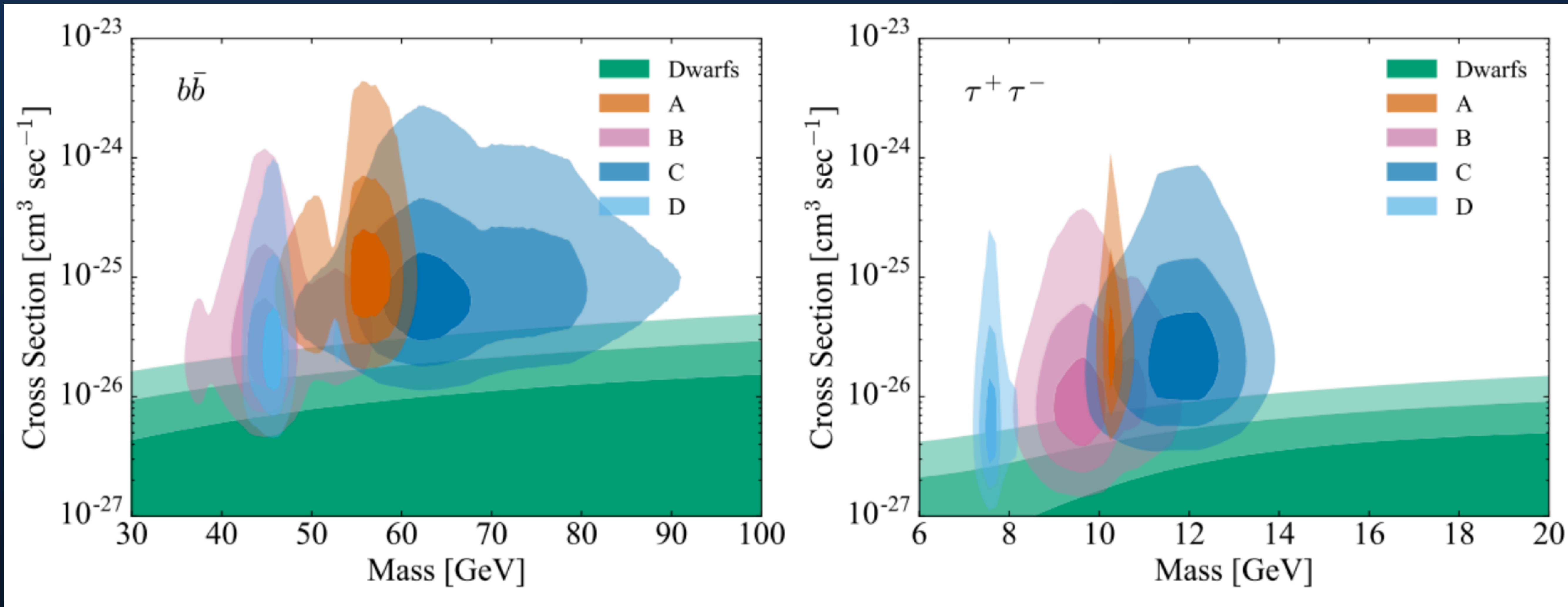

The major uncertainty in correlating the GCE and dwarf spheroidal galaxies is the local dark matter density.

Keeley et al. (2017; 1710.03215)

New Observations of the Local Dark Matter Density

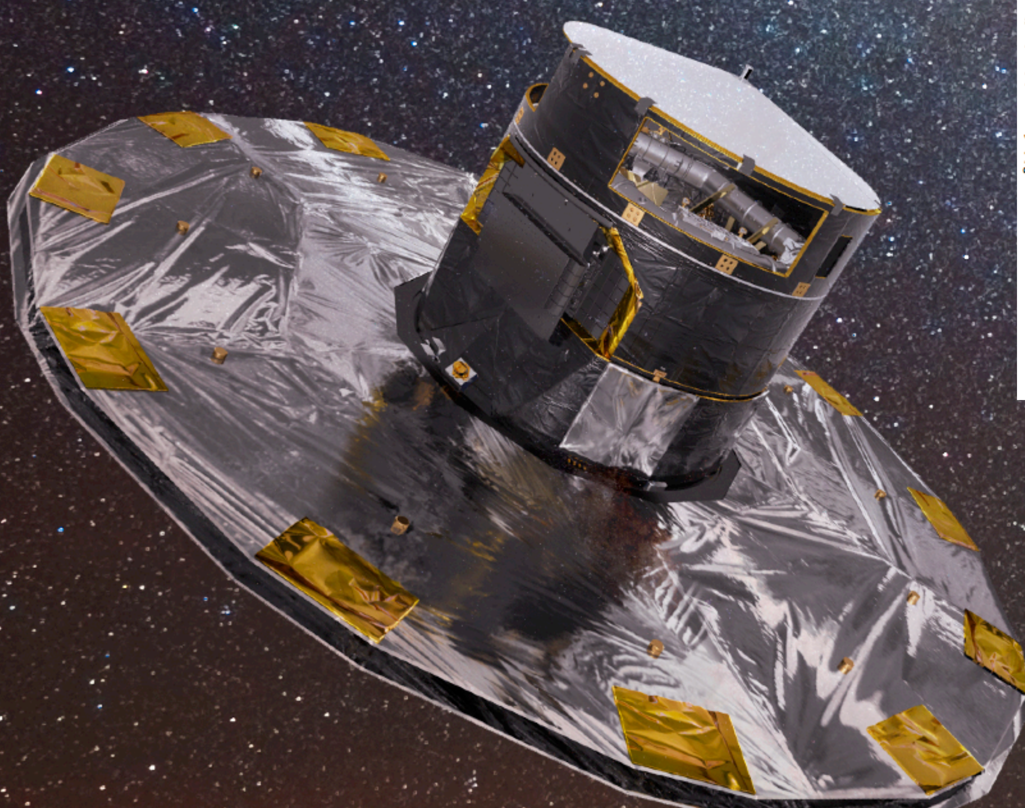

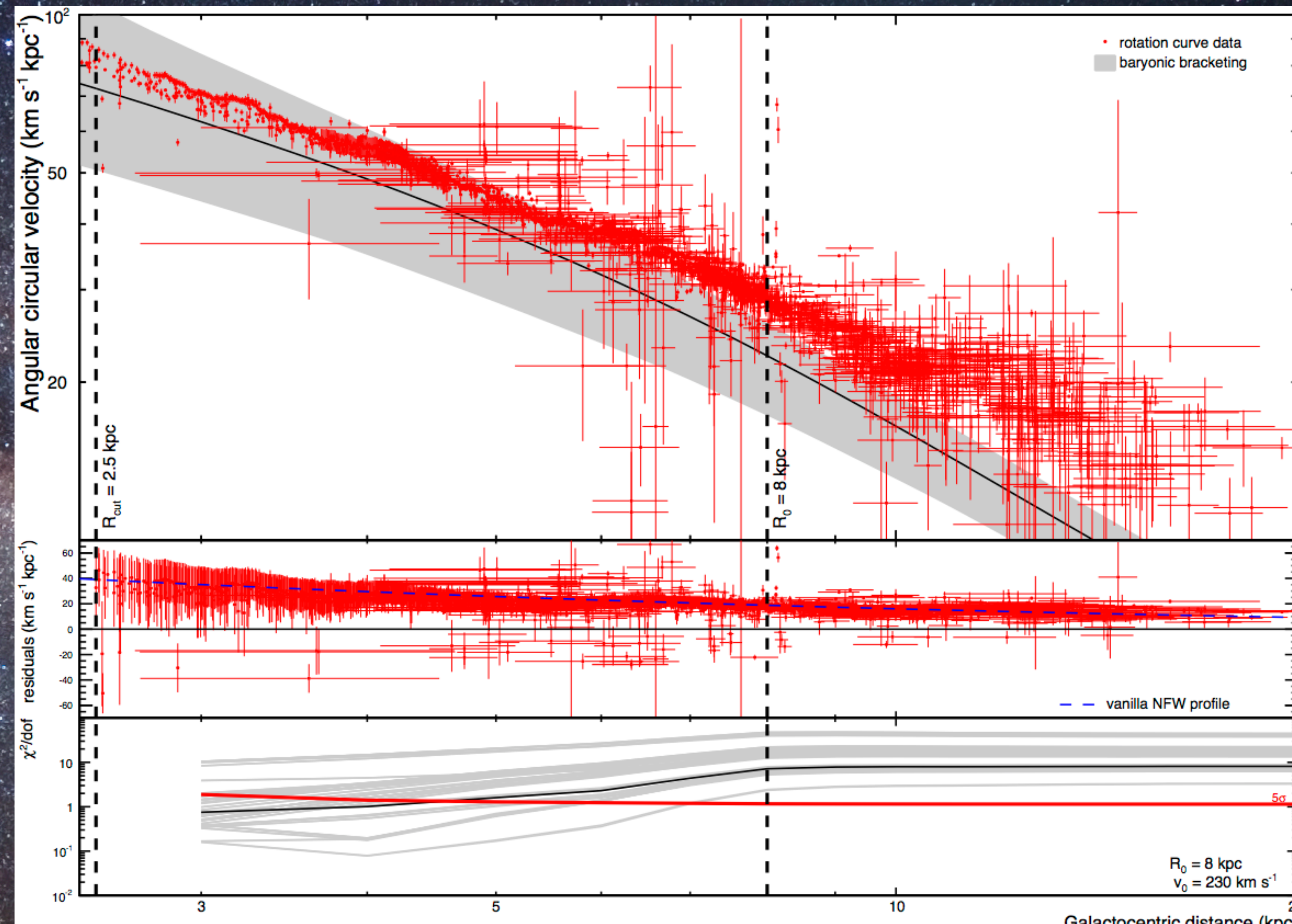

Iocco et al. (2015; 1502.03821)

New Insights into Cosmic-Ray Diffusion

H.E.S.S. Collaboration (2016; 1603.07730)

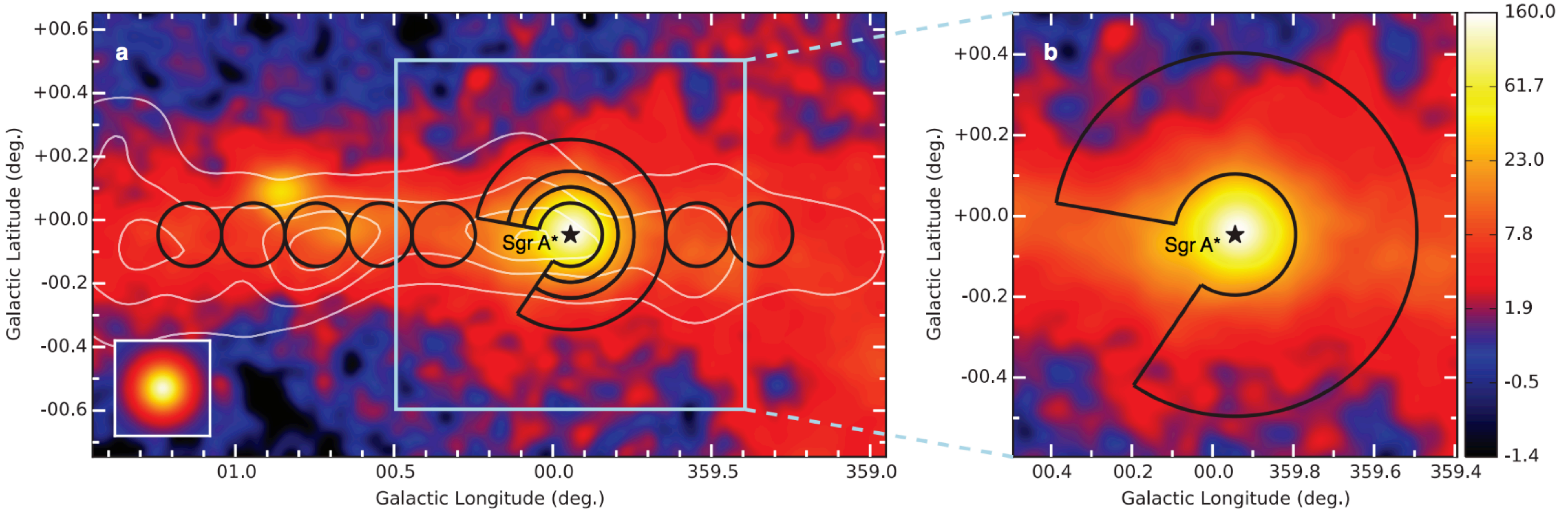

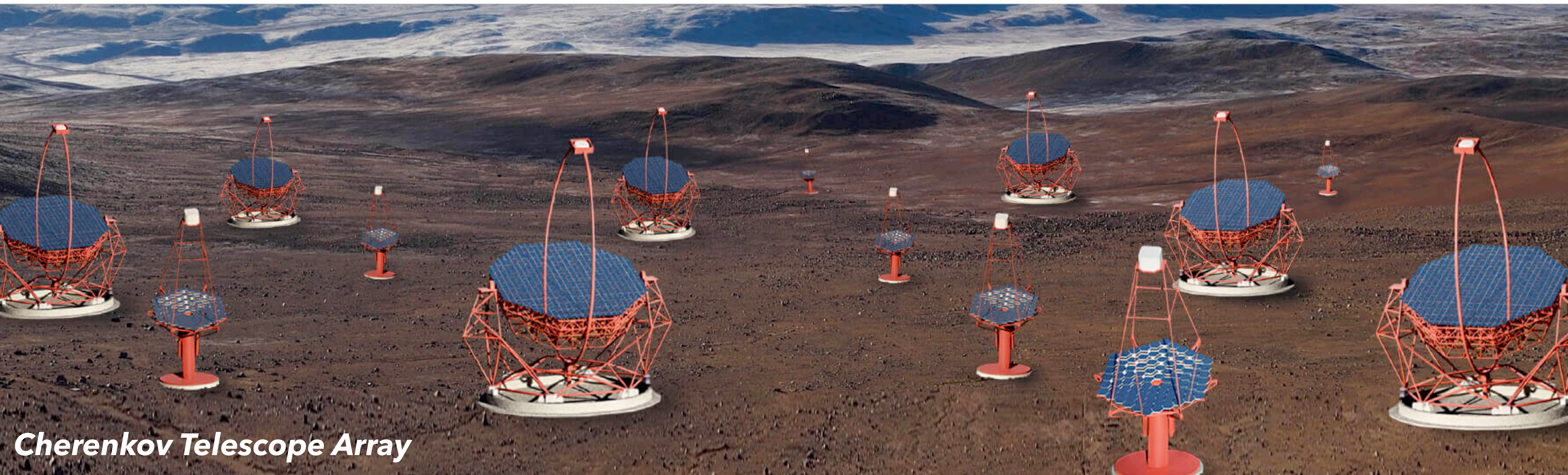

Cherenkov Telescope Array

New Dwarf Galaxies

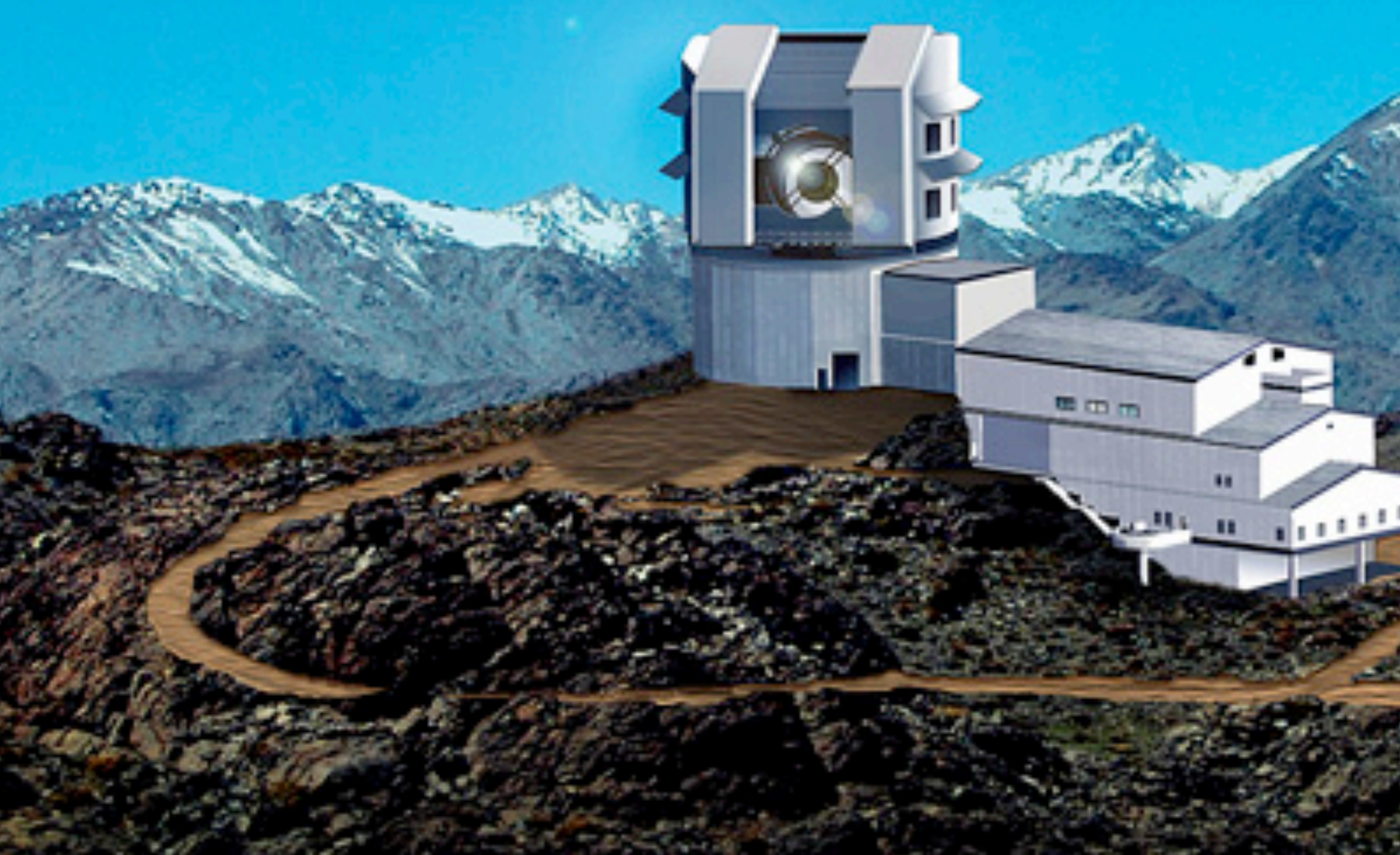

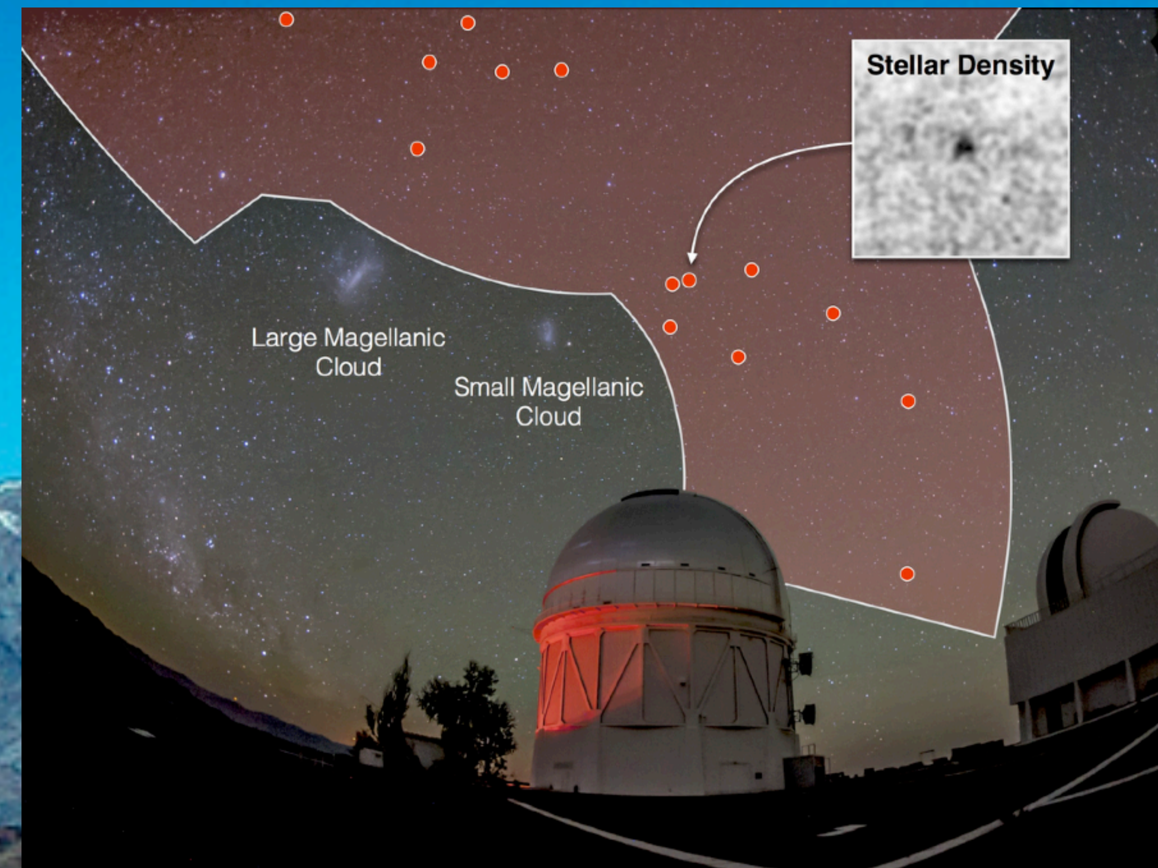

Continued DES observations, and upcoming LSST observations will find more (and smaller) dwarfs.

LSST

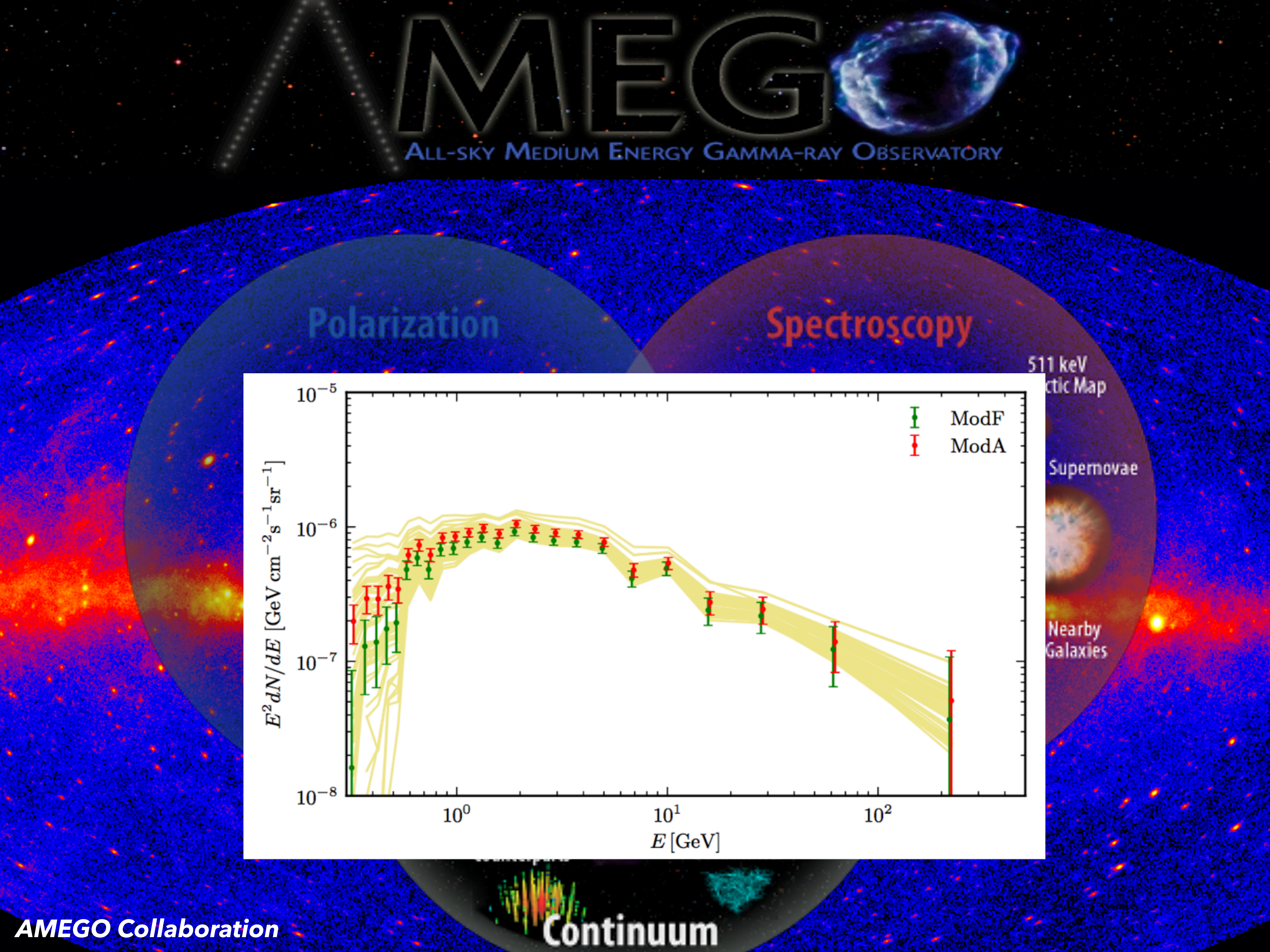

AMEGO
ALL-SKY MEDIUM ENERGY GAMMA-RAY OBSERVATORY
Polarization
Spectroscopy
511 keV
ctic Map
Supernovae
Nearby
Galaxies
Continuum
ModF
ModA
10^{-5}
10^{-6}
10^{-7}
10^{-8}
$E^2 dN/dE$ [GeV cm^{-2}s^{-1}sr^{-1}]
10^0
10^1
10^2
E [GeV]
AMEGO Collaboration

Continued Operation of the Fermi-LAT

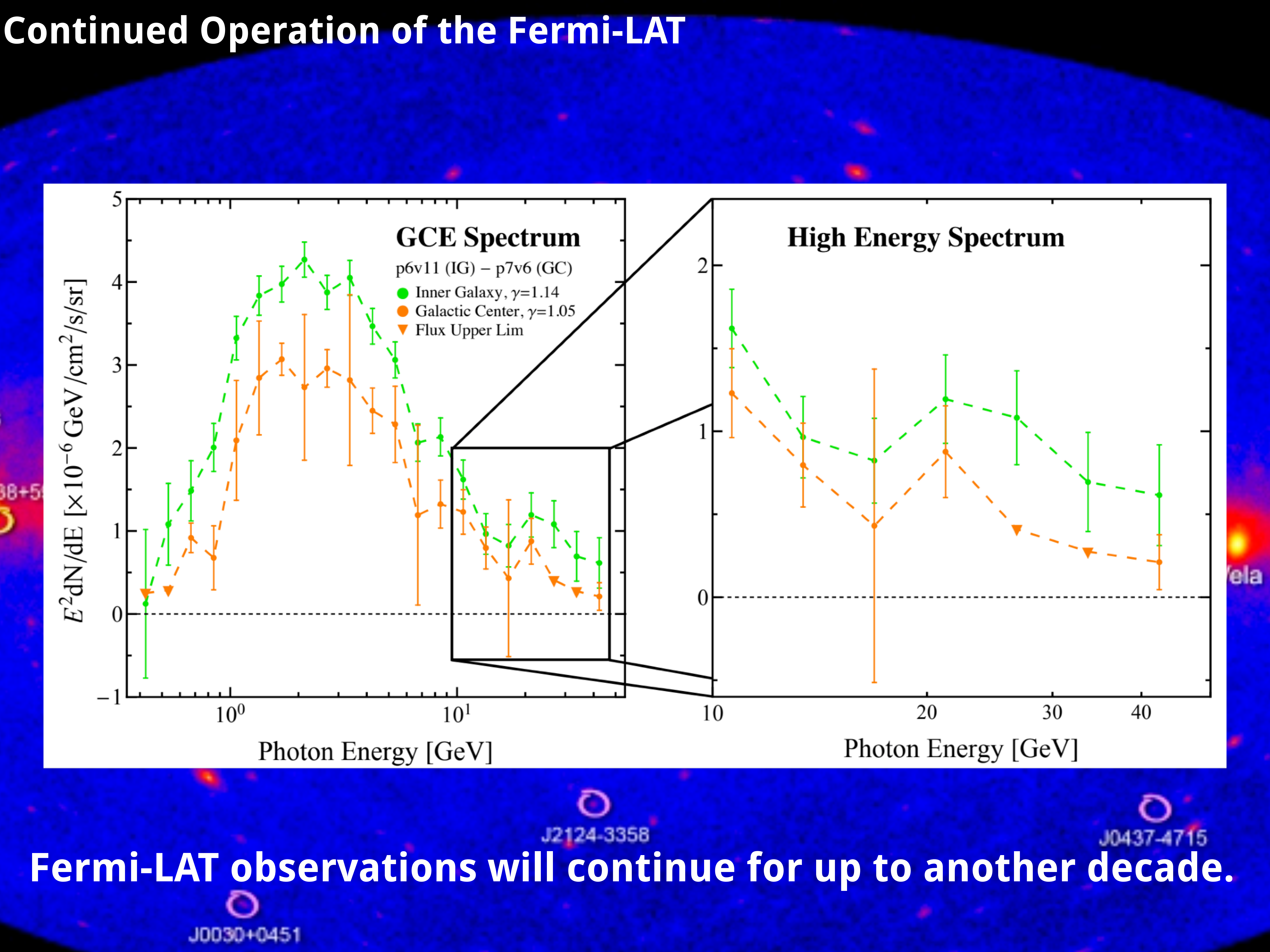

Fermi-LAT observations will continue for up to another decade.

Continued Operation of the Fermi-LAT

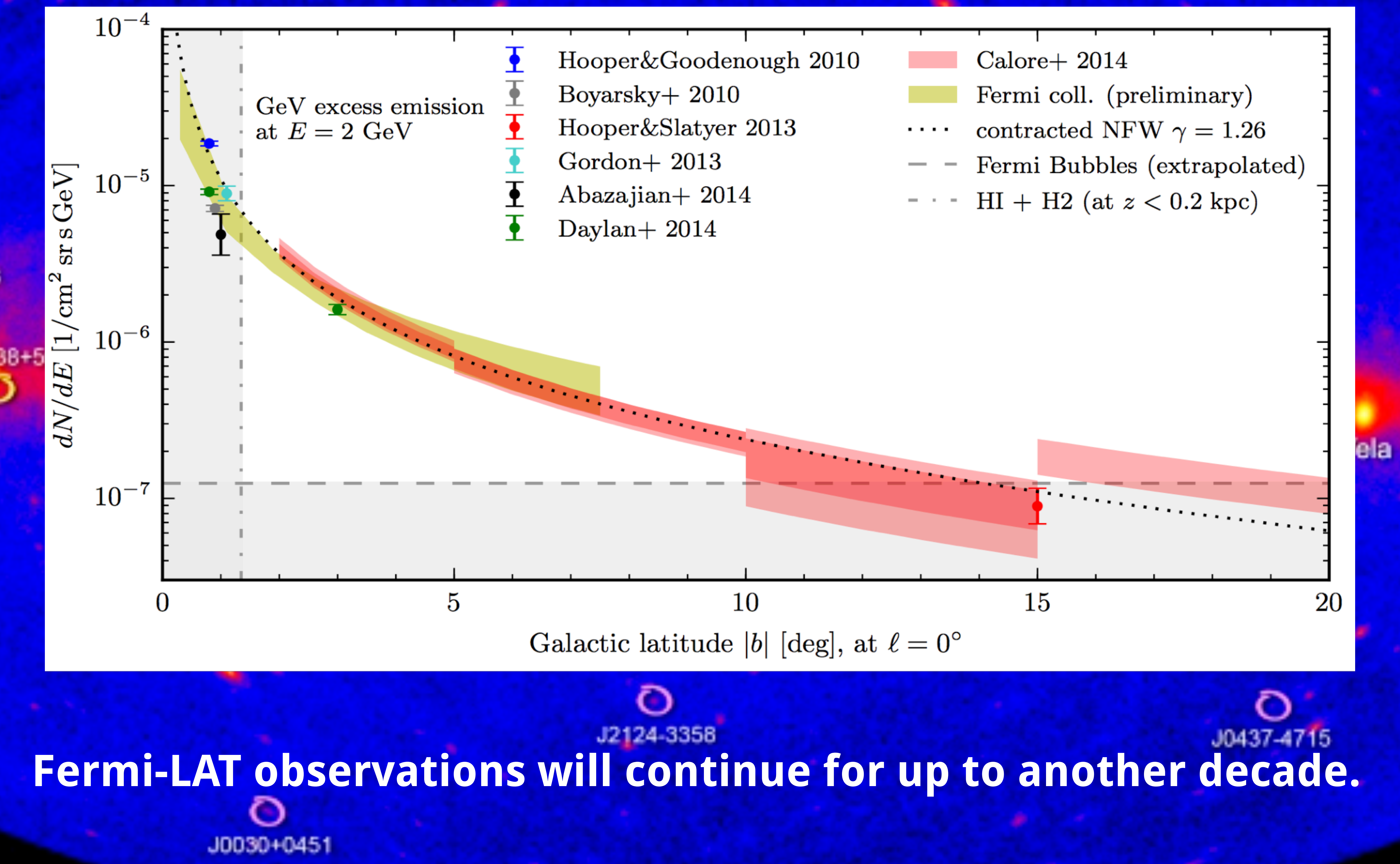

Fermi-LAT observations will continue for up to another decade.

Continued Operation of the Fermi-LAT

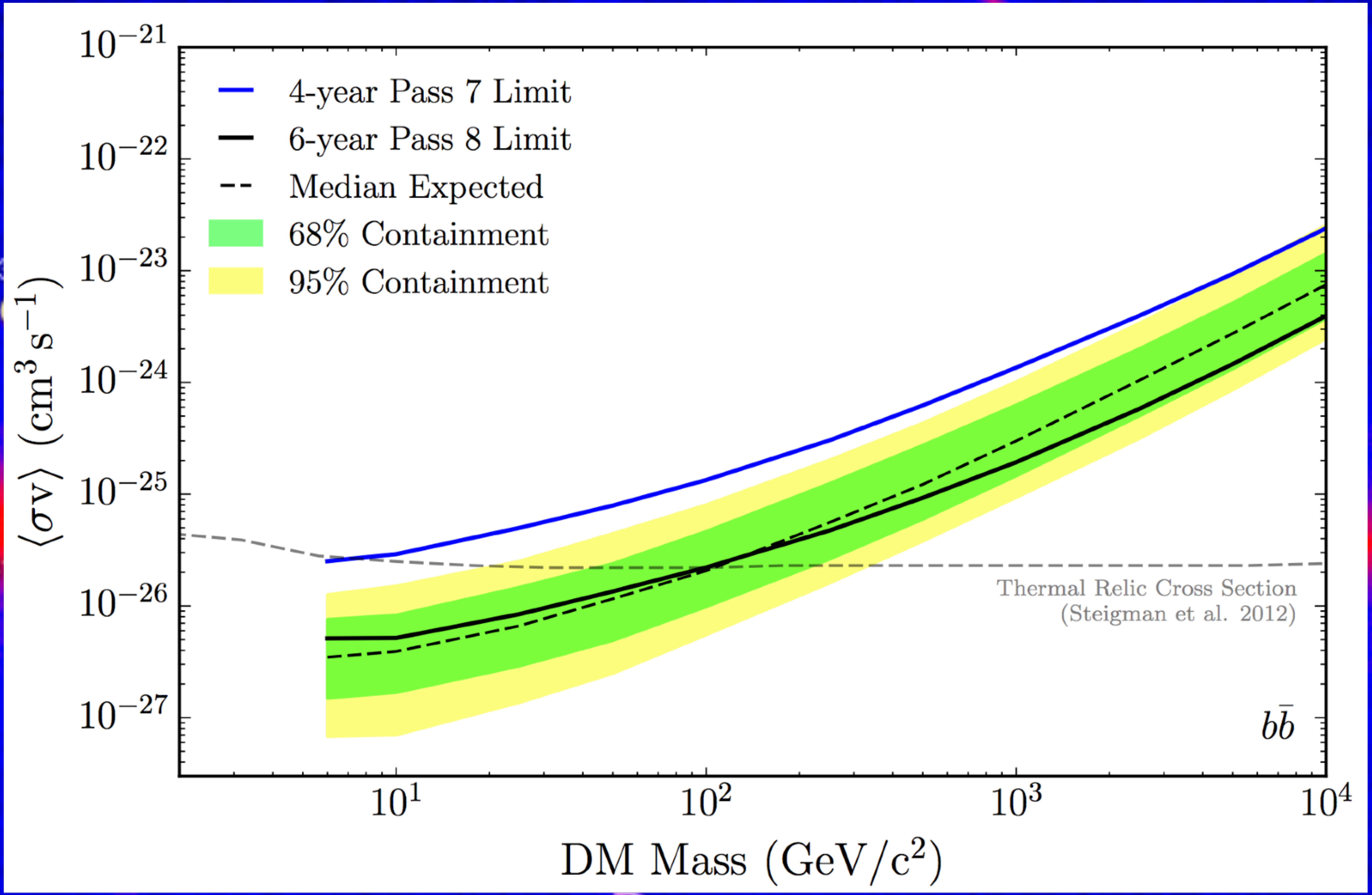

Fermi-LAT observations will continue for up to another decade.

Continued Operation of the Fermi-LAT

Fermi-LAT observations will continue for up to another decade.

Conclusions

1.) The Galactic Center Excess (compared to any standard model of astrophysical emission) is real.

2.) The two most promising models to explain the excess are dark matter and millisecond pulsars.

3.) New observations and models over the next decade offer the potential to understand the galactic center at GeV energies.

Diffuse Emission Models

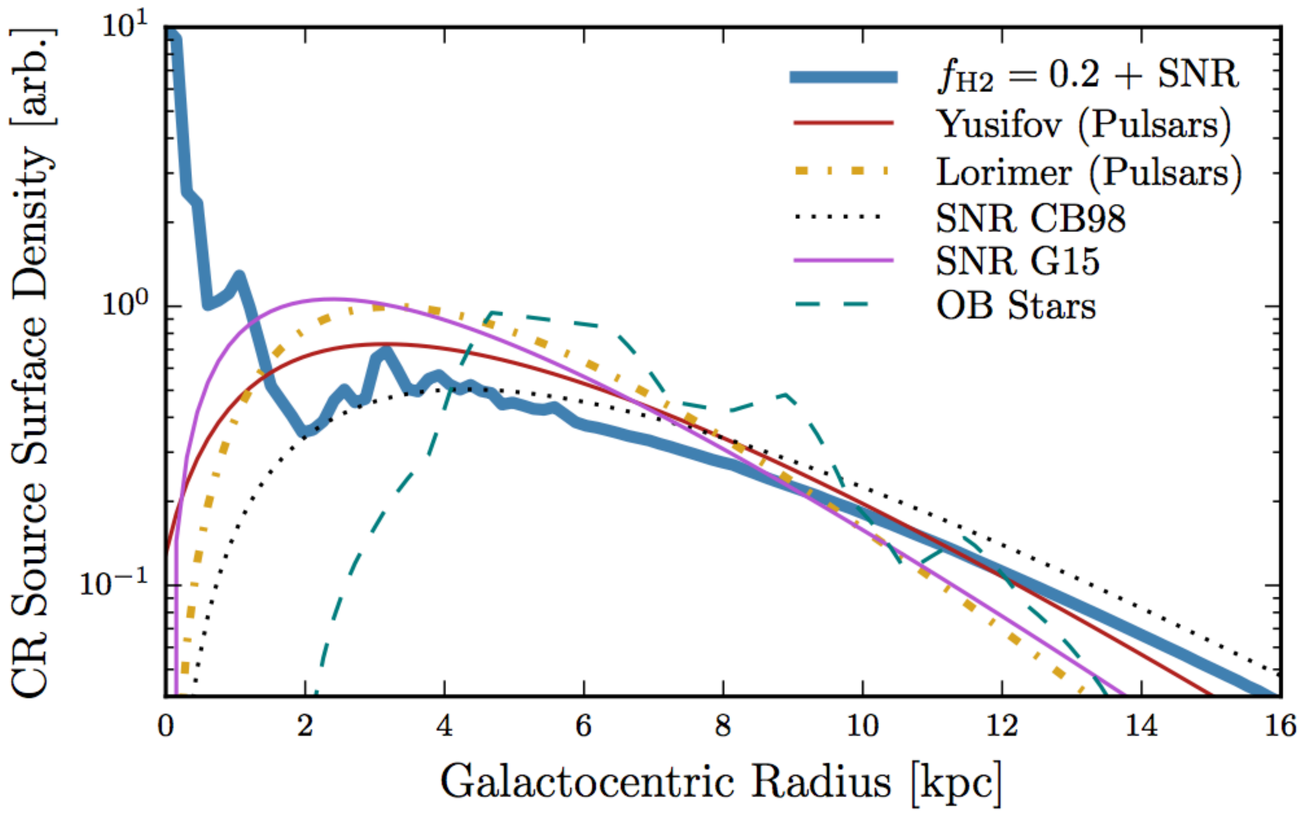

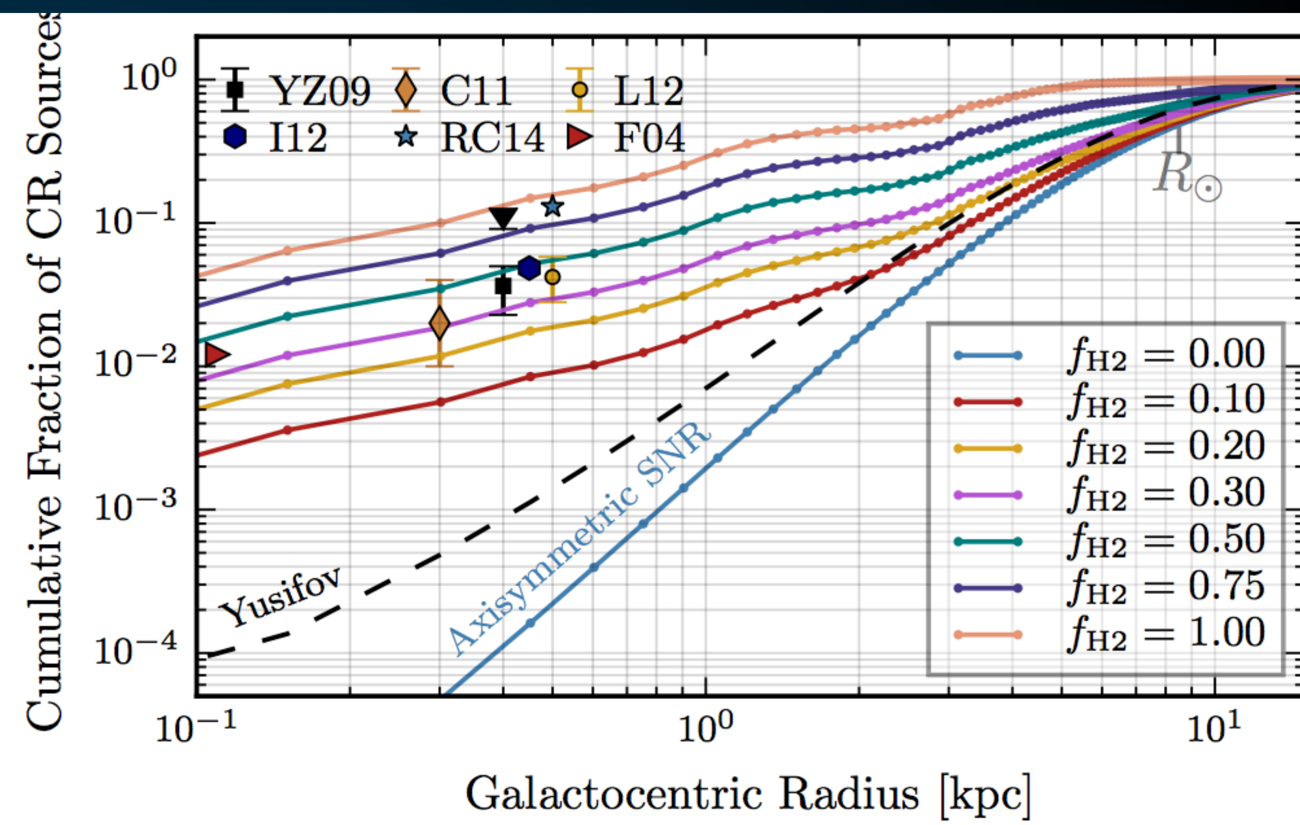

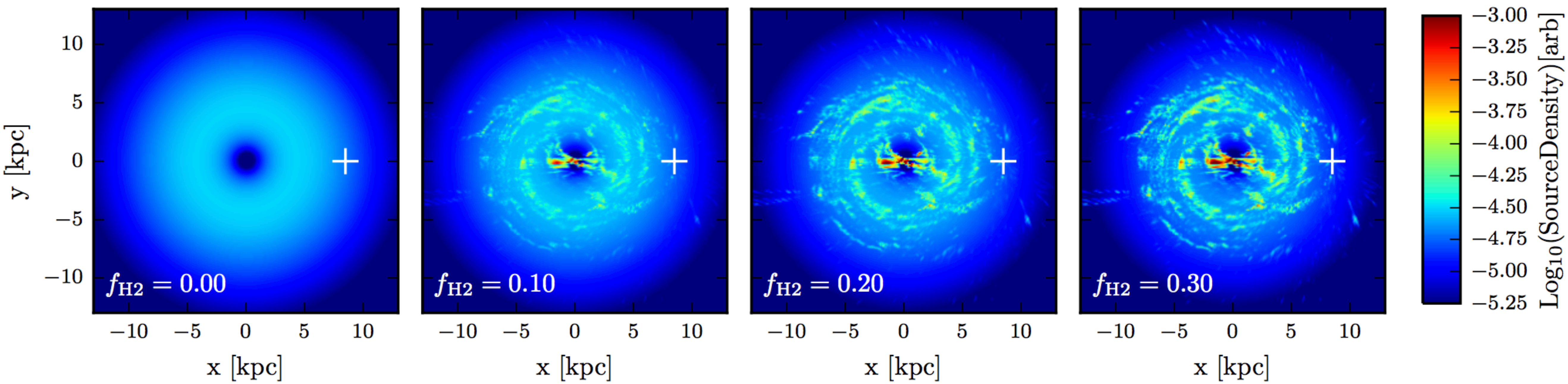

Can build models that inject cosmic-rays tracing gas in the CMZ.

Diffuse Emission Models

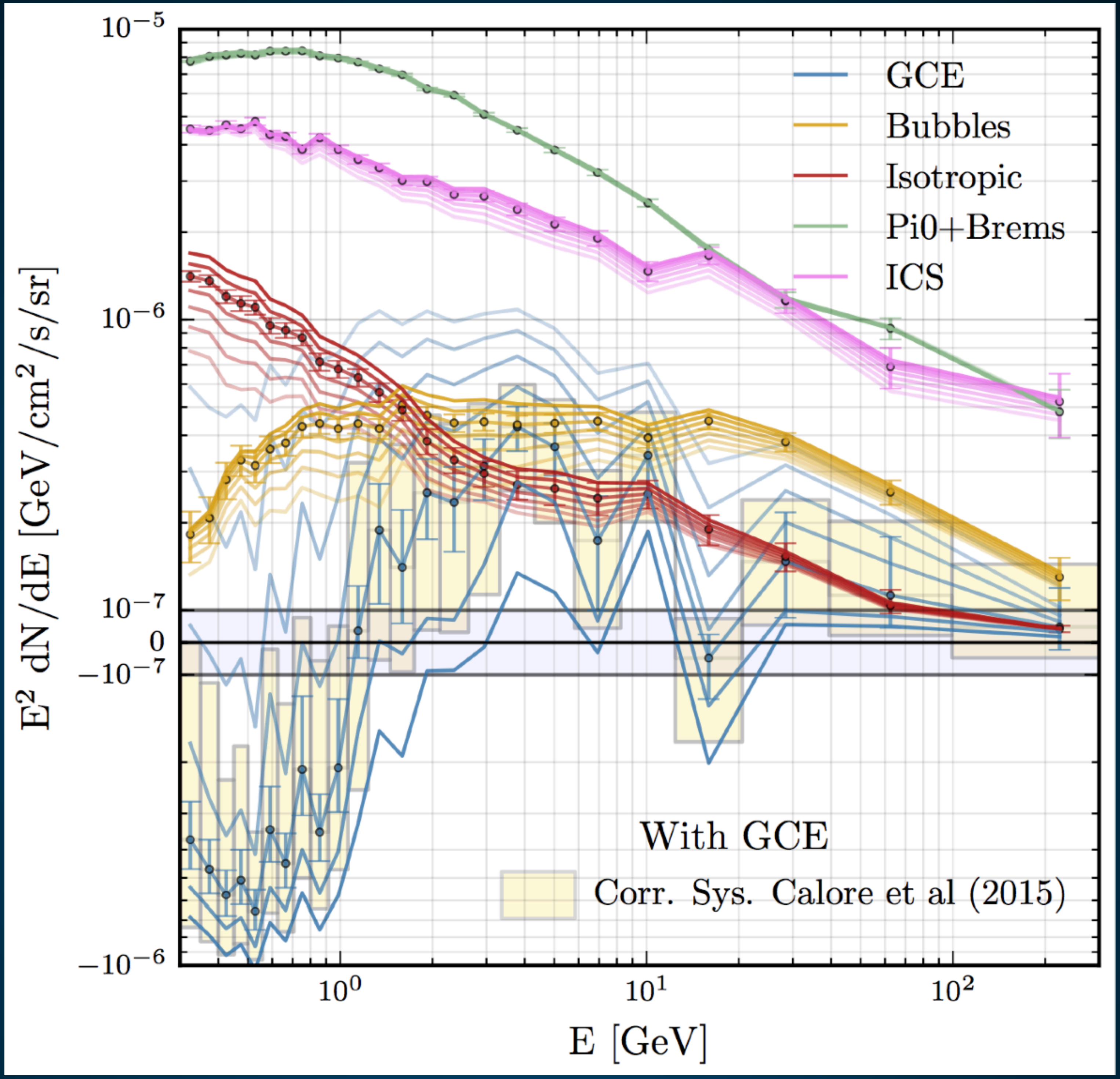

Cranking up the CR injection causes significant over subtraction at low energies. The GCE feature remains, but is zero-subtracted.

Diffuse Emission Models

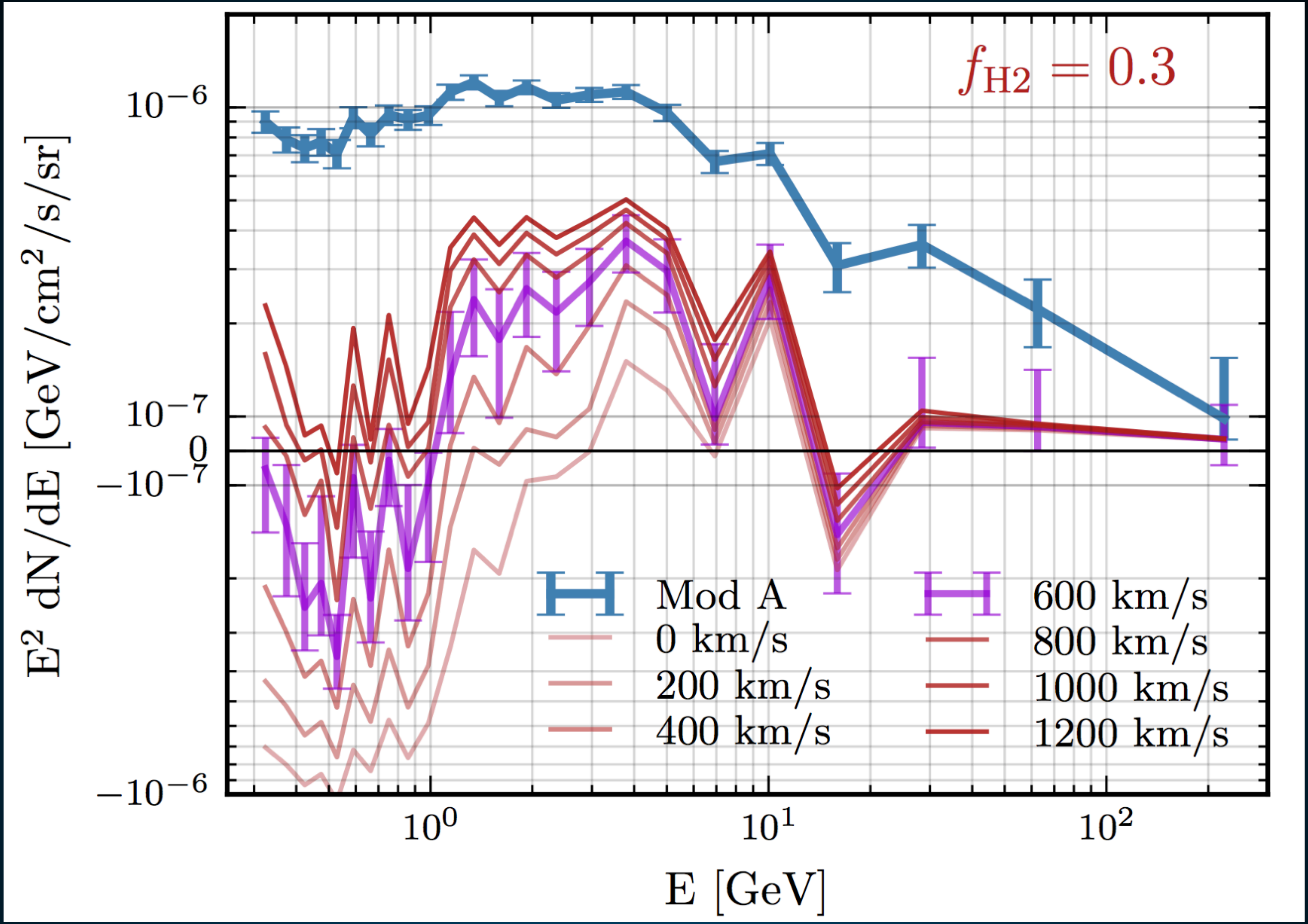

Better models fix this - GC excess returns!

Two Types of Models

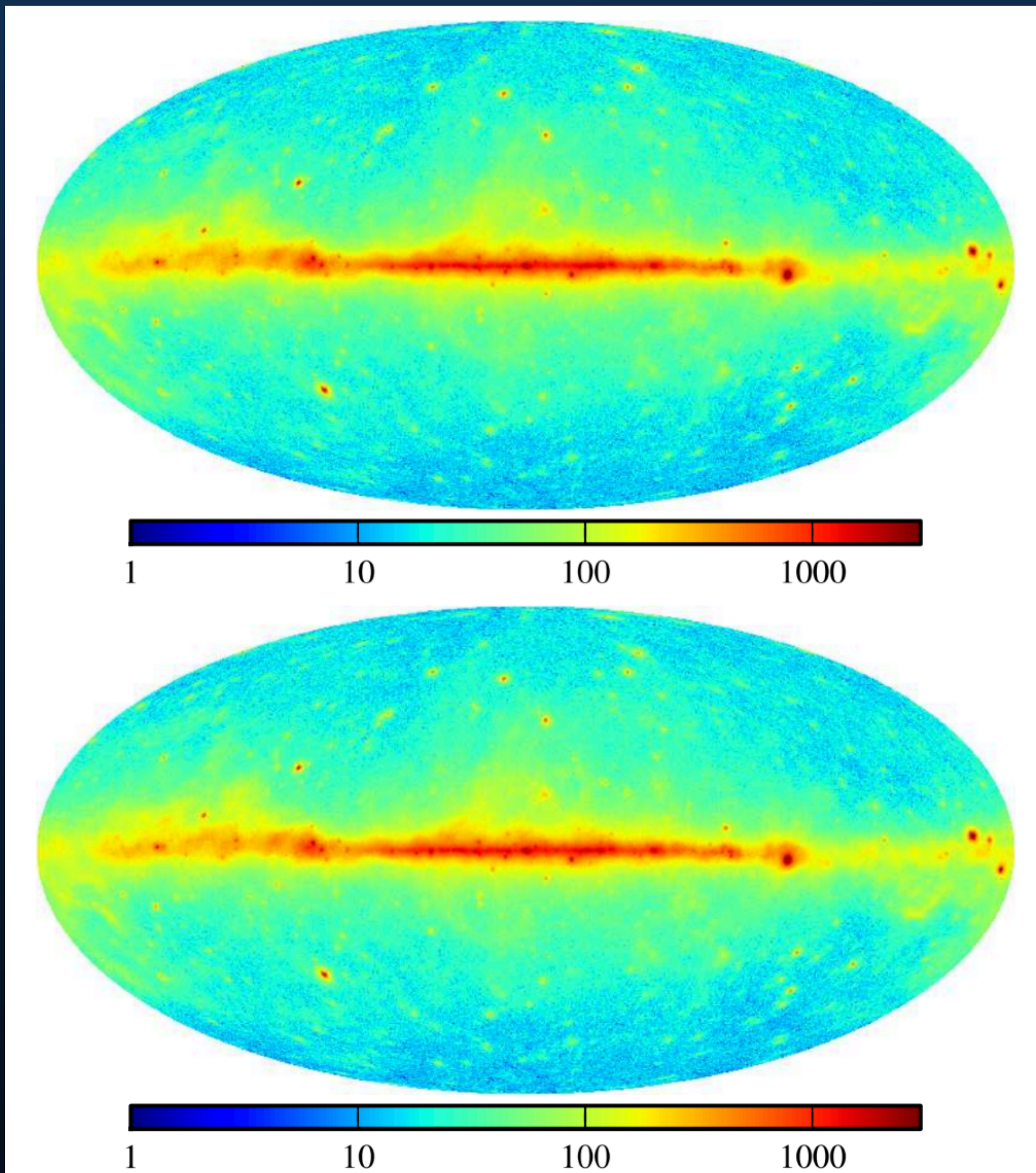

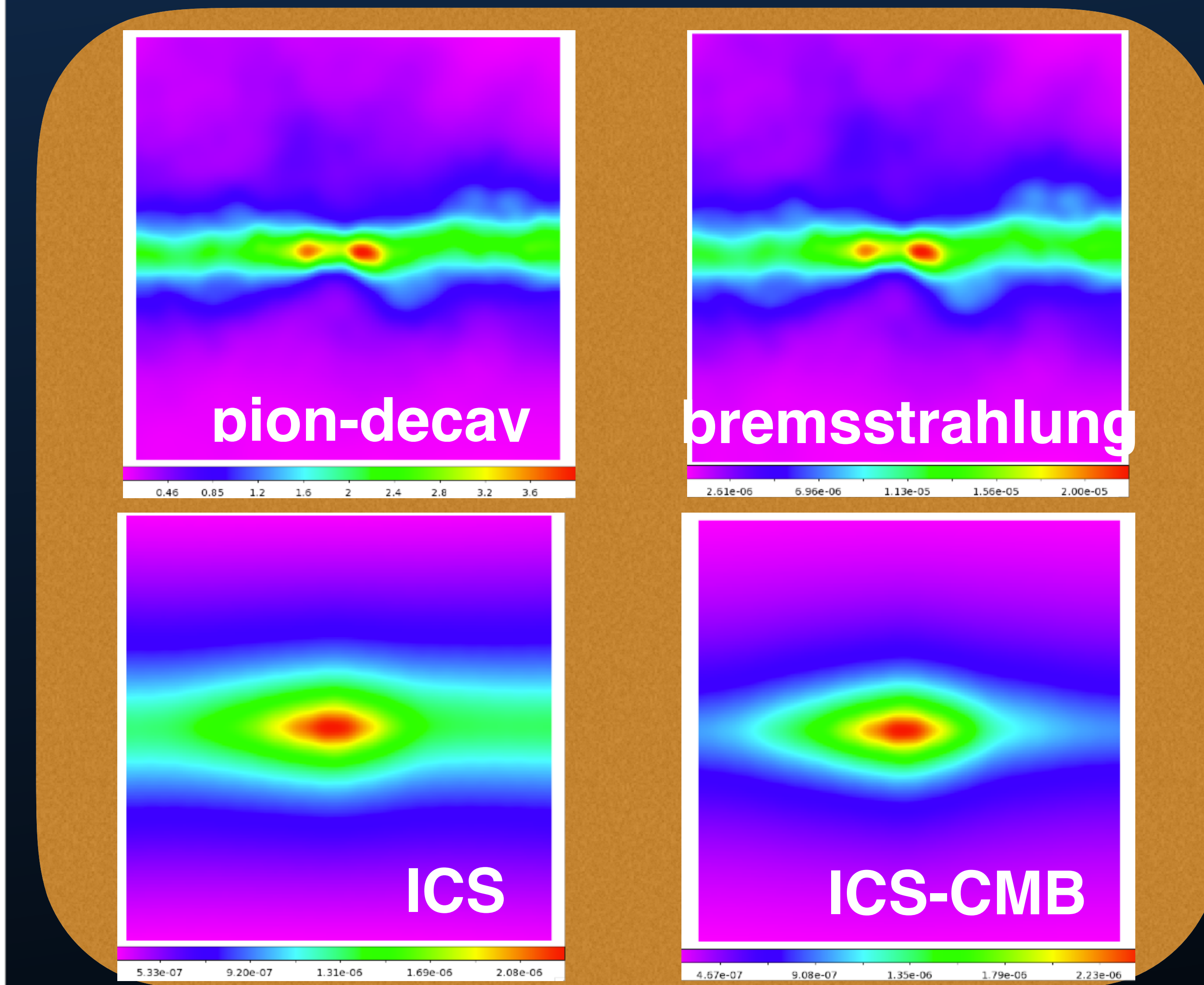

Template-Based

Galprop-Based